Zebrafish as a Model Organism to Study the *In Vivo* Role of G-Protein Coupled Receptor 17 in Myelination

---

Dissertation

zur

Erlangung des Doktorgrades (Dr. rer. nat)

der Mathematisch-Naturwissenschaftlichen Fakultät

der Rheinischen Friedrich-Wilhelms-Universität Bonn

vorgelegt von

Nina-Katharina Schmitt

aus München

Bonn 2019

Angefertigt mit Genehmigung der Mathematisch-Naturwissenschaftlichen Fakultät der Rheinischen Friedrich-Wilhelms-Universität Bonn.

1. Gutachter: Prof. Dr. Evi Kostenis

2. Gutachter: Prof. Dr. Benjamin Odermatt

Tag der Promotion: 21.02.2019

Erscheinungsjahr: 2019

Die vorliegende Arbeit wurde in der Zeit von November 2014 bis August 2018 am Institut für Pharmazeutische Biologie und am Anatomischen Institut der Rheinischen Friedrich-Wilhelms-Universität Bonn unter der Leitung von Frau Prof. Dr. Evi Kostenis angefertigt.

Für meine Lieben

Abstract

The sheathing of axons with myelin by oligodendrocytes constitutes a necessity for sufficient and rapid nerve conduction within the vertebrate central nervous system (CNS). However to date, the complex molecular mechanisms controlling distinct signalling cascades of myelination are still not decrypted. Recent studies have proposed G-protein coupled receptors (GPCRs), such as Gpr17, as crucial regulators of oligodendrocyte development and myelination. Herein, this study investigates the implication of Gpr17 in myelination in its native signalling environment by using zebrafish (Danio rerio), an ideal suited vertebrate model system for studying myelination *in vivo*. Additionally, further functionality studies evaluate responsiveness of zebrafish and chimeric human/zebrafish Gpr17 receptors in extrinsic mammalian cellular backgrounds.

While zebrafish Gpr17 transiently transfected in HEK293 cells remained unresponsive towards the small molecule agonist MDL29,951, stimulation of chimeric human/zebrafish receptors containing the human binding domain led to concentration-dependent response curves in Dynamic mass redistribution assays. These results, further confirmed by *in vivo* assays revealing unaffected oligodendrocyte development and myelination after bath treatment with MDL29,951, imply an impaired zebrafish receptor-ligand interaction both *in vivo* and *in vitro*. Investigations with zebrafish demonstrated sustained Gpr17 expression in oligodendrocyte lineage cells during CNS development from 1 to 5 dpf. Moreover, morpholino-induced receptor knockdown provoked a significant reduction of pre-mature and mature oligodendrocyte numbers and disturbed myelination. The reduced cell numbers are assumed to result from impaired migration of pre-mature pre-oligodendrocytes (pre-OLs) accumulating in the ventral spinal cord region. On the contrary, overexpression of Gpr17 in early stages did not influence oligodendrocyte development. Together, the data confirm a crucial role of zebrafish Gpr17 *in vivo*. Clearly, future studies with knockout animals are strictly necessary to corroborate these findings and conclusively delineate the impact of Gpr17 on oligodendrocyte development and myelination.

Kurzfassung

Im zentralen Nervensystem (ZNS) stellt die Myelinisierung durch Gliazellen, den sogenannten Oligodendrozyten, eine essentielle Grundlage für die erfolgreiche Reizweiterleitung von Nervenzellen dar. Trotz zahlreicher Studien bestehen jedoch weiterhin Unklarheiten bezüglich der Entwicklung von Oligodendrozyten sowie ihrer Aufgabe Myelin zu produzieren. Permanente Forschung in diesem Gebiet hat kürzlich erwiesen, dass G-Protein-gekoppelte Rezeptoren (GPCRs), wie etwa Gpr17, entscheidende Rollen in der Reifung von Oligodendrozyten sowie in der Myelinisierung übernehmen. Innerhalb dieser Arbeit wurde der Zebrafisch (Danio rerio) als Tiermodell verwendet, um den Einfluss von Gpr17 auf die Myelinisierung zu untersuchen. Des Weiteren wurden der Zebrafisch-Gpr17 sowie chimäre Human/Zebrafisch-Rezeptoren auf ihre Funktionalität gegenüber postulierten Gpr17 Liganden in zellulären Hintergründen überprüft.

Während der Agonist MDL29,951 den in HEK293 Zellen rekombinant überexprimierten Zebrafish-Gpr17 nicht zu aktivieren vermochte, führte die Stimulation von chimären Human/Zebrafisch-Rezeptoren zu einer konzentrationsabhängigen Zellantwort in dynamischen Massenumverteilungs-Experimenten. Diese Ergebnisse wurden durch weitere *in vivo* Studien bestätigt, die zeigten, dass die Reifungen von Oligodendrozyten sowie die darauffolgende Myelinisierung durch eine 5-tägige Applikation von MDL29,951 nicht beeinträchtigt wurde. Daher wurde geschlussfolgert, dass die Bindung von MDL29,951 am Zebrafisch-Rezeptor sowohl *in vitro* als auch *in vivo* verhindert sein muss.

Der zweite Teil dieser Arbeit befasste sich mit der Expression und der Rolle von Gpr17 im Zebrafisch. Zunächst konnte bewiesen werden, dass Gpr17 innerhalb der ersten 5 Tage während der ZNS Entwicklung von unreifen Oligodendrozyten-Vorläufer-Zellen exprimiert wird. Um weitere Rückschlüsse auf den Einfluss von Gpr17 auf die Oligodendrozyten-Reifung zu ziehen, wurde mittels Morpholino-Injektion ein Rezeptor-Knockdown hervorgerufen, der eine signifikante Reduktion von unreifen sowie reifen Oligodendrozyten im dorsalen Rückenmarksbereich und eine gestörte Myelinisierung zur Folge hatte. Hierbei wird vermutet, dass die Abwesenheit von Gpr17 nicht nur die Reifung, sondern auch die Migration von Oligodendrozyten zu den Axonen beeinträchtigt. Im Gegensatz zum Rezeptor-Knockdown bewirkte die Überexpression von Gpr17 in frühen embryonalen Phasen keinerlei Veränderung in der Entwicklung sowie in der Myelinisierung der Oligodendrozyten. Zusammenfassend implizieren die erhobenen Daten, dass Gpr17 eine wichtige Rolle während der Oligodendrozyten-Reifung im Zebrafisch einnimmt. Letztendlich sind jedoch weitere Studien, wie die Untersuchung von Knockout-Mutanten, unabdingbar, um die vorhandenen Hypothesen zu bestätigen.

Table of contents

Abstract ..... **IX**

Kurzfassung ..... **XI**

Table of contents ..... **XIII**

1 Introduction **1**

1.1 Myelination **2**

1.1.1 Oligodendrogenesis 2

1.1.2 Oligodendrocyte remyelination as therapy of demyelinating disorders 3

1.1.3 The role of G-protein coupled receptors in oligodendrocyte development and myelination 5

1.2 The G-protein coupled receptor 17 ..... **6**

1.2.1 Gpr17 localization 6

1.2.2 Ligand-mediated signaling of Gpr17 7

1.2.3 Role of Gpr17 during oligodendrocyte development 7

1.3 Zebrafish as a model to study myelination *in vivo* **8**

1.3.1 The zebrafish 8

1.3.2 Myelination and remyelination in zebrafish 9

1.3.3 Zebrafish as a model to study myelination and remyelination 11

1.3.4 GPCR's studied in zebrafish 12

1.4 Aims of this study **13**

2 Material **15**

2.1 Cell culture **15**

2.1.1 Mammalian cell lines 15

2.1.2 HEK293 cell culture medium 15

2.1.3 PAC2 cell culture medium 16

2.2 Zebrafish lines **16**

2.3 Zebrafish maintenance **17**

2.3.1 Zebrafish water 17

2.4 Antibodies **18**

2.4.1 Primary antibodies 18

2.4.2 Secondary antibodies 19

2.5 Media, buffers and solutions **19**

2.5.1 Media, buffers, supplements and growth factors 19

2.5.2 Solutions 20
2.6 Water purification 26
2.7 Chemicals 26
2.8 Enzymes 30
2.9 Oligonucleotides 31
2.10 Oligonucleotides for RT-qPCR 31
2.11 Morpholino oligonucleotides 32
2.12 Plasmids 32
2.13 Assay kits 34
2.14 Consumables 35
2.15 Sterilization method 36
2.16 Laboratory instruments and equipment 37
2.17 Software 41
3 Methods 43
3.1 Cell biological methods 43
3.1.1 Passaging cell lines 43
3.1.2 Cryopreservation and thawing of cells 44
3.1.3 Cell counting 44
3.1.4 Transient transfection of recombinant cells with FuGENE HD® 45
3.1.5 Coating cell culture dishes and plates 45
3.2 Cell based assays 46
3.2.1 Dynamic mass redistribution assay 46
3.2.2 Enzyme-linked immunosorbent assay 47
3.2.3 Immunocytochemistry assay 48
3.3 Methods in molecular biology 49
3.3.1 Preparation of LB plates 49
3.3.2 Heat shock transformation 49
3.3.3 Cryopreservation of bacterial strains 49
3.3.4 Preparative isolation of plasmid DNA 49
3.3.5 Determination of nucleic acid concentration by photometrical method 50
3.3.6 Analysis of protein expression by Western blot 50
3.4 Zebrafish maintenance and rearing conditions 52
3.5 Microinjections of zebrafish embryos 52
3.5.1 Morpholino injections 52
3.5.2 RNA injections 53

3.6 Drug treatment of zebrafish 54
3.6.1 Bathing in MDL29,951 54
3.6.2 TSA treatment 54
3.7 Zebrafish based methods 54
3.7.1 Two-photon imaging 54
3.7.2 EnSight™ imaging 55
3.7.3 Whole-mount in situ hybridization 56
3.7.4 Quantitative real time polymerase chain reaction 59
3.7.5 Whole-mount immunohistochemistry 61
3.7.6 Immunohistochemistry of zebrafish sections 62
3.7.7 Western blot analysis 63
4 Results 65
4.1 Functional analysis of zebrafish Gpr17 in HEK293 cells 65
4.1.1 Zebrafish Gpr17 version A is unresponsive to uracil nucleotides and cysteinyl leukotrienes 65
4.1.2 MDL29,951 fails to evoke DMR responses on zebrafish Gpr17 67
4.1.3 Zebrafish Gpr17 receptors display sufficient cell surface expression in HEK293 cells……. 68
4.1.4 No expression of zebrafish Gpr17 in fibroblast zebrafish cell line 70
4.2 Analysis of zebrafish embryos after bath treatment with MDL29,951 72
4.2.1 Differentiation of oligodendrocytes is unaffected by MDL29,951 treatment 72
4.2.2 MDL29,951 treatment does not alter myelin gene transcripts levels 73
4.2.3 Myelination is not impaired after MDL29,951 treatment 74
4.3 Construction and functional analysis of chimeric receptors 76
4.3.1 Chimeric receptors are localized in the cell surface membrane 77
4.3.2 MDL29,951 induces concentration-depended DMR responses at human Gpr17 with intracellular loops of zebrafish receptor 78
4.4 Gpr17 expression in zebrafish 80
4.4.1 Whole-mount in situ hybridization reveals *gpr17* expression during oligodendrocyte development 80
4.4.2 Gpr17 protein is expressed during zebrafish embryogenesis 82
4.5 Role of Gpr17 in zebrafish 84
4.5.1 Transient overexpression of Gpr17 in zebrafish embryos does not affect oligodendrocyte development and myelination 84

4.5.2 *ZfAgpr17* morpholino injections in zebrafish embryos causes reduced oligodendrocyte numbers and an impaired myelination 96

5 Discussion 109

5.1.1 Zebrafish Gpr17 lacks functionality *in vitro* 110

5.1.2 MDL29,951 treatment of zebrafish embryos does not influence myelination *in vivo*…….. 112

5.1.3 Chimeric Gpr17 receptors may represent suitable tools for target validation and drug discovery 114

5.1.4 Gpr17 is expressed in developmental stages of zebrafish CNS 115

5.1.5 The impact of zebrafish Gpr17 on myelination needs to be further explored 117

5.1.6 Conclusion & outlook 121

6 Summary 123

7 Supplementary 125

8 List of abbreviations 129

9 List of figures 133

10 Bibliography 137

Publications 149

Acknowledgments 151

1 Introduction

The central nervous system (CNS) consists of giant cells conducting electrical signals over long distances throughout the body of living beings to innervate their targets. These cells called neurons exhibit large calibre axons that are wrapped in multilamellar insulating myelin sheaths. Through periodic unmyelinated breaks on the neuronal plasma membrane, the nodes of Ranvier, enormous velocities of saltatory conduction between neurons and their targets are achieved (Hartline and Colman, 2007) allowing rapid physiological reactions. The importance of myelination in the CNS is underscored by several destructive neurological disorders such as multiple sclerosis (MS), an inflammatory autoimmune disease caused by myelin sheath breakdown (Compston and Coles, 2008). Moreover, Alzheimer's disease (George Bartzokis, 2011), cerebral palsy (Azzarelli *et al.*, 1996) or schizophrenia (Azzarelli *et al.*, 1996) display abundance of demyelination. Although a range of studies unveiled distinct signalling cascades controlling myelination of axons (Marinelli *et al.*, 2016), the complex molecular mechanism of myelin synthesis remain poorly explored. Thus, there is an urgent need of fundamental research to identify candidate pathways, targets and/or therapeutic molecules that promote myelination when endogenous remyelination fails. While *in vitro* studies help to uncover key molecules or downstream signalling cascades, *in vivo* models such as zebrafish present an ideal system to investigate myelination in its native signalling environment (Preston and Macklin, 2015).

Herein, this thesis aims to establish whether the zebrafish is useful as a model to study a potential target protein *in vivo*, the G-protein coupled receptor 17, which has been reported to modulate the myelination process in a crucial manner.

1.1 Myelination

1.1.1 Oligodendrogenesis

In the vertebrate central nervous system (CNS), specialized glia cells, so called oligodendrocytes, generate axon-wrapping myelin sheaths that promote rapid conduction of action potentials (Pfeiffer, Warrington and Bansal, 1993). During development, oligodendrocytes originate from multipotent neural precursor (NP) cells (or NG2 glia) that give rise to oligodendrocyte precursor cells (OPCs) within a region in the ventral neural tube, the primary motor neuron (pMN) domain (**Figure 1**). Through expression of transcription factors such as Olig2 and Sox10, OPCs proliferate and begin to migrate throughout the CNS (Sun *et al.*, 2006). The onset of terminal differentiation of OPCs into axon-associated, postmitotic pre-oligodendrocytes (pre-OLs) is initiated by the expression of Nkx2.2 transcription factor, while OPCs lacking Nkx2.2 expression remain as slowly dividing, non-myelinating OPCs throughout life (Kucenas, Snell and Appel, 2010). Pre-OLs extend numerous processes wrapping multiple neuronal axons, before finally transition into fully mature oligodendrocytes forming compact multilayer membrane sheaths, the myelin. This process is called myelination and is accompanied by the expression of a variety of terminal markers such as myelin basic protein (Mbp), proteolipid protein (Plp), myelin-associated glycoprotein (Mag) or myelin oligodendrocyte glycoprotein (Mog) (Pfeiffer, Warrington and Bansal, 1993).

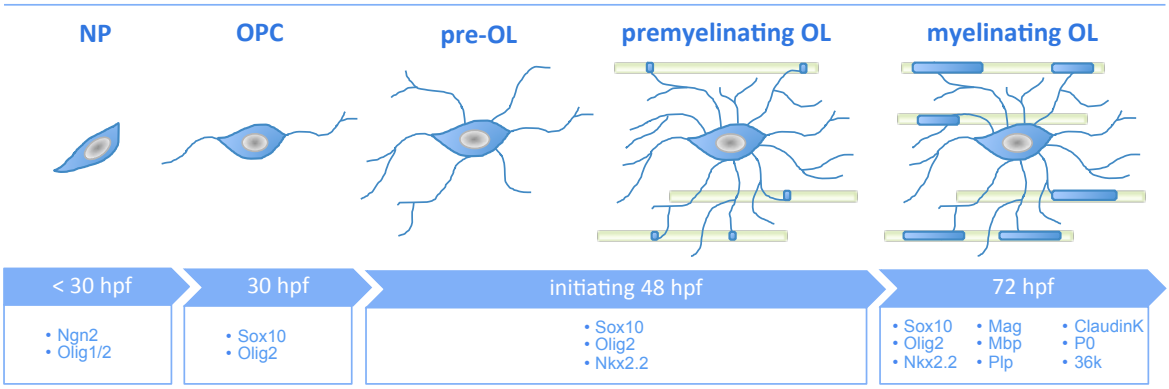

Figure 1: Oligodendrocyte development (Oligodendrogenesis) in zebrafish. Neural precursor (NP) cells give rise to oligodendrocyte precursor cells (OPCs) within the pMN domain of the neural tube. OPCs expressing Olig2 proliferate and start migrating dorsally throughout the developing CNS. The onset of terminal differentiation into pre-oligodendrocytes (pre-OLs) is accompanied by the expression of the transcription factor Nkx2.2. Pre-OLs extent processes that wrap axons, but do not myelinate yet. Finally pre-OLs transition into mature myelin-producing oligodendrocytes (OLs). Shown are lateral images of oligodendrogenesis, complemented with a table presenting the time line and corresponding characteristical markers.

1.1.2 Oligodendrocyte remyelination as therapy of demyelinating disorders

Myelination is a continuous process that does not only occur during developmental stages of the vertebrate system, but also persists until adulthood. Healthy adults display an increase of myelination, peaking in the mid-30s, that declined again beyond the middle age (Lu *et al.*, 2013). Meanwhile, it is known that myelination is not only required for efficient saltatory conduction of action potentials but also contributes to the stability and health of axons. Furthermore, it is assumed that myelination is necessary for higher cognitive function during learning phases both in child and adulthood (Emery, 2010; Nave, 2010). Thereby, adult OPCs remaining in the CNS retain the capability of proliferating and dividing into mature myelinating oligodendrocytes in health and also in disease (Harlow, Honce and Miravalle, 2015).

Loss of myelin during young adulthood, a defining pathological feature of demyelinating disorders such as multiple sclerosis (MS) (Compston and Coles, 2008), can be rescued by endogenous regenerative remyelination through adult OPCs. However, this repair exhibits abnormalities in myelin thickness and fails as the disease progresses (Perier, O. and Gregoire, 1965; van Wijngaarden and Franklin, 2013). Ongoing research has discovered impaired differentiation and maturation of OPCs accounting for demyelination and degeneration of

neurons in demyelinating injuries (Hagemeier, 2012). Hence, the identification of potential remyelinating strategies that promote the survival and maturation of oligodendrocytes could restore neuronal function and prevent clinical disabilities.

Though the repair mechanism is unknown, previous studies reported that established immunomodulatory therapies induce beneficial consequences on remyelination in animal models. However, MS patients treated with immunomodulators still revealed damaged myelin in the progressive phase of the disease (Aharoni and Aharoni, 2016). Promising results were achieved with a monoclonal antibody (Opicinumab) targeted to the Nogo receptor interacting protein-1 (Lingo-1), a protein negatively regulating both oligodendrocyte maturation and myelination. Inhibition of Lingo-1 promotes remyelination *in vitro* and *in vivo* (Mi *et al.*, 2005, 2007; Pepinsky *et al.*, 2011), hence it was evaluated in clinical trials. Although Opicinumab failed in reaching its primary goal in a phase 2 trail, a slight glimmer of hope emerged with a middle dose that seemed to be most beneficial for patients (Mellion *et al.*, 2017). Another recombinant human IgM antibody (rHIgM22) was found to promote oligodendrocyte remyelination. However, the mechanism is unclear since OPC differentiation is inhibited (Stoffels *et al.*, 2013; Watzlawik *et al.*, 2013). Nonetheless, a phase 1 clinical trial with rHIgM22 has been completed and subsequent trials follow (Acorda Therapeutics; PRA Health Sciences, 2015).

Noteworthy, a large number of nuclear (Marinelli *et al.*, 2016) and guanine nucleotide binding protein (G-protein) receptors (Mogha, Rozario and Monk, 2016) have been identified to intervene in oligodendrocyte developmental processes and consequently display therapeutic potential after injury and in myelin disorders.

1.1.3 The role of G-protein coupled receptors in oligodendrocyte development and myelination

The guanine nucleotide binding protein receptors (GPCRs) present the largest membrane receptor family of pharmacological drug targets in the mammalian genome (Bjarnadóttir, 2006). Involved in a variety of physiological events, many distinct diseases such as cardiovascular and neurodegenerative disorders or cancer can be modulated through their selective activation (Neves, Ram and Iyengar, 2002; Howard *et al.*, 2011). Intriguingly, recent studies implicate manifested key roles of GPCRs in PNS and CNS myelinating glia. Thereby, receptors belonging to the rhodopsin, frizzled, adhesion and glutamate families seem to control the development of myelinating cells in distinct manners and at different developmental time points (Mogha, Rozario and Monk, 2016) (**Figure 2**).

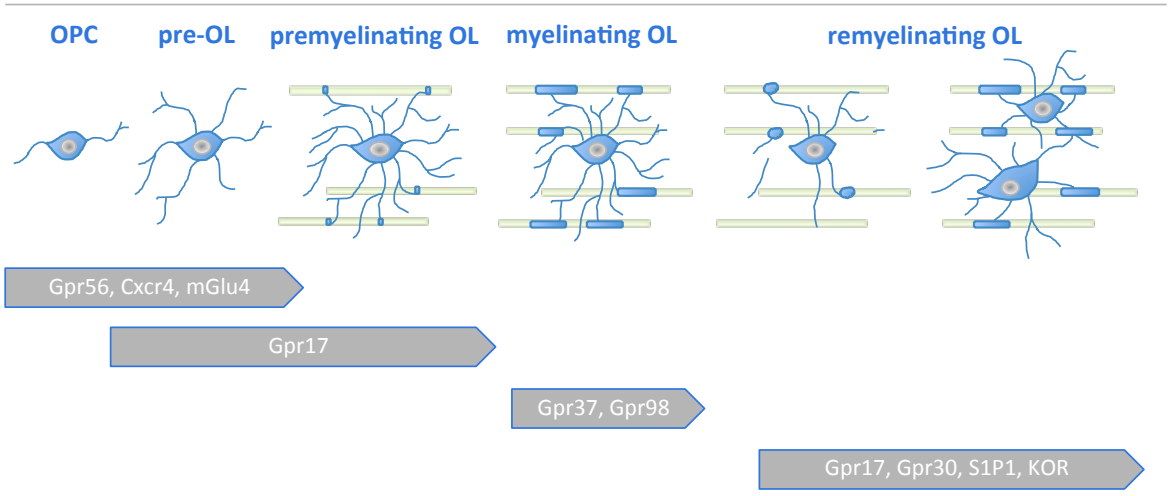

Figure 2: Expression of GPCRs during oligodendrocyte development. G-protein coupled receptors are known to regulate oligodendrogenesis in different developmental stages. Ongoing research revealed a handful GPCRs (Gpr17, Gpr30, S1P1, KOR) that might pose potential therapeutic targets for forcing remyelination when endogenous myelination fails. Modified from (Mogha, Rozario and Monk, 2016).

For instance, the adhesion Gpr56/Adgrg1, expressed in early stages during oligodendrocyte development, was reported as a crucial regulator of OPC proliferation and differentiation. Previous work in zebrafish and mice showed that depletion of Gpr56 produces hypomyelination resulting from decreased OPC proliferation (Ackerman *et al.*, 2015; Giera *et al.*, 2015). A further study in mice has shed light in how Gpr37, a rhodopsin family GPCR affects late-stage

oligodendrocyte development. Expressed and maintained in mature oligodendrocytes, absence of Gpr37 leads to precocious oligodendrocyte differentiation, entailing hypermyelination that persisted until adult stages (Yang *et al.*, 2016). Last but not least, a third GPCR, Gpr17, expressed in pre-mature stages of oligodendrocyte development and abundant in demyelination pathologies, will be portrayed more extensively in the next chapter (1.2).

Noteworthy, further GPCRs such as Gpr30, CxCr4, S1P1 and KOR were found to intervene in CNS remyelination, underscoring once more the potential of this receptor family as potential targets in injury and disease (Mogha, Rozario and Monk, 2016).

1.2 The G-protein coupled receptor 17

Gpr17 is a member of the superfamily of the rhodopsin-like, seven transmembrane (7TM) G-protein coupled receptors (Raport *et al.*, 1996). It is also called P2Y-like receptor, since it is phylogenetically located between P2Y purinergic and cysteinyl leukotriene receptors (CysLTRs) (Ciana, Fumagalli, L. Trincavelli, *et al.*, 2006).

1.2.1 Gpr17 localization

Two isoforms, a long form (Gpr17-L, 369 amino acids) that is present in heart and kidney and a short form (Gpr17-S, 339 amino acids) that adopts a role in brain and spinal cord were analysed by Benned-Jensen and Rosenkilde (2010). In the CNS, short form Gpr17 is mainly expressed in OPCs and pre-OLs and disappears when cells achieve functional maturation (Chen *et al.*, 2009) (**Figure 2**). While additionally expressed in ependymal cells, lining ventricle cavities (Marucci *et al.*, 2016), the occurrence of Gpr17 in neurons still remains controversial (Maisel *et al.*, 2007; Lecca *et al.*, 2008; Chen *et al.*, 2009). Due to this expression pattern, Gpr17 is assumed to be a regulator of the pre-mature stage during oligodendrogenesis (Ciana, Fumagalli, L. Trincavelli, *et al.*, 2006; Fumagalli *et al.*, 2011).

Besides its expression during oligodendrocyte development, Gpr17 was found to be upregulated under pathological conditions, such as traumatic brain injury or stroke (Lecca *et al.*, 2008; Ceruti *et al.*, 2009; Zhao *et al.*, 2012). Moreover, it was shown that experimental autoimmune encephalomyelitis (EAE) mouse models display abundance of Gpr17 in demyelinating regions (Fumagalli *et al.*, 2015). Similar observations were reported by Ou *et al.* (2016), additionally demonstrating that loss of Gpr17 in mice leads to an earlier onset of remyelination after lysolecitihin-induced demyelination. Last but not least, human white matter plaques of multiple

sclerosis patients exhibit high expression levels of Gpr17, suggesting that therapeutic inhibition of the receptor might foster remyelination (Chen *et al.*, 2009).

1.2.2 Ligand-mediated signaling of Gpr17

In search of the endogenous agonist, Ciana *et a*l. (2006) introduced uracil nucleotides and cysteinyl leukotrienes as activators of Gpr17. However, several independent laboratories failed to completely recapitulate the original deorphaning report (Bläsius *et al.*, 1998; Heise *et al.*, 2000; Benned-Jensen and Rosenkilde, 2010; Hennen *et al.*, 2013b; Qi *et al.*, 2013; Simon *et al.*, 2017), wherefore Gpr17 must still be considered as orphan. Conversely, a small synthetic molecule, MDL29,951 (2-carboxy-4,6-dichloro-1H-indole-3-propionic acid), was identified as a selective activator of Gpr17 in heterologous expression systems and primary oligodendrocytes (Hennen *et al.*, 2013b). So far, MDL29,951 is the only credible activator of Gpr17, thus this ligand provides the opportunity to further investigate the role of Gpr17 during oligodendrocyte development.

In addition, three different antagonists of uracil nucleotide (cangrelor) and cysteinyl leukotriene receptors (pranlukast, montelukast) were proposed to inhibit LTD4 and UDP-glc activated Gpr17 (Ciana, Fumagalli, M. L. Trincavelli, *et al.*, 2006). Here again, receptor inhibition was only reproducible for pranlukast (Hennen *et al.*, 2013).

1.2.3 Role of Gpr17 during oligodendrocyte development

Since high expression of Gpr17 was found in oligodendrocyte lineages cells, researchers aimed to investigate the role of Gpr17 during oligodendrogenesis. Studies in mice revealed that receptor loss induces an early onset of oligodendrocyte maturation, while overexpression results in impaired oligodendrocyte differentiation and myelination (Chen *et al.*, 2009). These results were supported by further studies with primary rat oligodendrocytes, that demonstrated decreased Mbp expression levels upon receptor activation, mainly mediated through the $G\alpha_{i/o}$ pathway (Simon *et al.*, 2016). Furthermore, it has been shown that Gpr17 desensitization leads to terminal differentiation of OPCs (Daniele *et al.*, 2014). However, findings obtained by other research groups implicate opposing results, whereby Gpr17 activation through postulated endogenous ligands resulted in promoted OPC maturation and myelination, while receptor inhibition by antagonists as well as specific silencing RNAs caused opposite effects (Ceruti *et al.*, 2009; Fumagalli *et al.*, 2011). Contradicting their own findings, some years later, the same research group presented Gpr17, overexpressed in cultured OPCs, as an inhibitor of oligodendrocyte maturation (Fumagalli *et al.*, 2015).

1.3 Zebrafish as a model to study myelination *in vivo*

In scientific research, cell cultures or tissue samples are extremely useful in providing initial approaches for probing human diseases and discovering new human drugs. However, to ascertain whether patient's symptoms are caused by genetic alternations or alleviated by therapeutical compounds, the use of *in vivo* model organisms is still the gold standard. Likewise, for the identification of pathways and key molecules that control developmental processes, an analysis in a native *in vivo* environment is superior to *in vitro* systems.

In the field of myelination, rodents display the preferred animal models since over 90 % of their genes can be aligned with the human genome (Waterston *et al.*, 2002). However, long rearing periods and low-throughput evince limitations of this model organism (Cole *et al.*, 2017). Nevertheless, during the last couple of decades, a smaller vertebrate animal, the zebrafish, has emerged as powerful model system to study myelination and remyelination *in vivo* (Driever *et al.*, 1994; Buckley, Goldsmith and Franklin, 2008; Ackerman and Monk, 2015; Preston and Macklin, 2015).

1.3.1 The zebrafish

At the first sight the zebrafish (Danio rerio), a small freshwater teleost native to South-East Asia (Kari, Rodeck and Dicker, 2007), seems to have not much in common with humans, but its remarkable genome homology over 70% with mammals made it a very useful vertebrate genetic model organism to study key developmental processes, investigate human diseases or conduct pharmacological drug screenings (Langheinrich, 2003; Howe *et al.*, 2013). One of its unique advantages includes the short life circle accompanied by a rapid ex utero development that can be perused by distinct non-invasive imaging methods. The ability to follow developmental processes in a live intact organism is further supported by the optical clarity of the embryos. Within 5 days, a zebrafish develops from a fertilized egg to a fish exhibiting most of the mammalian organs (**Figure 3**) (Kari, Rodeck and Dicker, 2007). The ability of zebrafish to produce every two to three days large clutch sizes with hundreds of individuals, already at the age of three months, displays a feature that facilitates genetic analysis, since research depends on fast and reproducible replication (Driever *et al.*, 1994). Noteworthy, low costs and less space for maintenance makes this animal especially attractive in the scientific community (Goldsmith and Solari, 2003).

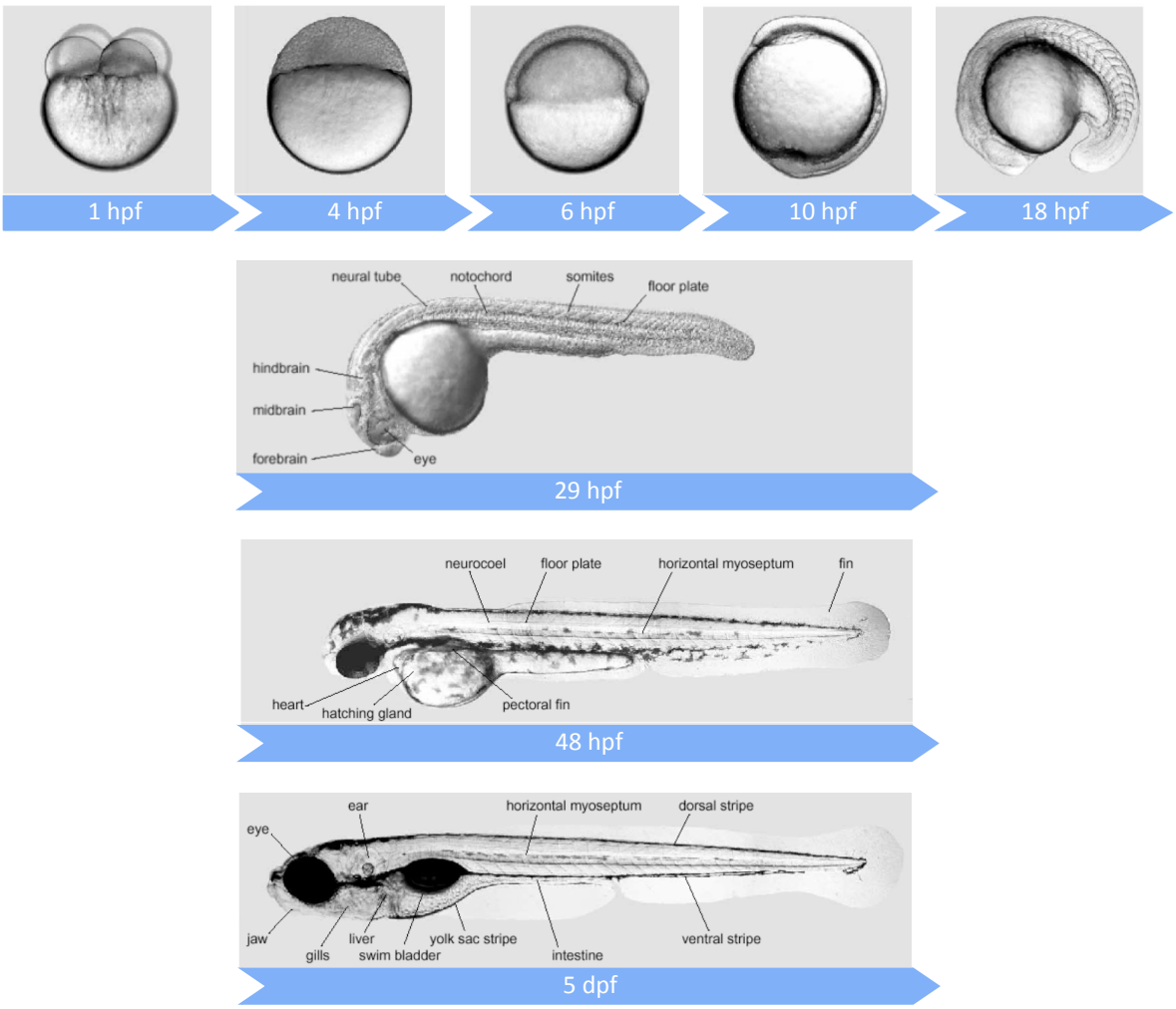

Figure 3: Development of zebrafish during the first 5 days post fertilization (dpf). hpf = hours post fertilization. Modified from (Haffter *et al.*, 1996)

1.3.2 Myelination and remyelination in zebrafish

Studies with zebrafish established that oligodendrocyte development and myelination is conserved from fish to mammals (Raphael and Talbot, 2011). Expression of transcription factors such as Olig1 and Olig2, Sox10 and Nkx2.2. is identical across species (Monk and Talbot, 2009; Kucenas, Snell and Appel, 2010) and although there is some variation in expression pattern compared to mammals, homologs for myelin proteins such as myelin basic protein (Mbp) (Nawaz *et al.*, 2013), proteolipid protein (Plp/DM20) (Schweitzer *et al.*, 2006) and myelin protein zero (P0) (Bai *et al.*, 2011) are present in zebrafish. Besides the major proteins, several novel myelin membrane-associated proteins like Zwilling-A and -B (Schaefer and Brosamle, 2009) and Claudin K (Münzel *et al.*, 2012) have been identified, although their roles in mammalian myelination still

remain unknown. Another interesting protein, the short-chain dehydrogenase/reductase protein 36k was also found to be highly expressed in oligodendrocytes in the CNS of teleosts, while it is missing in rodents (Morris *et al.*, 2004). However, Morris *et al.* (2004) determined a human homolog (FLJ13639) that is abundant in oligodendrocytes and neurons of the adult human brain. Probably, the presence of these newly discovered proteins implicates an evolutionary adaption of the aquatic vertebrate zebrafish (Buckley, Goldsmith and Franklin, 2008). Since the initiation of developmental and myelinating processes occurs earlier in zebrafish, at 3 dpf (Brösamle and Halpern, 2002) compared to mice exhibiting myelination at P6 (Foran and Peterson, 1992), the zebrafish represents an ideal model to follow myelination in real-time in its native environment.

In comparison to mammals, zebrafish exhibit the unique ability to regenerate injured axons by continuous endogenous remyelination (Becker and Becker, 2008; Ohnmacht *et al.*, 2016). Goldsmith *et al.* (2012) assumed that efficient axon regeneration capability is likely to be present because of lacking glial scar formation. Since major reasons remain speculative at the time, further studies with zebrafish may help to elucidate pathways or tractable key molecules that are necessary for successful and continuous OPC differentiation, thus following remyelination in health and disease.

1.3.3 Zebrafish as a model to study myelination and remyelination

During the last decades a wide variety of different techniques for studying myelination and remyelination in zebrafish have been created. One big strength was the generation of transgenic zebrafish reporter lines that express exogenous proteins under control of cell or subcellular structure specific regulatory DNA. Meanwhile, hundreds of different lines, expressing fluorescent proteins in distinct cell types are available (Preston and Macklin, 2015). Beside others, reporter lines such as tg(*olig2*:EGFP) (Shin *et al.*, 2003), tg(*claudinK*:Gal4;UAS:mGfp) (Münzel *et al.*, 2012), tg(*plp*:EGFP) (Yoshida and Macklin, 2005) or tg(*mbp*:EGFP) (Jung *et al.*, 2009) label oligodendrocyte lineage cells or myelin sheaths and provide the opportunity to gain profound insights in OPC generation, migration and myelination in the spinal cord. Furthermore, expression of specific proteins can be easily obtained by microinjections of either capped mRNA or plasmids into the one- or two-cell stage of zebrafish embryos, leading to an expression throughout the whole animal, unless the injected nucleic acids contain tissue specific promoters (Kari, Rodeck and Dicker, 2007). In doing so, zebrafish can also be humanised with genes involved in human diseases (Goldsmith, 2004). On the contrary, Zink Fingers (Urnov *et al.*, 2010), TALEN's (Campbell *et al.*, 2012) or more current CRISPR (Blackburn *et al.*, 2013) methodologies display the opportunity to generate knockout zebrafish. A timesaving alternative to knockout animals offers the morpholino antisense oligonucleotides mediated gene knockdown, which impairs the translation machinery by hybridizing to translation-initiating or splicing donor sites of specific mRNAs. However, this method provides no guaranty for a transient protein disruption, wherefore it has to be demonstrated by rescue experiments (Corey and Abrams, 2001; Zon and Peterson, 2005).

Besides genetic screening, zebrafish are well suited as a pharmacological tool for small-molecule drug discovery (Langheinrich, 2003; Goldsmith, 2004; Kari, Rodeck and Dicker, 2007). As producing high numbers of offspring, they provide a rapid and low cost high-throughput screening model. Drugs can be easily administered by bath treatment. From 1 to 3 dpf, embryos are able to absorb substances across the skin, while after 3 dpf the oral route dominates (Goldsmith, 2004). At this, compounds have to overcome the blood brain barrier that allows the transition of molecules smaller than 1000 kD (Joeng *et al.*, 2008). In case of large molecule drugs, microinjection of embryos display an alternative drug administration (Goldsmith, 2004). After treatment, several methods such as fluorescent and electron microscopy, quantitative polymerase chain reaction (qPCR), Whole-mount in situ hybridization (WISH) or immunohistochemistry (IHC) assays can be performed to examine potential effects (Pruvot *et al.*, 2014; Guo *et al.*, 2015). Until now a few chemical-screening studies have been published. For

instance, Buckley *et al.* (2010) generated a robust screening platform and identified several compounds with pro-myelinating features. Recently it has been shown that treatment of zebrafish larvae with the antihistaminic drug clemistine rescued hypomyelination in mct8 mutants that display a key symptom of Allan-Herndon-Dudly syndrome (ADHS) (Zada *et al.*, 2016). Noteworthy, Kulkarni *et al.*, (2017) developed an adult EAE zebrafish model as a quick *in vivo* screening system that serves for the identification of premyelinating drugs.

1.3.4 GPCR's studied in zebrafish

Since researchers discovered that G-protein coupled receptors intervene in the myelination process (Mogha, Rozario and Monk, 2016), a zebrafish myelination screen identified the orphan Gpr126/Adgrg6 as a crucial regulator of Schwann cells differentiation in the PNS. It was shown that absence of Gpr126 restrains Schwann cells in its premyelinating stage (Monk *et al.*, 2009, 2011). Meanwhile, two different working groups postulated type IV collagen (Paavola *et al.*, 2014) as well as Laminin-211 (Petersen *et al.*, 2015) as activators of Gpr126 by means of zebrafish animal models. Another GPCR, Gpr56, enriched in oligodendrocyte lineage cells, was found to be a key regulator of oligodendrocyte development in the central nervous system (Giera *et al.*, 2015). Ongoing studies in zebrafish, uncovered $G\alpha_{12/13}$-Rho signalling as key pathway for Gpr56 dependent OPC proliferation (Ackerman *et al.*, 2015). These studies further demonstrate the strength of the zebrafish model system to investigate key regulators and pathways controlling myelination *in vivo*.

1.4 Aims of this study

Since the orphan G-protein coupled receptor Gpr17 was first characterized by Raport *et al.* in 1996, several working groups have made great efforts in order to prove that this receptor is, inter alia, a crucial regulator of oligodendrocyte development in health and disease (Lecca *et al.*, 2008; Ceruti *et al.*, 2009; Chen *et al.*, 2009b; Fumagalli *et al.*, 2011; Coppi *et al.*, 2013; Hennen *et al.*, 2013b; Schneider *et al.*, 2016; Simon *et al.*, 2016; Seyedsadr and Ineichen, 2017). However, discrepancies between published literature query Gpr17 agonist and antagonist profiles as well as its function in demyelinating pathologies (Marucci *et al.*, 2016). Thus, further studies are necessary to clarify its role and discover new therapeutic compounds with activity on human Gpr17. Herein, this thesis scrutinize whether the zebrafish (Danio rerio) is a suitable animal model, not only in terms to confirm receptor's role in myelination but also in relation of presenting an *in vivo* screening platform for new ligands of human Gpr17 as modulators of CNS remyelination.

The first element of this work intends to verify activity of zebrafish Gpr17 upon expression in mammalian cells towards the postulated ligands (Ciana, Fumagalli, M. L. Trincavelli, *et al.*, 2006), and the small-molecule agonist MDL29,951 (Hennen *et al.*, 2013b) by label-free Dynamic mass redistribution (DMR) technology. At this, two variants of zebrafish Gpr17, zfAGpr17 and zfBGpr17 sharing an AA-identity of 56 and 44 % with the human Gpr17 (Kleinert, 2018) are examined with a special focus on zfA. To further investigate zebrafish Gpr17 in its native environment, zebrafish embryos are bath exposed to MDL29,951 and screened for alterations in oligodendrocyte development and myelination. Additionally, chimeric receptors containing the ligand binding domain of human Gpr17 and the intracellular loops of zebrafish Gpr17 are constructed and evaluated in functional DMR assays as potential tools for an *in vivo* zebrafish screening platform.

The second part of the thesis focuses on Gpr17 expression and role in the zebrafish itself. To this end, expression pattern will be analysed by Whole-mount in situ hybridization (WISH) and Western blot analysis. Finally, genetic manipulation of transgenic zebrafish lines such as tg(*olig2*:EGFP) and tg(*claudinK*:EGFP) through receptor overexpression and morpholino antisense oligonucleotide mediated gene knockdown sheds light on Gpr17 function *in vivo*.

2 Material

2.1 Cell culture

2.1.1 Mammalian cell lines

Table 1. Cell lines

Name	Biological source	Producer/Owner
HEK293	Human embryonic kidney	Research group of Prof. Dr. Evi Kostenis, Institute of Pharmaceutical Biology, University of Bonn, Germany
PAC2 fibroblasts	Zebrafish	Research group of Prof. Dr. Nicholas Foulkes, Karlsruhe Institute of Technology (KIT), Germany

2.1.2 HEK293 cell culture medium

Table 2. HEK293 cell medium

Constituent	Volume (mL)	Final concentration
Dulbecco's Modified Ea- gle Medium (DMEM)	500	
Fetal calf serum (FCS)	50	≈10 %
Penicillin-Streptomycin	5	≈100 U/mL Penicillin, 0.1 mg/mL Streptomycin

2.1.3 PAC2 cell culture medium

Table 3. PAC2 cell medium

Constituent	Volume (mL)	Final concentration
Leibovitz's L15 Medium	500	
Fetal bovine serum (FBS)	75	≈15 %
Penicillin-Streptomycin	5	≈100 U/mL Penicillin, 0.1 mg/mL Streptomycin
Gentamicin	0.5	0.05 mg/mL

2.2 Zebrafish lines

Table 4. Zebrafish lines

Name	Producer/Owner
Tg(*cldnk*:GAL4, UAS:EGFP)	Münzel et al., 2012
Tg(*olig2*:EGFP)	Shin et al., 2003
TU (wild type)	Item #1173 European Zebrafish Resource Center, Karlsruhe, Institute for technology
TL (wild type)	Item #1174 European Zebrafish Resource Center, Karlsruhe, Institute for technology

2.3 Zebrafish maintenance

2.3.1 Zebrafish water

Table 5. Danieau 300%

Constituent	Volume (mL)	Concentration (M)	Final concentration (mM)
NaCl	60	2.9	174
KCl	30	0.07	2.1
$MgSO_4x7H_2O$	30	0.04	1.2
$Ca(NO_3)_2$	30	0.06	1.8
HEPES	30	0.5	15
MilliQ water	820	-	-

Table 6. Danieau 30 %

Constituent	Volume (L)
Danieau 300 %	1
MilliQ water	9

Table 7. Danieau 30 % with Methylenblue

Constituent	Volume (mL)	Final concentration
Methylenblue 500x	2	10^{-5} %
Danieau 30 %	998	

Table 8. Danieau 30 % with PTU

Constituent	Volume (mL)	Final concentration
N-Phenylthiourea 50x	20	0.003 %
Danieau 30 %	980	

2.4 Antibodies

2.4.1 Primary antibodies

Table 9. Primary antibodies

Antibody	Species	Product number	Company
Anti-36k (flj13639)	rabbit	QPE0580	Thermo Fisher Scientific
Anti-β-actin-HRP	mouse	A3854	Sigma-Aldrich
Anti-ClaudinK	rabbit	QPE0581	Thermo Fisher Scientific
Anti-Cleaved Caspase3	rabbit	9579	Cell Signaling Technology
Anti-Digoxigenin-AP	sheep	11093274910	Roche
Anti-EGFP	mouse	JL8-632381	Takara Clontech
Anti-HA	mouse	11583816001	Roche
Anti-MbpA	guinea pig	QOJ1724	Thermo Fisher Scientific
Anti-P0	rabbit	QOJ1722	Thermo Fisher Scientific
Anti-zfAGpr17	chicken	QOJ1726	Thermo Fisher Scientific
Anti-zfBGpr17	rabbit	QoJ1723	Thermo Fisher Scientific

2.4.2 Secondary antibodies

Table 10. Secondary antibodies

Antibody	Species	Product number	Company
Anti-chicken-HRP	goat	ab97150	Abcam
Anti-guinea pig-AlexaFlour546	goat	A-11074	Molecular Probes
Anti-mouse-HRP	goat	115-035-003	Jackson Immuno Research
Anti-mouse-HRP	goat	A4416	Sigma-Aldrich
Anti-rabbit-HRP	goat	111-035-144	Jackson Immuno Research
Anti-mouse-Cy2	goat	AP124J	Millipore

2.5 Media, buffers and solutions

2.5.1 Media, buffers, supplements and growth factors

Table 11. Media, buffers, supplements and growth factors

Name	Product number	Company
Ampicillin-Natrium	10835242001	Roche
CutSmart® 10x	B72049	New England Biolabs®
Dulbecco's Modified Eagle Medium (DMEM)	41965	Thermo Fisher Scientific
DPBS 1x	14190-094	Gibco by life technologies™
Fetal calf serum (FCS)	P30-3702	PANTM Biotech GmbH
Fetal bovine serum (FBS)	F7524	Sigma-Aldrich
Hank's balanced salt solution (HBSS)	14025050	Thermo Fisher Scientific

Leibovitz's L15 Medium	11415064	Thermo Fisher Scientific
Normal Goat Serum	G9023	Sigma-Aldrich
Nuclease-free water	129144	Qiagen
Opti-MEM	1616013	Thermo Fisher Scientific
Penicillin-Streptomycin solution	15140122	Thermo Fisher Scientific
Pierce Ripa Buffer	89900	Thermo Fisher Scientific
Sheep Serum	S2263	Sigma-Aldrich
SSC buffer 20x	15557-044	Gibco by life technologies™
T4 DNA Ligase buffer 10x	EL0011	Thermo Fisher Scientific
Trypsin-EDTA (0.05 %)	25300054	Thermo Fisher Scientific

2.5.2 Solutions

Solution 1. 1 M HEPES

Component	Total amount	Final concentration
HEPES	23.8 g	1 M
NaOH	q.s.	pH 7.2-7.4
dH_2O	ad 100 mL	

After adjusting the pH to 7.2-7.4 with NaOH, solution was sterilized by sterile filtration and stored at - 20 °C.

Solution 2. ELISA Blocking buffer

Component	Total amount	Final concentration
Dry milk	3 g	3 %
Tris-HCl 1 M, pH 7.4-7.8	5 mL	50 mM
MilliQ water	ad 100 mL	

Solution 3. ICC Blocking buffer

Component	Total amount	Final concentration
Normal goat serum	5 mL	10 %
Bovine serum albumin	0.5 mL	1 %
MilliQ water	ad 50 mL	

Solution 4. WB Lysis buffer

Component	Volume (mL)	Final concentration
Tris 1 M, pH 7.4	1.5	25 mM
NaCl 5 M	1.8	150 mM
EDTA 0.5 M	0.12	1 mM
TritonX100	0.6	1 %
IGEPAL®	0.6	1 %
MilliQ water	ad 60	

1.5 mL aliquots were prepared and stored at - 20°C.

Solution 5. WB Washing buffer

Component	Volume (mL)	Final concentration
Tween20	1	0.1 %
PBS	1000	

Solution 6. PBST

Component	Total amount	Final concentration
Tween20 20 %	25 µL	0.1 %
DPBS 1x	ad 500 mL	

Solution 7. 4 % paraformaldehyde (PFA)

Component	Total amount	Final concentration
Paraformaldehyde	4 g	4 %
Citric acid monohydrate	q.s.	pH 7.3
DPBS 1x	ad 100 mL	

After regulation of the pH to 7.2-7.4 with citric acid, the solution was sterilized by sterile filtration and 10 mL aliquots were stored at - 20 °C.

Solution 8. Buffer I Dot blot

Component	Volume (mL)	Final concentration
Tris-HCl 1 M pH 7.5	20	100 mM
NaCl 5 M	6	150 mM
DEPC water	ad 200	

Solution 9. Buffer II Dot blot

Component	Volume (mL)	Final concentration
Tritron^{TM}X-100	0.05	0.1 %
DPBS 1x	ad 50	

Solution 10. Buffer III Dot blot

Component	Volume (mL)	Final concentration
Tris-HCl 1 M pH 9.5	5	100 mM
NaCl 5 M	1	100 mM
$MgCl_2$ 1 M	2.5	50 mM
Tween20 20 %	0.25	0.1 %
DEPC water	ad 50	

Solution 11. WISH Hybridization buffer (HM) for probe

Component	Volume (mL)	Final concentration
Formamide	25	50 %
SSC 20x	12.5	SSC 5x
Heparin 5 mg/mL	0.5	50 µg/mL
tRNA 10 mg/mL	2.5	500 µg/mL
Tween20 20 %	0.5	0.2 %
Acide citrique 1 M	q.s	pH 6
DEPC water	ad 50	

Solution 12. WISH Hybridization buffer (HM wo) for washing steps

Component	Volume (mL)	Final concentration
Formamide	25	50 %
SSC 20x	12.5	SSC 5x
Tween20 20 %	0.25	0.1 %
Acide citrique 1 M	q.s	pH 6
DEPC water	ad 50	

Solution 13. WISH Alkaline tris buffer

Component	Volume (mL)	Final concentration
Tris-HCl 1 M pH 9.5	5	100 mM
NaCl 5 M	1	100 mM
$MgCl_2$ 1 M	2.5	50 mM
Tween20 20 %	0.25	0.1 %
DEPC water	ad 50	

Solution 14. WISH NBT/BCIP labelling solution

Component	Volume (mL)
NBT (Nitro Blue Tetrazolium)	0.0225
BCIP (5-Bromo 4-Chloro 3-indolyl Phosphate)	0.175
Alkaline tris buffer	ad 50

Solution 15. IHC Tris buffer

Component	Total amount	Final concentration
Tris Base	1.8171 g	150 mM
HCl	q.s.	pH 9
DEPC water	ad 100 mL	

Solution 16. IHC Sodium phosphate buffer

Component	Total amount	Final concentration
NaH_2PO_4	3.1 g	100 mM
Na_2HPO_4	10.9 g	100 mM
DEPC water	ad 1000 mL	

The buffer can be stored up to one month at 4 °C.

Solution 17. IHC PBTx

Component	Total amount	Final concentration
TritonX100	800 µL	0.8 %
100 mM IHC sodium phosphate buffer	ad 100 mL	

Solution 18. IHC NGS/BSA/PBTx blocking solution

Component	Total amount	Final concentration
Normal goat serum	1 mL	10 %
Bovine serum albumin	0.2 g	2 %
IHC PBTx	ad 10 mL	

Solution 19: IHC NGS/BSA/PBTx antibody blocking solution

Component	Total amount	Final concentration
Normal goat serum	200 µL	2 %
Bovine serum albumin	0.2 g	2 %
IHC PBTx	ad 10 mL	

2.6 Water purification

Purified water was generated by the MilliQ-Water system (AG Kostenis) and the Reverse Osmosis Mobil Filtration System MobilRO16 (AG Odermatt) and used for all for media and solutions.

2.7 Chemicals

Table 12. Chemicals

Substance	Product number	Company
Agarose Type IX-A, Ultra-low Gelling Temperature	A2576	Sigma-Aldrich
LE Agarose	840004	Biozym
Albumin Fraction V (pH 7.0) for western blotting	A1391	PanReac Applichem
Ampuwa, water for injections	40676.00.00	Fresenius Kabi Deutschland
BCIP/NBT	S3771	Promega
Blotting-Grade Blocker, Dry milk for western blotting applications	1706404	Bio-Rad Laboratories
Carbachol	212385	Merck
Citric acid monohydrate	100244	Merck
Complete Tablets Easypack Protease Inhibitor	046931166001	Roche

DEPC water	T143.3	Roth
DMSO	A1584	PanReac Applichem
DNA Loading Dye 6x	R0611	Thermo Fisher Scientific
dNTP Set, 100 mM Solutions	R0182	Thermo Fisher Scientific
EDTA-disodium	39760.01	Serva
Ethanol absolute	A1613	PanReac Applichem
Ethidiumbromide 1 %	46067	Sigma-Aldrich
Ethyl 3-aminobenzoate methansesulfonate salt (MS222)	A5040	Fluka Analytical
NorthernMax®Formaldehyde Load Dye	AM8552	Thermo Fisher Scientific
Formamide	47671	Sigma Life Science
FuGENE HD® Transfection Reagent	E2312	Promega
GeneRuler 1 kb DNA Ladder	SM0311	Thermo Fisher Scientific
GeneRuler 100 bp Plus DNA Ladder	SM0321	Thermo Fisher Scientific
Glycerol	104093	Merck
Heparin Sodium Salt from porcine intestinal mucosa	H3393	Sigma-Aldrich
HEPES (4-(2-hydroxyethyl)-1-piperazineethanesulfonic acid)	54457	Fluka
Hydrochloric acid 37 %	9057	Merck
IGEPAL®	CA-630	Sigma-Aldrich
Kaleidoscope Prestained Standard	161-0324	Bio-Rad Laboratories

MagicMark™ XP Western Protein Standards	LC5602	Invitrogen
Magnesium chloride hexahydrate	A4425	PanReac Applichem
MDL29,951	SEWO6645SC	Maybridge
Methanol	131091.1212	PanReac Applichem
Mineral Oil	M5904	Sigma-Aldrich
Mowiol	81381	Sigma-Aldrich
Normal Goat Serum	G9023	Sigma-Aldrich
NuPAGE® Antioxidant	NP0005	Novex™ by Life Technologies
NuPAGE® LDS Sample Buffer 4x	NP0007	Novex™ by Life Technologies
NuPAGE® MOPS SDS Running Buffer 20x	NP0001	Novex™ by Life Technologies
NuPAGE™ Novex™ 10 % Bis-Tris Protein Gels, 1.5 mm, 10-well	NP0315Box	Novex™ by Life Technologies
NuPAGE® Sample Reducing Agent 10x	NP0009	Novex™ by Life Technologies
NuPAGE® Transfer Buffer 20x	NP000P-6	Novex™ by Life Technologies
Paraformaldehyde	158127	Sigma-Aldrich
Pierce™ Comassie Plus (Bradford)	23236	Thermo Fisher Scientific
Phenol red solution	P0290	Sigma-Aldrich
N-Phenylthiourea	P7629	Sigma-Aldrich
Poly-D-lysine hydrobromide (PDL)	P6407	Sigma-Aldrich
N-Propylgallate	P3130	Sigma-Aldrich

Protease inhibitor cocktail	P8340	Sigma-Aldrich
Protease from Streptomyces griseus Type XIV	P5147	Sigma-Aldrich
Proteinase K	A3830	PanReac Applichem
Ribonucleic acid from torula yeast Type VI	R6625	Sigma-Aldrich
Roti®-Block	A151.2	Roth
Sodium actetate anhydrous	6268	Merck
Sodium chloride	A2942	PanReac Applichem
Sodium dihydrogen phosphate, anhydrous	71640	Fluka
Sodium hydrogen phosphate	131679.1211	PanReac Applichem
Sulfuric acid	109073	Merck
3,3',5,'- Tetramethylbenzidine Liquid substrate system (TMB)	T8665	Promega
TRIS PUFFERAN® ≥99,9 % Ultra Qualität	5429.3	Roth
Tritron™X-100	X100	Sigma-Aldrich
TRIzol Regent	T9424	Ambion by life technologies™
Tween20	P9416	Sigma-Aldrich
UltraPureTM Distilled water	10977035	Thermo Fisher Scientific

2.8 Enzymes

Table 13. Enzymes

Enzyme	Product number	Company
DreamTaq® DNA Polymerase	EP0701	Thermo Fisher Scientific
EcoRI-HF	R3101S	New England Biolabs®
FastAP Thermosensitive Alkaline Phosphatase	EF0651	Thermo Fisher Scientific
HindIII	R0104S	New England Biolabs®
iScript™ Reverse Transcription Supermix for RT- qPCR	170-8841	Bio-Rad Laboratories
KpnI-HF	R3142S	New England Biolabs®
MfeI	R3589S	New England Biolabs®
Phusion® High-Fidelity DNA Polymerase	F-534S	Thermo Fisher Scientific
SacI-HF	R3156S	New England Biolabs®
SpeI-HF	R3133S	New England Biolabs®
T4 DNA Ligase	EL0011	Thermo Fisher Scientific
XhoI	R0146S	New England Biolabs®

2.9 Oligonucleotides

2.10 Oligonucleotides for RT-qPCR

Table 14. Oligonucleotides for RT-qPCR from Sigma Aldrich

Name	Sequence 5'-3'	ZFIN ID
actin_forward	GCCAACAGAGAGAAGATG	ZDB-GENE-000329-1
actin_reverse	GCGTAACCCTCATAGATG	
actin_reverse_probe	[6FAM]ACCATCACCAGAGTCCATCACAAT[BHQ1]	
ef1a_forward	GGAGTGATCTCTCAATCTTG	ZDB-GENE-990415-52
ef1a_reverse	CTTCCTTCTCGAACTTCTC	
ef1a_reverse_probe	[6FAM]TCTCTTGTCGATTCCACCGCA[BHQ1]	
mbp_forward	CTGGGCAGAAAGAAGAAG	ZDB-GENE-030128-2
mbp_reverse	GATGACCACGAAATGAAC	
mbp_forward_probe	[HEX]CTCCTCCGAAGAACCTGCTGAT[BHQ1]	
plp_forward	CAGGAATCACCCTTCTTG	ZDB-GENE-030710-6
plp_reverse	GAACCTAGCAACGGATTC	
plp_forward_probe	[HEX]CCACCACCTACAACTACGCTATTCT [BHQ1]	

2.11 Morpholino oligonucleotides

Table 15. Morpholino oligonucleotides from Gene Tools, LLC

Name	Sequence 5'-3'	Concentration
zfAgpr17 MO	GTTCTGTCAAGGAGGACTCCATTT	2.54 mg (300 nmol), M=8465
Control MO	CCTCTTACCTCAGTTACAATTTATA	0.833 mg (100 nmol), M=8328

2.12 Plasmids

Table 16. Plasmids

Plasmid	Size (bp)	Host
pBlueskriptII SK	2961	Invitrogen™
pcDNA3.1+	5428	Invitrogen™
EGFP in N1	720	Addgene
hGpr17 in pcDNA3.1+	1020	Research group of Prof. Dr. Evi Kostenis, Institute of Pharmaceutical Biology, University of Bonn, Germany
3HA-hGpr17 in pcDNA3.1+	1151	Research group of Prof. Dr. Evi Kostenis, Institute of Pharmaceutical Biology, University of Bonn, Germany
3HA-zfAGpr17 in pcDNA3.1+	1155	Research group of Prof. Dr. Evi Kostenis, Institute of Pharmaceutical Biology, University of Bonn, Germany
3HA-zfBGpr17 in pcDNA3.1+	1080	Research group of Prof. Dr. Evi Kostenis, Institute of Pharmaceutical Biology, University of Bonn, Germany

3HA-h+zfAGpr17 in pcDNA3.1+	1137	Research group of Prof. Dr. Evi Kostenis, Institute of Pharmaceutical Biology, University of Bonn, Germany
3HA-h+zfBGpr17 in pcDNA3.1+	1110	Research group of Prof. Dr. Evi Kostenis, Institute of Pharmaceutical Biology, University of Bonn, Germany
3HA-zfA+hGpr17 in pcDNA3.1+	1149	Research group of Prof. Dr. Evi Kostenis, Institute of Pharmaceutical Biology, University of Bonn, Germany
3HA-zfB+hGpr17 in pcDNA3.1+	1107	Research group of Prof. Dr. Evi Kostenis, Institute of Pharmaceutical Biology, University of Bonn, Germany
mbpA in pGEM®-T Easy Vektor	411	Research group of Dr. Hauke Werner, Department of Neurogenetics, MPI for Experimental Medicine, Göttingen, Germany
nkx2.2 in pBlueskriptII SK	700	Research group Bart and Wilson, Developmental Biology Research Centre, Randall Institute, King's College London, UK
tdTomato in pBlueskriptII SK	1428	Clontech Laboratories
zfAGpr17 in pBlueskriptII SK	1020	Research group of Prof. Dr. Benjamin Odermatt, Institute of Anatomy, University of Bonn, Germany

2.13 Assay kits

Table 17. Assay kits

Assay Kit	Product number	Company
Amersham ECL prime Western Blotting Detection	RPN2236	GE Healthcare
DIG RNA Labeling Kit (SP6/T7)	11175025910	Roche
DyNAmo® Flash Probe qPCR Kit	F-455S	Thermo Fisher Scientific
iScript™ cDNA synthesis Kit	170-8890	Bio-Rad Laboratories
mMessage mMachine™ T7 Ultra Kit	AM1345	Invitrogen by Thermo Fisher Scientific
NucleoBondR Xtra Maxi	740414.10	Macherey-Nagel
NucleoSpin Gel and PCR Clean-UP	740609.250	Machery-Nagel
Qubit RNA HS Assay Kit	Q32855	Molecular Probes by life technologies™
Rapid DNA Ligation Kit	K1422	Thermo Fisher Scientific
Pierce BCA Protein Assay Kit	23225	Thermo Fisher Scientific

2.14 Consumables

Table 18. Consumables

Consumables	Product number	Company
Assay plate, 384 well	784080	Greiner
Blue 1000 µL tips	686290	Greiner bio-one
Cell culture flasks, 25/75/175 cm^2	430168/430729/431079	Corning
Cell scraper	3926.90.97	Corning
Centrifuge tubes, 15ml/50mL	430791/430829	Corning
Compound plate, 384 well g	3657	Corning
Cryogenic vials	5000-1020 Nalgene®	Nalgene® by Thermo Fisher Scientific
Culture dishes 21/55 cm^2	430166 / 430167	Corning
Culture dishes (untreated)	430591	Corning
Disposable filter unit 0.2 µL	FB30/0.2 CA-s	Whatman®
EPIC cell assay plate, 384 well	9027.90.50	Corning
Glass Bottom viewplate, 96-well, high performance #1.5 cover glass	P96-1.5H-N	Cellvis
Gelloading 200 µL tips	B71932	Bioplastics
MicroSeal B Seal Hard-Shell PCR Plate 96-well, thin-wall	HSP9601	Bio-Rad Laboratories
Nitrocellulose membranes HybondTM-C Extra	RPN203E	GE Healthcare
ParafilmTM	1447011	Labomedic

Pasteur pipettes, glass	447016	Labomedic
Precellys Bulk beads for 500pp Zirconium oxie beads	KT03961-1-103.BK	PEQLAB Biotechnologie
SNAP i.d.® 2.0 MultiBlot Holders (4.5 x 8.4 cm)	SNAP2BHMB-K	Merck
Sponge Pad for Blotting	EI9052	Thermo Fisher Scientific
Stripette® serological pipettes	4486 – 4490	Corning
TC-Platte 24-well Standard, F	83.3922.005	Sarstedt
Tip, Gelloading	B71932	Bioplastics BV
Whatman paper	GB005	Biometra
Yellow 200 µL tips	760.002	Sarstedt

2.15 Sterilization method

All heat-stable solutions and materials were autoclaved at 121 °C and 1.2 bar for 21 min with the Varioklav®. All other solutions were sterilized with a membrane filter of 0.2 µm pore size.

2.16 Laboratory instruments and equipment

Table 19. Laboratory instruments and equipment

Instruments/ Equipment	Product number	Company
Apotome.2 microscope	-	Zeiss
Apochromat 63x/1.4 objective	-	Zeiss
Autoclave Varioklav®	-	H+P Labortechnik
Axiocam 503 mono	-	Zeiss
Balances TE64 (precision balance) TE6101	BL310	Satorius
Biofuge pico	-	Hereaus by Thermo Fisher Scientific
Biofuge primo	-	Hereaus by Thermo Fisher Scientific
Camera CoolSNAP HQ2	DFC 360 FX	Photometrics Leica
CFX96™ Real-Time System	185-5196	Bio-Rad Laboratories
Counting chamber	Neubauer	Labomedic
Detection System DeVision DBOX Detection System	-	Decon
Digital Sight DS-U3	-	Nikon
Dual-Stage Class Micropipette Puller	PC-10	Narishige
EnSight™	HH34000000	Perkin Elmer
Epic System Reader	-	Corning
Eppendorf BioPhotometer®D30	6133000001	Eppendorf AG

Eppendorf µCuvette® G1.0	6138000018	Eppendorf AG
Eppendorf Multipipette M4	4982000012	Eppendorf AG
Eppendorf ThermoMixer®	5436	Eppendorf AG
Fluorescence microscope DM IL LED Fluo	-	Leica
Freezer (-80 °C)	-	Heraeus
Freezer (liquid nitrogen)	MVE 815P-190	Chart BioMedical Ltd
Geldoc 2000	-	Bio-Rad Laboratories
CO2 incubator (cell culture)	HERAcell® 240	Heraeus
Incubator IN	ASTM304	Memmert
Assab CO2-Inkubator	T303	Medicin AB
Innova 4000 Incubator	8261-30-1007	New Brunswick Scientific
InSight™ DeepSee™	-	Spectra Physics
Intenslight CHFIE	-	Nikon
KL 1500 LED Plus	150500	Lighting and Imaging Schott
KL 200 LED	120200	Lighting and Imaging Schott
KL 2500 LED	250400	Lighting and Imaging Schott
TriM scope 2	-	LaVision BioTec
Microscope	CKX31SF	Olympus
Microscope Stemi	Stemi 508	Zeiss
Model 302 RM	-	ConOptics
MPPI-3 Pressure Injector	-	Applied Scientific Instrumentation, Inc.

Nikon AZ100	-	Nikon
Nikon Eclipse Ni-U	-	Nikon
PerfectSpin Mini	91-PSPIN-M	PEQLAB Biotechnologie
pH electrode	-	Mettler Toledo
Pipettes 0.5-10 µl; 10-100 µl; 100- 1000 µl		Eppendorf
Pipetboy acu2	612-0926	Integra Bioscience
PlateFuge™ Microplate Microcentrifuge	C2000	Benchmark Scientific
Power Pac 300	164-5070	
Precellys 24	91-PCS24	PEQLAB Biotechnologie
Qubit® 2.0 Fluorometer	Q32866	Life Technologies
RMS-30V Roller	-	NeoLabs
Semi-automatic pipettor CyBi®-Selma	-	Cybio
SevenEasy™ pH-meter	-	Mettler Toledo
SNAP i.d.® 2.0 Protein Detection System	SNAP2MB1	Merck
T100 Thermal Cycler	1861096	Bio-Rad Laboratories
Tecan Sunrise	-	r-biopharm
UV/VIS spectrophotometer SmartSpecTM Plus	-	Bio-Rad Laboratories
Vacuum pump system AP 15 Membrane Vacuum Pump	-	HLC BioTech
Vacuum pump system 220V/50HZ	WP6122050	Merck

Vortex Mixer	F202A0173	Velp Scientifica
Water purification A Milli-Q Water System	-	Merck Millipore
XCell SureLock® Mini-Cell and XCell II™ Blot Module	EI0002	Thermo Fisher Scientific
X-Cite SERIES	120Q	Excelitas Technologies

2.17 Software

Table 20. Software

Software	Company
Application Suite 3.3.1	Leica
CFX Manager	Bio-Rad Laboratories
ChemDraw	PerkinElmer
ImageJ	NIH
ImSpector	LaVision
MikroWin2000	Berthold Technologies GmbH & Co. KG
NIS-Elements Viewer 4.20	Nikon Instruments Europe B.V.
Gel-Pro Analyzer	Media Cybernetics, L.P
Gelscan software V6.0	Bioscitec
GraphPad Prism6	GraphPad Software
Microsoft Exel 2010	Microsoft® Corporation
Microsoft PowerPoint 2010	Microsoft® Corporation
Microsoft Word 2010	Microsoft® Corporation
Serial Cloner 2.6	http://serialbasics.free.fr/Serial_Cloner.html
XFluor4	Microsoft® Corporation/Tecan sunrise

3 Methods

3.1 Cell biological methods

Human embryonic kidney cells (HEK293) were cultivated at 37 °C in a 5 % CO_2 and 96 % humidity air atmosphere until they were ready to be subcultured. Zebrafish PAC2 fibroblast cells were kept in room atmosphere at 28 °C. To prevent contamination, all cell culture procedures were performed under sterile conditions by using laminar airflow cabinets. All solutions, buffers and media were pre-warmed to the appropriate culturing temperatures before use.

3.1.1 Passaging cell lines

3.1.1.1 HEK293 cells

The immortalized cell line was passaged two times a week and used for experiments until passage 70-80 was achieved. Under laminar air flow conditions, HEK293 cell medium (Table 2) was removed and cells were rinsed once with 5 mL PBS. Subsequently, 2 mL of 0.05 % Trypsin-EDTA were added and flasks were incubated for 1-5 min at 37 °C until complete detachment of the cells was achieved. By adding 8 mL of HEK293 cell medium trypsination was stopped and cell solution was thoroughly resuspended to disperse clumps. Cells were splitted 1:10 in a 75 cm^2 cell culture flask and supplied with 14 mL of fresh cell medium.

3.1.1.2 PAC2 fibroblast cells

PAC2 fibroblast cells proliferate rather slowly. Hence, they were passaged every 10 days after reaching 100 % confluency. Cells were washed once a week with 15 mL PBS and provided with new L15 medium (Table 3). For passaging, cell medium was removed and cells were washed twice with 10 mL of PBS to remove trypsin inhibitors of the serum. 2 mL of 0.05 % Trypsin-EDTA was added and cells were incubated for 10-15 min at 28 °C. As soon as cells were fully detached, 8 mL PAC2 medium was added. Cells were splitted 1:2 and supplemented with fresh medium to a total volume of 20 mL.

3.1.2 Cryopreservation and thawing of cells

3.1.2.1 HEK293 cells

To avoid aging, mammalian cells were cryopreserved and stored in liquid nitrogen vapour phase at - 196 °C. For this purpose, cells were trypsinized as described (see 3.1.1.1) and subsequently centrifuged at 800 g for 4 min. After removing the supernatant, the pellet was resuspended in 1 mL freshly prepared freezing medium (= growth medium containing 20 % FCS, 10 % DMSO) and transferred into cryogenic vials. To achieve a freezing rate of - 1 °C/min, vials placed in a warm styrofoam box were frozen at - 80 °C and the day after transferred into the liquid nitrogen tank for long-time conservation.

For insuring the highest level of viability after long-time storage, cells were quickly thawed at 37 °C in the water bath and supplied with 10 mL pre-warmed medium. After centrifugation at 800 g for 4 min, supernatant was discarded and cells were gently resuspended in the respective HEK293 cell medium without antibiotic. After 24 h medium was exchanged to standard HEK293 cell medium.

3.1.2.2 PAC2 fibroblast cells

Cryopreservation and thawing was conducted as described in 3.1.2.1, however distinct media were used. The L15 freezing medium for PAC2 fibroblasts was L15 medium containing 30 % FBS and 10 % DMSO. For thawing growth medium with antibiotic was used. Additionally, cells were washed 24 h after revitalization with 10 mL PBS and then passaged as described in 3.1.1.2.

3.1.3 Cell counting

Cell counting was conducted with Neubauer counting chamber that contained two counting areas. Before loading 10 µL of cell suspension, a glass cover was placed over the central area of the chamber. Using a microscope, cells were counted in four of nine squares without taken those into account that touched the upper and the left limits. Cell number was averaged and cell density calculated with following formula: cell density [cells/mL] = counted cells x dilution factor x 10^4.

3.1.4 Transient transfection of recombinant cells with FuGENE HD®

Transient transfection is a temporary non-viral delivery of genetic material into cultured eukaryotic cells.

The non-liposomal transfection with FuGENE® HD was conducted according to manufacturer's instructions. One day before transfection, 5 x 10^6 cells were plated on 6 cm cell culture dishes such that they reached a confluency of 50 % at the day of transfection. For medium-DNA-FuGENE complex formation, 19 µL of FuGENE® HD reagent were gently added to 6 µg of DNA in 500 µL of pre-warmed Opti-MEM and mixed by brief pipetting. After 5 min incubation at RT, transfection mixture was pipetted in drops onto the cells in the dish. Cell-based assays were performed 48 h after transfection.

3.1.5 Coating cell culture dishes and plates

For ELISA and ICC experiments, culture plates and coverslips were coated with poly-D-lysine (PDL) for achieving sufficient attachment and effective growth of cells. Cell culture surfaces were covered with 0.1 mg/mL PDL solution and incubated for 1 h in a 37 °C incubator. The coating solution was aspirated and surfaces were washed three times with sterilized PBS. After drying under UV light, plates were stored at 4 °C until needed.

3.2 Cell based assays

3.2.1 Dynamic mass redistribution assay

Dynamic mass redistribution (DMR) is a pathway-unbiased and label-free technology to examine receptor functionality in living cells in real-time. Upon application of stimuli, a holistic cell response emerging as a movement of biomass (mass redistribution) is captured by a resonant waveguide grating (RWG) biosensor (Fang *et al.*, 2007). Distinct events including ligand binding, receptor activation, internalization or recycling as well as protein recruitment can be recorded by this method. The readout is based on changes of the wavelength of polarized broadband light reflected by the biosensor depending the optical density of the cell layer within 150 nm from the plate bottom. The shifts in wavelength (Δpm) are recorded over time relative to the baseline value. An accumulation of mass causes positive DMR responses (reflection of longer wavelength), while reduction of mass leads to negative shifts (reflection of shorter wavelength) (Schröder *et al.*, 2011).

3.2.1.1 Experimental procedure

The day prior to the assay, transiently transfected cells were seeded with a density of 21 kc/well in a fibronectin-coated 384-well Epic® biosensor microplate. The plate was centrifuged at 800 g for 10 s and incubated at 37 °C and 5 % CO_2 for 24 h. The next day, cells were washed twice with HBSS containing 20 mM HEPES (Solution 1) and 0.4 % DMSO to match exactly with respect to the DMSO content of compound dilutions. Buffer was aspirated by using a manifold and a final volume of 30 µL was added to each well. The microplate was equilibrated 1 h at 37 °C onto the DMR reader. In the meantime a serial dilution of the compound was produced and transferred in a 384-well compound plate. With respect to the compound dilution during addition to the biosensor plate, compounds were prepared 4-fold concentrated. The compound plate was kept for 30 min at 37 °C in the incubator of the semi-automatic pipetting system CyBi® Selma. Before starting the measurement, the cell plate was aligned to the camera by using the Epic® Aligner tool. A baseline signature was recorded for 5 min and subsequently compound solutions of 10 µL/well were transferred with CyBi® Selma into the plate. Optical changes were measured in real-time for at least 4800 s.

DMR measurements of PAC2 fibroblast cells were conducted at 28 °C, hence the compound plate was kept at 28 °C equally.

3.2.1.2 Data evaluation

Once the measurement was finished, data were transformed with the Transform table to column macro and finally analysed with GraphPad Prism®. All DMR data were buffer-corrected and concentration-effect curves were calculated based on maximal response until 1800 s. Representative optical traces were illustrated as mean values (+ SEM), while resulting concentration-effect curves were shown as mean values (± SEM).

3.2.2 Enzyme-linked immunosorbent assay

In this thesis Enzyme-linked immunosorbent assay (ELISA) was used to quantify the amount of N-terminally 3HA-tagged GPR17 receptors on the cell surface. The measurement is based on an indirect detection strategy, where an antigen targeted by a primary antibody is detected with an HRP-conjugated secondary antibody.

3.2.2.1 Experimental procedure

24 h after transfection, HEK293 cells were detached and seeded into PDL-coated 96-well microtiter plates at a density of 50 kc/well. Cells were cultivated overnight at 37 °C under 5 % CO_2 conditions. On the day of the assay (48 h after transfection), cell medium was quickly aspirated and cells were fixed with 4 % paraformaldehyde (100 µL/well) for 20 min at RT. After fixation, cells were washed three times for 5 min with 200 µL PBS at RT and blocked with blocking buffer containing 3 % dry milk (Solution 2) for 60 min at 37 °C. Blocking buffer was removed and 75 µL of first antibody (mouse anti-HA, 2.4.1) diluted 1:400 in blocking buffer were added to the wells. Following incubation for 1 h at 37 °C, cells were washed three times with 200 µL PBS for 15 min at 37 °C. Subsequently, 75 µL HRP-conjugated goat anti-mouse (Sigma, 2.4.2) diluted 1:1000 were added and cells were kept for 1 h at 37 °C. After three washes, secondary antibody was detected by adding 100 µL/well of the colorimetric horseradish peroxidase substrate 3,3',5,5'-tetramethylbenzidine (TMB). After 3-5 min, reaction was terminated with 50 µL/well of 0.5 M H_2SO_4. 130 µL supernatant were transferred into a new 96-well plate with clear bottom and colorimetric readings were obtained using Tecan Sunrise reader at 450 nm.

3.2.2.2 Data determination

The resulting sample data were subtracted by the value of the empty vector control and normalized in GraphPad Prism®. Quantified results were shown as mean values (+ SEM).

3.2.3 Immunocytochemistry assay

Immunocytochemistry (ICC) is a fluorescent dye-based laboratory technique that uses specific antibodies to visualize the localization of proteins in cells. In this case, a primary antibody targeted against the N-terminal 3HA-tag of GPR17 constructs was used in conjunction with a fluorescent-labelled secondary antibody.

3.2.3.1 Experimental procedure

The day prior to the assay, transiently transfected HEK293 cells were seeded onto PDL-treated cover-slips lying in 24-well-plates at a density of 80 kc/well and cultivated overnight at 37 °C and 5 % CO_2. Next day, medium was removed and cells were fixed with 4 % paraformaldehyde for 30 min at RT. After three washing steps with 500 µL PBS for 15 min at 37 °C, cells were incubated with 300 µL blocking buffer (Solution 3) per well for 1 h at 37 °C. Blocking buffer was replaced with 250 µL primary antibody (mouse anti-HA, 2.4.1) diluted 1:500 in blocking solution. After an incubation of 1 h at 37 °C, extent of antibody was removed by three washing steps with PBS and 250 µL secondary antibody (goat anti-mouse-Cy2, 2.4.2) diluted 1:500 in blocking buffer were added to the wells. Cells were incubated for 1 h at 37 °C and subsequently washed three times with PBS. Finally, 8 µL of Mowiol were pipetted onto glass object holders and cover slips were fixed upside-down. Samples were stored at 4 °C for further analysis.

3.2.3.2 Data determination

Images were obtained with the Zeiss® Apotome.2 microscope by using the Plan-Apochromat 63x oil-objective with a resolution of 1.4 megapixels and the Zeiss® Axiocam 503 mono. Pictures were pseudo-colored with Zeiss® ZEN Imaging Software. All experiments were conducted at least three times and show representative images.

3.3 Methods in molecular biology

3.3.1 Preparation of LB plates

500 mL of Luria Bertani (LB) agar were solved and cooled down to 50 °C before adding 100 µg/mL ampicillin. Later, agar was casted into petri dishes (30 mL/dish) to firm up. Plates were stored at 4 °C with agar-side up.

3.3.2 Heat shock transformation

Transformation is a non-viral process by which external DNA molecules are introduced in host cells, in this case, E.coli XL1Blue. To this end, chemically competent bacteria were thawed for 5 min on ice. 50 ng of plasmid DNA were added, mixed carefully and left to incubate for 30 min on ice. Subsequently, bacteria were heat shocked at 42 °C for 90 s and immediately stored for 2 min on ice. 850 µL of LB medium were added and solution was cultured under vigorous shaking (220 rpm) for 45 min at 37 °C. Following centrifugation at 13,000 rpm for 1 min, supernatant was discarded leaving 200 µL in the eppendorf vial. Bacteria were resuspended and plated onto pre-warmed LB plates containing 100 µg/mL ampicillin. Plates were incubated at 37 °C and clones were picked after 24 h.

3.3.3 Cryopreservation of bacterial strains

For long-time storage of transformed bacterial strains, cells were cryopreserved as glycerol stocks. For that, 200 µL glycerine were added to 800 µL bacterial suspension and stored at - 80 °C.

3.3.4 Preparative isolation of plasmid DNA

Preparative isolation of plasmid DNA such as necessary for transfection experiments was conducted by using NucleoBond® Xtra Maxi Kit. To this end, 20 µL of thawed glycerine culture were pipetted in 300 mL of LB medium containing the respective antibiotic and cultivated under vigorous shaking (220 rpm) overnight at 37 °C. Plasmid isolation was processed according to manufacturer's instructions.

3.3.5 Determination of nucleic acid concentration by photometrical method

DNA concentrations (ng/µL) were determined with Eppendorf BioPhotometer® D30 at 260 nm. 3 µL of DNA sample were analyzed with the Eppendorf µCuvette® G1.0. The purity of DNA was estimated by validation of the A_{260}/A_{280} (should be 1.8-2) and A_{260}/A_{230} (should be ≥ 2) ratio.

3.3.6 Analysis of protein expression by Western blot

3.3.6.1 Preparation of lysates

In order to analyse protein expression in HEK293 cells by Western blot analysis, cell lysates were prepared. Cells were seeded and transfected like described in 3.1.4. 48 h after transfection, medium was removed and cells were washed twice with ice-cold PBS. Subsequently, lysis buffer (Solution 4) containing 10 µL/mL protease inhibitors was added and lysed cells were rotated for 20 min at 4 °C. Finally, lysates were centrifuged at 15,000 g for 10 min at 4 °C and supernatants were frozen at - 20 °C.

3.3.6.2 Determination of the protein content of lysates

Protein concentration was determined by Pierce™ BCA Protein Assay Kit according to the manufacturer`s recommendations. The detection is based on reduction of Cu^{2+} to Cu^{1+} in an alkaline medium followed by a chelation of two bicinchoninic acid (BCA) molecules with one cuprous ion. The incurred chelate complex exhibits a strong linear absorbance at 562 nm within increasing concentrations of proteins. In brief, 10 µL of each sample were diluted 1:5 with 0.1 M NaOH and a standard dilution series of bovine serum albumin (0 µg/µL - 10 µg/µL) was prepared. 200 µL of fresh protein detection reagent were added to each sample and mixtures were incubated for 30 min at 37 °C. Finally, absorption was measured at 560 nm using the Tecan Sunrise reader. Protein concentrations were computed based on the BSA standard curve.

3.3.6.3 SDS-Polyacrylamide-Gel-Electrophoresis (SDS-PAGE)

After determination of protein amount, NuPage® Sample Reducing Agent (10x) and NuPage® Sample Buffer (2-4x) were added to 15 µg cell lysate. Proteins were separated by their mass at 60 V for 3 h in 10 % NuPage® Bis-Tris Protein Gels. Gels were fixed in a chamber with running buffer, while the inner part of the chamber was subjoined with 500 µL NuPage Antioxidant. 5 µL Kaleidoscope marker and 2.5 µl Magic marker were used as molecular weight standards.

3.3.6.4 Western blot analysis

Following separation, protein transfer procedure was conducted at 25 V for 2 h by using a wet blotting module. Briefly, a sandwich of successive layers of prewetted sponges, filter papers, protein gel and nitrocellulose membrane was prepared and fixed in the blotting chamber filled with NuPage® Transfer Buffer including 20 % of methanol.

3.3.6.5 Protein detection

After blotting, membranes were rinsed twice with washing buffer (Solution 5) and blocked with Roti-Block® in 50 mL tubes, rotating for 1 h at RT. First antibody, diluted in blocking solution, was added and incubated at 4 °C overnight. Next morning, the extent of antibody was removed by three washing steps, each 5 min at RT. Membranes were incubated for 1 h with the respective horseradish peroxidase-conjugated secondary antibody and washed again three times with washing buffer. Finally, proteins were detected by chemiluminescence using Amersham ECL Prime Western Blotting Detection Reagent according to the manufacturer's recommendations.

3.3.6.6 Data determination

Quantification was achieved by scanning the blot with an imager and densitometric analysis of bands using Gel scan software. To account for possible loading as well as transfer errors, samples were normalized to β-actin acting as an internal loading control. All data are shown as means (+SEM).

3.4 Zebrafish maintenance and rearing conditions

Zebrafish lines were maintained at 28 °C in the Zebrafish facility of the Institute of Anatomy, University of Bonn according to previously described standard protocols (Westerfield, 2007).
Embryos were collected from mating pairs and reared at 28.5 °C in 30 % Danieau egg water (17.4 mM NaCl, 0.21 mM KCl, 0.12 mM $MgSO_4$, 0.18 mM $CaCl_2$, 1.5 mM HEPES) containing 10^{-5} % methylene blue for the first 24 h. To inhibit pigmentation of embryos older than 1 dpf, egg water was supplemented with 0.003 % phenylthiourea (PTU). Embryos were staged to hours post fertilization (hpf) or days post fertilization (dpf). All experiments were conducted in compliance with the Belgium and European laws (Ethical commission protocols ULg1076 and ULg624).

3.5 Microinjections of zebrafish embryos

3.5.1 Morpholino injections

The antisense *zfAgpr17* morpholino (MO) 5'GTTCTHTCAAGGAGGACTCCATTT3' and a control morpholino 5' CCTCTTACCTCAGTTACAATTTATA3' were purchased as lyophilized stocks from Gene Tools, LLC, and solved in sterile DEPC water to a stock concentrations of 2 mM. For injections a 20 µL master mix containing 0.25 mM MO, 5 % cutsmart buffer 10x and 10 % phenol red were heated for 10 min to 65 °C and filled in a pulled class capillary micropipette opened with forceps. The injection volume was calibrated by adjusting the diameter of droplets spreading in mineral oil to 135 µm on micrometer slides. This spawned a droplet of 1.3 nL containing 2.75 ng *zfAgpr17* MO. Once the parameters were adjusted, embryos at one- or two-cell stage were placed in an injection mold and injected into the yolk.

The amount of injected MO was calibrated by the master student Philip Reinoß. For further information refer to the master thesis 'Functional analysis of the transmembrane receptor Gpr17 in CNS myelination in zebrafish' (Reinoß, 2014).

$$V_{injection} = \frac{4}{3} \times \pi \times \left(\frac{135\ \mu m}{2}\right)^3 = 12288249\ \mu m^3$$

$$1\ \mu m^3 = 1 \times 10^{-9}\ \mu L$$

$$12288249\ \mu m^3 \times 1\ 10^{-9} \frac{\mu L}{\mu m^3} = 0{,}0013\ \mu L = 1{,}3\ nL$$

$$n = c \times V = 0{,}25 \times 10^{-3}\ \frac{mol}{L} \times 1{,}3 \times 10^{-9}\ L = 3{,}25 \times 10^{-13}\ mol$$

$$m = n \times M = 3{,}25 \times 10^{-13}\ mol\ x\ 8465\ \frac{g}{mol} = 2{,}1 \times 10^{-9}\ g = 2{,}75\ ng$$

Figure 4: Calculation of injected amount of morpholino.

3.5.2 RNA injections

3.5.2.1 RNA synthesis

For the *in vitro* synthesis of *zfA* and *zfBgpr17* as well as *tdTomato* RNA the mMessage Maschine Kit T7 Ultra Kit® was used. Therefore, plasmids of 3HA-tagged Gpr17 constructs (Table 16) were linearized with XhoI and transcribed as mentioned in the protocol. Linearization of control tdTomato plasmid was conducted with MfeI. Finally, RNA was obtained by lithium chloride precipitation, quantified with the Qubit RNA HA Assay Kit® and frozen as aliquots at - 80 °C.

3.5.2.2 Overexpression

RNA injections were performed like described in chapter 3.5.1. 2.2 µg of *zfA* and *zfBgpr17* RNA were diluted with 1 µL phenol red and RNase-free water to 5 µL. Finally 1.8 nL (refers to 150 µm droplets diameter) containing 800 pg RNA were injected into the yolk of embryos at the one- cell stage. As a control for the successful *in vivo* transcription *tdTomato* RNA was generated and injected equally.

3.5.2.3 Rescue experiment

For the rescue experiment 3 µg RNA were mixed with 2.5 µL pre-heated MO stock solution (0.5 mM) and adjusted with RNase-free water to 5 µL. Finally 1.3 nL (refers to a droplets diameter of 135 µm) containing 800 pg RNA and 2.75 ng *zfAgpr17* MO were injected into embryos at the one-cell stage.

3.6 Drug treatment of zebrafish

3.6.1 Bathing in MDL29,951

Before treatment was applied, 1 dpf embryos were enzymatically removed from their chorion with 2 mg/mL pronase in 30 % Danieau. 10 mM MDL29,951/DMSO stock solution was diluted with 30 mL 30 % Danieau containing 0.003 % PTU to 10 and 30 µM working solution. 0.1 % and 0.3 % DMSO were used as controls. Larvae were exposed to the compound for 5 days in a light cycle incubator at 28.5 °C. The treatment solution was renewed every 24 h. Therefore 1.5 mL solution with all embryos were transferred in an Eppendorf tube and 28.5 mL of fresh Danieau solution containing MDL29,951 were poured in a new petri dish. Finally 1.5 mL of zebrafish embryos were added to the renewed drug solution. At 5 dpf zebrafish were imaged like described in chapter 3.7.1 or collected for qPCR and Western blot analysis.

3.6.2 TSA treatment

Treatment with Trichostatin A (TSA) was carried out as described in 3.6.1. Zebrafish were exposed to 100 ng/mL TSA for 5 days analysed by WISH as described in chapter 3.7.3.4.

3.7 Zebrafish based methods

3.7.1 Two-photon imaging

Two-photon imaging experiments were conducted by using the scan head based laser-scanning microscope TriMScope (LaVision, BioTec, Bielefeld, Germany). Spinal cord segments 4–10 were imaged with a 20x water-immersion objective lens (NA 1.0, W Plan-Apochromat, Zeiss®) directing the laser beam (930 nm) of a near-infrared laser (InSight™ DeeepSee™, Spectra-Physics, Santa Clara, USA) into the sample. Images were acquired as z-stacks (z-step 2 µm) with a field of view of 449 µm x 111 µm and a resolution of 2730 x 678 pixel (1 pixel was 0.16 µm).

3.7.1.1 Mounting of zebrafish

To inhibit pigmentation interfering with the imaging process, embryos were maintained after 24 h in 30 % Danieau containing 0.003 % PTU. For exempting zebrafish larvae from their chorions, embryos were incubated with 2 mg/mL pronase in 30 % Danieau for 5-10 min at 28 °C. Larvae were mounted laterally in 1.25 % low melting agarose containing 5 % MS222 for preventing movement during the imaging procedure.

3.7.1.2 Analysis

Analysis of the images was performed blindly by using Image J®. Cells were counted in single stacks and numbers were transferred to GraphPad Prism®. For all experiments D'Agostino-Pearson omnibus normality test was used to check the distribution of the values. In case of a Gaussian distribution, one-way ANOVA (parametric) was applied for statistical analysis. When the assumption of normality was not met, the non-parametric Kruskal-Wallis test was conducted.

3.7.2 EnSight™ imaging

The EnSight™ is a label-free, well imaging multimode reader that was used for high-throughput imaging and analysis of fluorescent zebrafish. The master student Enrico Mingardo established a protocol as an alternative for the time consuming screening with Two-photon microscopy. The fluorescent excitation measurements were performed at 465 nm with an exposure time of 50 ms. To visualized the entire animal, each well was imaged as a stack of six distinct focus channels with a height of 25 µm. Images were analysed using a semi-automatic counting plugin installed in ImageJ®. For more detailed information refer to the master thesis of Enrico Mingardo titled 'Establishing a multi-well plate reader system for high- throughput imaging and analysis of fluorescent zebrafish larvae to investigate the central nervous system' (Mingardo, 2017).

3.7.2.1 Mounting of zebrafish in the 96-well plate

After anaesthetizing with MS222 in the petri dish, one zebrafish per well was transferred to a 96-well glass bottom plate. The larvae were mounted laterally with an injection tip in the middle of the well and subsequently centrifuged at 300 rpm for 5 s.

3.7.3 Whole-mount in situ hybridization

The Whole-mount in situ hybridization (WISH) protocol used in this thesis was adapted from Thisse Lab – In situ hybridization Protocol – Update 2010 (Thisse and Thisse, 2008). The principle is based on the complementary hybridization of digoxigenin-labelled RNA to the specific RNA of interest. Subsequently, an alkaline phosphatase-conjugated antibody binds to digoxigenin and finally converts the colourless NBT/BCIP compound by removing phosphate into a purple dye.

3.7.3.1 RNA preparation

For RNA transcription, plasmids including T7/T3/SP6 promoters were linearized with corresponding enzymes (Table 21) at 37 °C overnight. The next day, templates were separated in a 1 % agarose gel and extracted from the gel by using the NucleoSpin Gel and PCR Clean-UP Kit. Afterwards, probes were synthesized as described in the protocol of the DIG RNA Labeling Kit (SP6/T7) from Roche.

Table 21: Probes for WISH

Plasmid	Probe	Restriction enzyme	Promoter
mbpA in pGEM®-T Easy Vektor	antisense	SpeI, SacI	T7
	sense	BamHI, ApaI	SP6
nkx2.2 in pBlueSkriptII SK	antisense	SacII, XbaI	T7
	sense	XhoI, KpnI-HF	T3
zfAGpr17 in pBlueSkript II SK	antisense	HindII, EcoRI	T7
	sense	XhoI, KpnI-HF	T3

RNA precipitation was conducted by adding 10 µL 3 M natrium acetate and 200 µL 100 % ethanol to 100 µL sample. After vortexing thoroughly, samples were chilled at - 20 °C at least for 30 min and subsequently centrifuged with 13,000 rpm for 30 min at 4 °C. Finally, the supernatant was discarded and the pellet resolved in RNase-free water after air-drying under the hood.

3.7.3.2 Dot blot

To determine labelling efficiency and concentration of each probe, spots of different dilutions (1:10, 1:50, 1:100, 1:500, 1:1000) were applied to a hybond membrane. Nucleic acids were fixed on the membrane by baking at 120 °C for 30 min. Afterwards, membranes were washed twice for 5 min under gentle agitation with Dot blot buffer I (Solution 8) and incubated in Dot blot buffer II (Solution 9) at RT for 30 min. Anti-DIG antibody was diluted 1:2000 in buffer II and added for 30 min. After removing the excess of antibody by washing twice with Dot blot buffer I, membranes were incubated for 5 min in Dot blot buffer III (Solution 10). At least, 50 µL NBT and 37 µL BCIP were mixed with 10 mL Dot blot buffer III and added for 5 min to the membrane until the spots were visible. The intensity of the different spots indicated the required dilution of the probe for the WISH.

3.7.3.3 Larvae preparation

After 24 hpf, 30 % Danieau fish water should include PTU, since pigmentation needs to be prevented for WISH. Larvae younger than 3 dpf were removed from their chorions by using pronase enzyme like described in chapter 3.6.1. In brief, larvae were fixed with 4 % paraformaldehyde in PBS at 4 °C overnight and dehydrated the next day in a series of 25 %, 50 % and 75 % methanol in PBS for 20 min, respectively. Finally the samples were stored in 100 % methanol at - 20 °C at least for 2 h before use.

3.7.3.4 In situ hybridization

At the first day, zebrafish samples were rehydrated like described in the Thisse protocol, always for 10 min. For permeabilization, zebrafish embryos were digested with proteinase K in PBST (final concentration of 20 µg/mL) for different periods of time depending on the age of the animal (Table 22).

Table 22. Incubation times for permeabilization of zebrafish embryos

Age of zebrafish (dpf)	Incubation time with proteinase K (min)
1	15
2	30
3	40
4	75
5	90

Likewise, the post fixation time in paraformaldehyde was enhanced to 30 min. After pre-hybridization for 3 h at 70 °C in hybridization buffer (HM) (Solution 11), samples were dosed with the digoxigenin-labelled probe diluted in HM (1:400 for *zfAgpr17* and *mpb*, 1:500 for *nkx2.2*) and incubated at 70 °C overnight. Next morning, the probe was washed out like described by Thisse, however for 20 min instead of 10 min. Subsequently, three longer washing steps followed, including 30 min with 0.2x SSC and two times 30 min with 0.1x SSC at 70 °C. All room temperature washing steps were conducted with 0.1x SSC diluted in the described concentration with PBST. After blocking for 2-3 h with 2 mg/mL BSA /2 % Sheep serum/ PBST, samples were exposed to the anti-DIG antibody (1:20,000) at 4 °C overnight. Next morning embryos were washed with PBST and pre-incubated in alkaline tris buffer (Solution 13) like described in the protocol. Afterwards, alkaline tris buffer was replaced by 700 µL labelling solution including NBT/BCIP (Solution 14). Once the desired staining intensity was reached, 1 mM EDTA (pH 5.5) in PBS was used to stop the labelling reaction. For reducing the background, 3 dehydration steps with 25 % and two times with 50 % methanol in PBST followed. Samples were kept for several days in 100 % methanol at 4 °C and rehydrated with the solutions mentioned before. Finally, stained embryos were stored in 100 % glycerol prevented from light at 4 °C.

3.7.3.5 Imaging

All images were acquired by using the NIS-Elements Viewer 4.20 on a Nikon Eclipse microscope. For imaging, embryos were transferred with a pipette on an object slide and mounted laterally or dorsally with a cat whisker fixed tip in 100 % glycerol.

3.7.4 Quantitative real time polymerase chain reaction

The combination of a reverse transcription (RT) followed by a quantitative polymerase chain reaction (qPCR) is a powerful tool to quantify the expression of genes (Livak and Schmittgen, 2001). In this thesis, gene-specific fluorescent probes including a reporter dye at the 5' and a quencher at the 3' were used for the quantitative detection of the amplicons. The probe binding between the primer pairs is hydrolysed by the polymerase and due to the separation of fluorophore and quencher a fluorescent signal arises. The signal increases equally to the amount of generated DNA.

3.7.4.1 RNA isolation

For qPCR experiments 25 zebrafish per sample were collected at different time points and stored without water at - 80 °C. RNA was extracted using 1 mL of TRIzol Reagent per sample. Solutions were transferred to Precellys tubes filled with beads and homogenized with the Precellys 24 setting 5000-1x10-005. Following homogenization, supernatants were pipetted into RNase-free tubes and centrifuged at 12,000 x g for 10 min at 4 °C. Subsequently, samples were incubated for 5 min at RT, mixed with 0.2 mL chloroform and vortexed for 15 s. After incubation of 2-3 min at RT a centrifugation at 12,000 x g for 15 min at 4 °C followed. The upper aqueous phases were placed into new RNAse-free tubes and supplemented with 100 % isopropanol. After briefly vortexing, samples were incubated again for 10 min at RT and centrifuged again at 12,000 x g for 10 min at 4 °C. Supernatants were discarded and the pellets were washed with 70 % ethanol. Finally the air-dried pellets were resolved in 20 µL RNase-free water and RNA concentration was determined with Qubit RNA HA Assay Kit®. Until needed, samples were stored at - 80 °C.

3.7.4.2 cDNA preparation

Reverse transcription of 1 ug RNA was carried out with iScript™ cDNA synthesis Kit following the manufacturer's instructions.

3.7.4.3 Polymerase chain reaction

Primers listed in Table 14 were designed by using Sigma Oligoarchitect. To amplify *mbp* and *plp*, as well as the controls *ef1a* and *β-actin*, DyNAmo Flash Probe qPCR Kit was used and qPCR conducted in the CFX96™ Real-Time System. All reactions had a volume of 20 µL containing 2 µL cDNA mix, 0.4 µL of each forward and reverse primer (25 µM), 0.2 µL respective probe (25 µM), 10 µL Polymerase mix and 7 µL DEPC water. The reactions run under following conditions: 95 °C for 7 min, followed by 40 cycles at 95 °C for 5 s and 60 °C for 30 s.

3.7.4.4 Analysis

Samples were analysed by using the relative quantification method $\Delta\Delta C_q$-method that is based on the expression level of a target gene relative to a reference gene (Livak and Schmittgen, 2001). The calculation uses C_q values, which represent the number of cycles that are needed to generate a constant defined fluorescent level. C_q values were generated after importing the data into the CFX Manager, labelling the wells, choosing the fluorophore and setting the thresholds. Triplicates of the C_q values were averaged and the expression of the target genes ($C_{q(TAR)}$) was normalized to the non-targeted reference gene expression ($C_{q(REF)}$) within the same sample to determine ΔC_q ($C_{q(TAR)}$-$C_{q(REF)}$). Afterwards ΔC_q values of the control groups ($\Delta C_{q(Control)}$) were subtracted from the treatment groups ($\Delta C_{q(Treatment)}$) to achieve $\Delta\Delta C_q$. Finally, $\Delta\Delta C_q$ was exponentially transformed to $2^{-\Delta\Delta Cq}$. This calculation assumes amplification efficiencies of the target and references genes of 100 % (E= 2). All calculations were conducted with this assumed efficiency of 2. The threshold that was used to generate the C_q values was manually determined by analysing different dilutions of pooled RNA from 1-10 dpf old zebrafish and taken for all experiments. Results were obtained by using D'Agostino & Pearson omnibus tests to check for equal variances and normality of data and one-way ANOVA or two-tailed Student's t-test for statistical significance. All error bars were expressed as standard errors of the mean (± SEM).

3.7.5 Whole-mount immunohistochemistry

The Whole-mount immunohistochemistry (IHC) is a useful technique to determine the expression of protein within retained tissues. Genetex – Whole-mount IHC protocol for zebrafish embryos was modified in spots and used for all experiments.

3.7.5.1 Larvae preparation

The rearing the larvae was as described in 3.7.3.3. 4 dpf old zebrafish were fixed for 2 h in 4 % paraformaldehyde at RT and subsequently washed three times for 10 min with PBS. Afterwards, dehydration steps (3.7.3.3) followed and samples were stored in 100 % methanol at - 20 °C.

3.7.5.2 Immunohistochemistry

Initially, zebrafish were rehydrated like described in chapter 3.7.3.4 and washed three times for 5 min with PBST. To break methylene bridges formed during the fixation, heat-induced epitope retrieval was performed with 150 mM Tris buffer (Solution 15) for 5 min at RT, followed by an incubation with exchanged solution for 15 min at 70 °C in the water bath. After two washing steps with PBST for 5 min, 4 dpf embryos were permeabilized with 10 mg/mL proteinase K in PBST for 90 min at RT. Digestion was stopped with 4 % paraformaldehyde for 20 min at RT. For the entire removal of the fixation solution, embryos were washed five times for 5 min with PBST and subsequently blocked with NGS/BSA/PBTx blocking solution (Solution 18) for 4 h at 4 °C. Mbp antibody (Table 9) was diluted 1:200 in blocking solution with 2 % normal goat serum (Solution 19) and incubated for three days at 4 °C. After washing five times with PBTx for 1 h at RT, AlexaFluor546 secondary antibody (Table 10) diluted 1:1000 in Solution 19 was added to the sample. The incubation was carried out for two days at 4 °C protected from light. For the removal of unbound antibody and the reduction of background signal, samples were washed once again six times for 15 min and five times for 5 min with PBST. A post-fixation with 4 % paraformaldehyde for 20 min at RT followed. Embryos were washed again five times for 5 min at RT and finally immersed through a series of 25 % glycerol, 50 % glycerol, 75 % glycerol in PBST, for 20 min respectively. Protected from light, samples were stored at 4 °C in 100 % glycerol.

3.7.5.3 Imaging

Images of embryos laterally mounted in 100 % agarose were recorded with TriMScope microscope (3.7.1) and a laser beam of 860 nm. Thicknesses of myelin sheaths were measured using Image J® and statistical analysis was carried out with GraphPad Prism®. All data are shown as means (+ SEM).

3.7.6 Immunohistochemistry of zebrafish sections

Immunohistochemistry analysis (IHC) of zebrafish spinal cord sections were conducted by Dr. Anna Sophia Japp (Institute of Neuropathology, Medical Centre, University of Bonn). 3 dpf zebrafish were fixed in 4 % formalin and stored at 4 °C. All experiments were performed on Ventana Benchmark XT Immunostainer (Roche Ventana, Darmstadt, Germany) with the antibody against Cleaved Caspase-3 (2.4.1) diluted 1:200. Object slides were automatically scanned and adapted with Panoramic Viewer.

3.7.7 Western blot analysis

3.7.7.1 Protein sample preparation

To analyze protein expression, 20 zebrafish embryos were collected in a pre-cooled Eppendorf tube. After anaesthetization on ice for 5 min and entire removal of water, zebrafish were solubilized with 90 µl ice cold RIPA lysis buffer supplemented with protease inhibitor mix and rotated for 30 min at 4 °C. Subsequently, by using a pellet pestle fish tissues were homogenized until uniform in consistency and centrifuged at 13,000 rpm for 30 min at 4 °C. The supernatant was transferred to another tube and frozen by - 20 °C.

3.7.7.2 Determination of protein concentration

Protein concentration was analyzed by the Bradford dye assay that is based on a colorimetric change of Coomassie Blue G-250 dye. While under acid conditions the dye is protonated and shines brown, binding of protein stabilizes the blue form that has an absorption maximum at 595 nm. The increase of absorbance is proportional to the amount of protein present in the sample. Therefore, 2 µL of each sample was diluted with 38 µl of 0.1 M NaOH and a standard of bovine serum albumin (0 µg/µl-1 µg/µl) was prepared. 10 µL samples as duplicates were transferred to a 96-well flat bottom plate and diluted with 200 µl Bradford reagent. After 5 min absorption of the blue protein/dye complex was measured at 595 nm with Tecan Sunrise reader and calculation of protein concentrations was performed by BSA standard curve.

3.7.7.3 SDS-Polyacrylamide-Gel-Electrophoresis

SDS-polyacrylamide-gel-electrophoresis (SDS-PAGE) was conducted like described in 3.3.6.3. However, 70 µg lysate mixed with NuPage® Sample Reducing Agent (10x) and NuPage® Sample Buffer (2-4x) were heated for 5 min at 95 °C before loading on the gel.

3.7.7.4 Western blot

Western blotting procedure was carried out like already described in 3.3.6.4.

3.7.7.5 Protein detection

To prevent unspecific binding, membranes were blocked in blocking solution (5 % non-fat dried milk diluted in TBST 0.01 %) by rotating at 4 °C overnight. Protein detection was carried out by using the vacuum driven SNAP i.d. 2.0 Protein detection system. Therefore, membranes were inserted in a blot holder placed in a blot holder frame and spilled with 30 mL of blocking solution.

The vacuum was applied until the frame was completely empty. Next, 7 mL of first antibody diluted in blocking solution were added to the blot holder frame and incubated for 10 min. Membranes were washed three times with 30 mL washing buffer (TBST 0.01 %) and incubated again with 10 mL of the respective horseradish peroxidase-conjugated secondary antibody diluted in blocking buffer. After three additional washing steps with 30 mL washing buffer, proteins were detected by chemiluminescence using Amersham ECL Prime Western Blotting Detection Reagent according to the manufacturer's recommendations.

3.7.7.6 Data determination

Data were determined like described in 3.3.6.6.

4 Results

4.1 Functional analysis of zebrafish Gpr17 in HEK293 cells

The first chapter will explore receptor functionality of zebrafish Gpr17 in mammalian HEK293 cells. Since signalling of zebrafish Gpr17 was unknown, the pathway-unbiased DMR assay represented an elaborate method to study live-cell responses upon receptor activation.

4.1.1 Zebrafish Gpr17 version A is unresponsive to uracil nucleotides and cysteinyl leukotrienes

Previous published data postulated uracil nucleotides and cysteinyl leukotrienes as endogenous ligands of the G-protein coupled receptor 17 (Ciana, Fumagalli, M. L. Trincavelli, *et al.*, 2006). However, several independent laboratories failed to confirm the deorphaning report (Heise *et al.*, 2000; Maekawa *et al.*, 2009; Benned-Jensen and Rosenkilde, 2010; Simon *et al.*, 2017). As differences in activity of GPCR agonists are known to occur among species orthologues (Milligan, 2011), it was essential to interrogate whether the putative agonists which are inactive on human, mouse and rat orthologues, might stimulate zebrafish Gpr17.

To this end, HEK293 cells transiently transfected with zebrafish Gpr17 version A (zfAGpr17) were exposed to the purported endogenous agonists and receptor mediated cell-responses were monitored by holistic DMR assays. None of the ligands displayed any sign of activity at all applied concentrations (**Figure 5**). Loss of cell viability as reason for the missing response can be excluded, since carbachol and ATP elicited robust DMR signals in HEK293 cells upon acting on endogenously expressed muscarinic M3 and adenosine A1 receptors.

These data demonstrate that zfAGpr17 is completely inert towards uracil nucleotides and cysteinyl leukotrienes, supporting once more the notion that Gpr17 must still be considered as orphan.

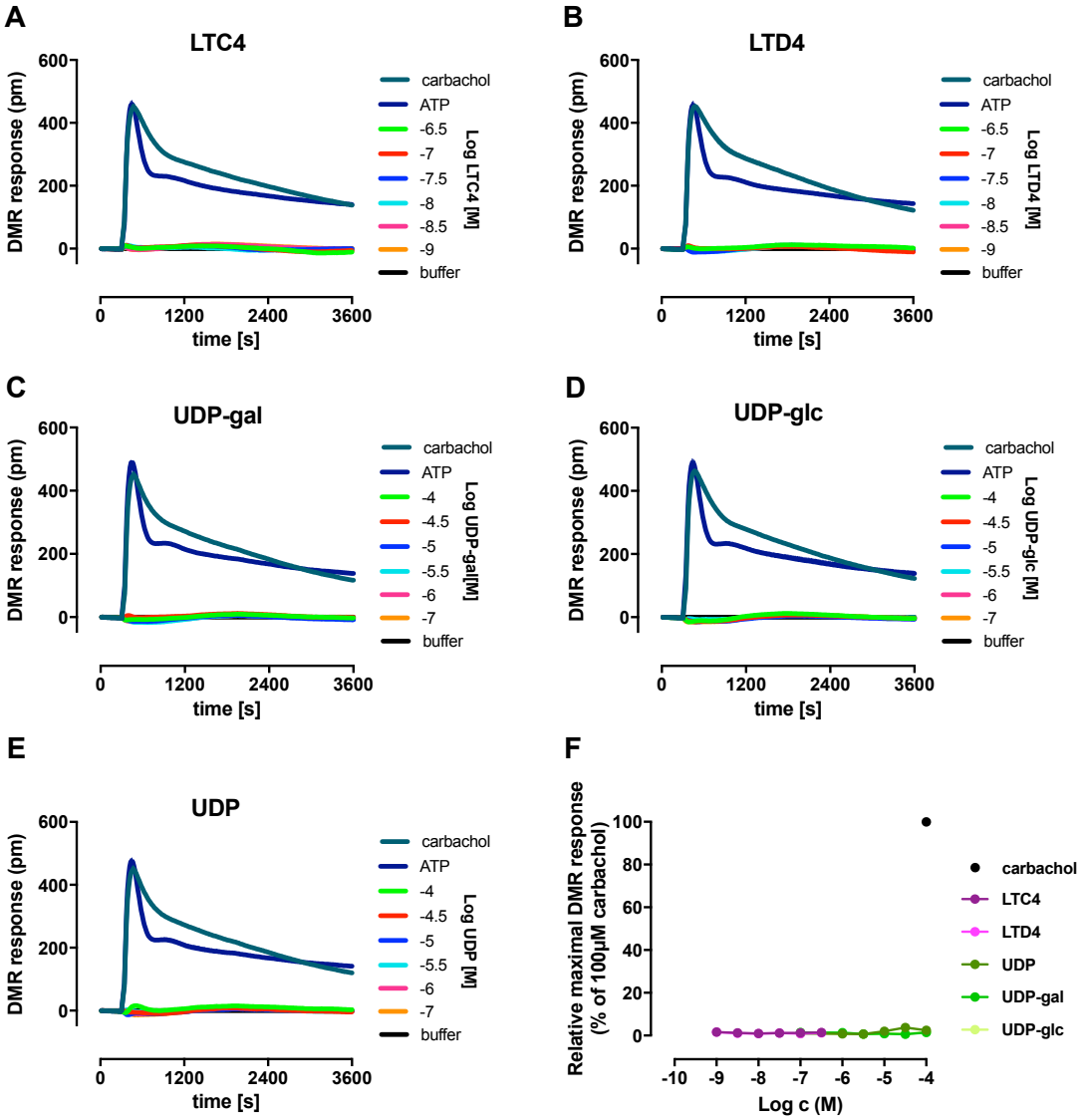

Figure 5: Zebrafish Gpr17 version A is unresponsive towards uracil nucleotides and cysteinyl leukotrienes. HEK293 cells transiently transfected with zfAGpr17 revealed no receptor specific functional activity after stimulation with putative endogenous ligands (LTC4, LTD4, UDP, UDP-gal, UDP-glc) (**A-E**). Signatures are representative traces (means + SEM) from at least three independent experiments, each performed in triplicates. Concentration-effect curves (**F**) were generated by calculation of the maximal response within 1800 s (means ± SEM).

4.1.2 MDL29,951 fails to evoke DMR responses on zebrafish Gpr17

Besides uracil nucleotides and cysteinyl leukotrienes, a small synthetic molecule, MDL29,951 (2-carboxy-4,6-dichloro-1H-indole-3-propionic acid), has been identified in previous studies as a selective agonist for human and rodent Gpr17 (Hennen *et al.*, 2013b). Further studies reported that Oli-neu cells and primary rat oligodendrocytes, which endogenously express Gpr17, displayed decreased myelin expression upon stimulation with MDL29,951 (Simon *et al.*, 2016). Hence, in search to find a compound serving as a tool to study receptor functionality and role of zebrafish Gpr17 *in vivo*, whole-cell activity of zebrafish Gpr17 towards MDL29,951 was determined by DMR assays.

3HA-tagged zebrafish Gpr17 version A (zfA) and B (zfB), transiently transfected in HEK293 cells were seeded in DMR plates and treated with increasing concentrations of the agonist. Cells transfected with empty pcDNA3.1 vector remained unaffected towards MDL29,951, which indicates that the agonist did not evoke unspecific background responses **(Figure 6, A)**. As expected, MDL29,951 led to robust, concentration-dependent traces on HEK293 cells expressing human Gpr17 **(Figure 6, B, E)**, thereby reaffirming the functionality on this species. However, MDL29,951 even in the highest concentration, displayed no functional activity on zfA **(Figure 6, C, E)** and zfBGpr17 **(Figure 6, D, E)**.

Together, these data demonstrate that zebrafish Gpr17 was neither sensitive to the postulated agonists nor to MDL29,951. The unresponsiveness towards MDL29,951 was rather unexpected, since human and zfAGpr17 display 55 % homology. Hence, reasons for the lacking response were examined by further experiments.

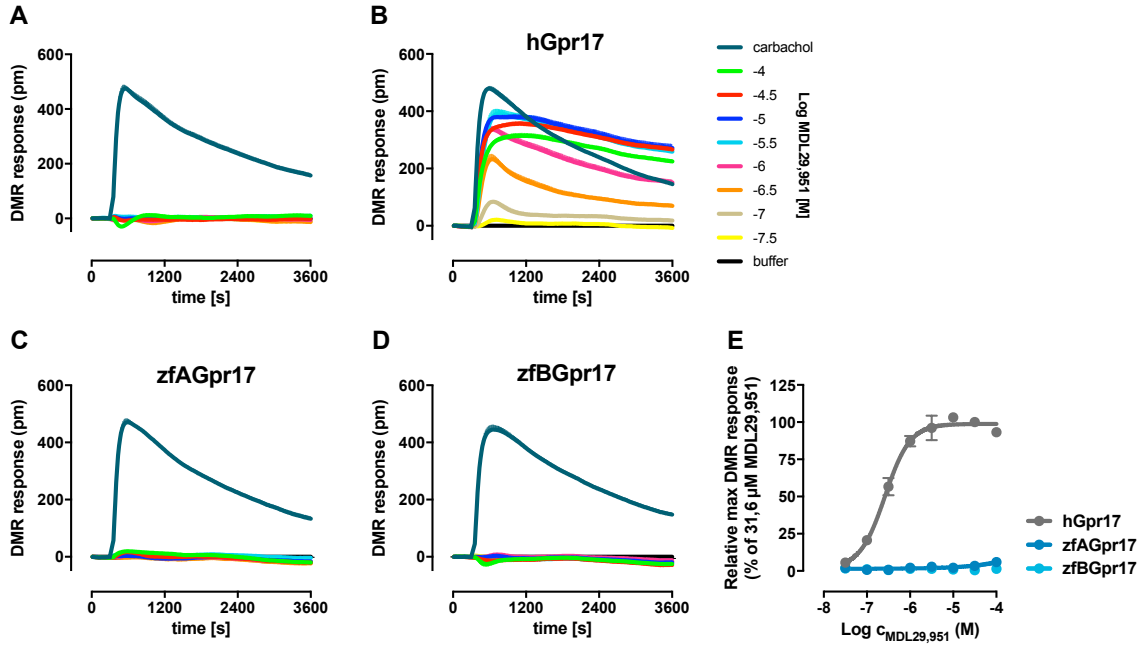

Figure 6: Stimulation of zebrafish Gpr17 with MDL29,951 does not display any sign of activity in holistic DMR assays. In DMR experiments, MDL29,951 did not produce a signal in cells lacking Gpr17 (**A**). HEK293 cells transiently transfected with 3HA-tagged zebrafish Gpr17 versions A (**C**) and B (**D**) showed no responses towards MDL29,951, while human 3HA-Gpr17 (**B**) displayed robust concentration-dependent signals after stimulation with agonist. Label-free recordings are shown as representative traces, each performed in triplicates (means + SEM) (**E**). Concentration response curves were quantified by calculation of the relative maximum DMR response within 1800 s. Data are means (± SEM) from three independent experiments.

4.1.3 Zebrafish Gpr17 receptors display sufficient cell surface expression in HEK293 cells

To account for potential discrepancies in subcellular localisation of the orthologous receptors, cell surface expression of 3HA-tagged Gpr17 constructs was analysed by fluorescent Immunocytochemistry (ICC). Thereby, 80,000 HEK293 cells seeded on coverslips were imaged 48 h post transfection. The data revealed equivalent membrane expression within all constructs (**Figure 7, B, C, D**), while control transfection with pcDNA3.1 displayed no fluorescence at all (**Figure 7, A**). Accumulation of receptors in the cytosol was comparable.

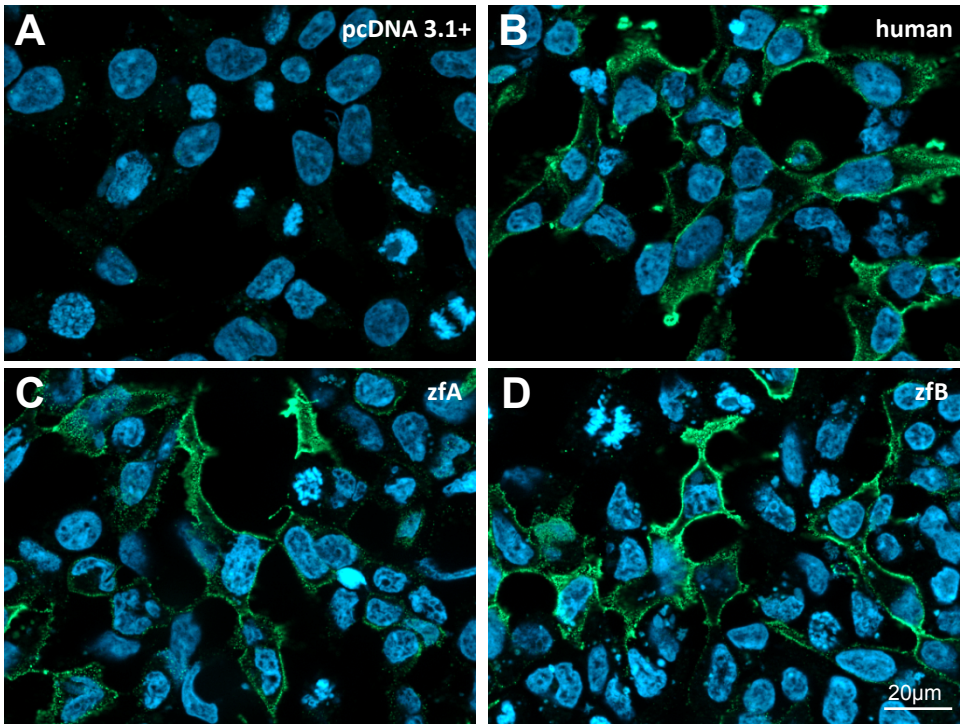

Figure 7: Immunocytochemical localisation of 3HA-tagged Gpr17 constructs reveals no difference. Representative images of HEK293 cells, transiently transfected with human (**B**) and zebrafish Gpr17 (**C, D**), were obtained 48 h after transfection. Cells were treated with an antibody directed against the N-terminal 3HA-Tag of Gpr17 constructs and then incubated with a Cy2-conjugated goat anti-mouse antibody. No specific fluorescence was detected in empty vector control transfected HEK293 cells (**A**). Experiments were conducted at least three times.

To further quantify expression levels, Enzyme-linked immunosorbent assays (ELISA) were performed. Empty HEK293 cells as well as HEK293 cells transiently expressing 3HA-tagged Gpr17 constructs were seeded in 96-well plates at a density of 50 kc/well and analysed 48 h after transfection. The obtained cell surface expressions were remarkably similar between human and both zebrafish Gpr17s (**Figure 8**).

In conclusion, the lack of agonist activity of MDL29,951 at the zebrafish Gpr17 receptors was not caused by impaired cell surface expression. Therefore it became evident that either the zebrafish receptors did not respond towards the agonist or the mammalian cell background was unsuitable for functional analysis of zebrafish receptors. To address the latter, a fibroblast zebrafish cell line was taken into account.

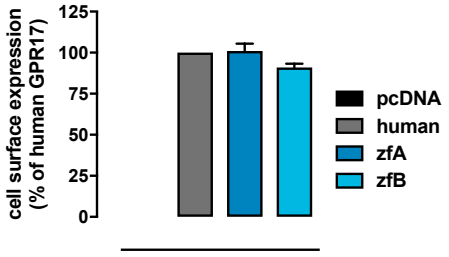

Figure 8: Quantification of cell surface expression of Gpr17 constructs displays almost equivalent expression levels in HEK293 cells. 48 h after transient transfection, cell surface expression of 3HA-tagged Gpr17 constructs was determined by ELISA. 3HA-epitope allowed a comparable quantification of protein expression in the cell membrane. Shown are representative data (means + SEM) of at least three independent experiments.

4.1.4 No expression of zebrafish Gpr17 in fibroblast zebrafish cell line

There are several publications studying zebrafish receptors in mammalian cell lines, however some of them claim about discrepancies in functional assays due to the distinct cellular background (Ringvall, Berglund and Larhammar, 1997; Starback *et al.*, 1999). To this end, a fibroblast zebrafish (PAC2) cell line, kindly provided by Prof. Dr. Foulkes of Karlsruhe Institute of Technology (KIT), was transiently transfected with human and zebrafish Gpr17 to be analysed in DMR assay for receptor function. Various amounts of DNA as well as different transfection methods were applied. Notably, it was not possible to achieve agonistic activities neither at the human (**Figure 9, B**) nor at the zebrafish Gpr17 (**Figure 9, C**). Cells lacking Gpr17 receptors (**Figure 9, A**) displayed similar trace shapes. The FCS control elicited responses on all cell lines, indicating that cell viability and assay conditions were suitable. Carbachol and ATP were unusable as positive controls, since their receptors are not expressed in this zebrafish cell line.

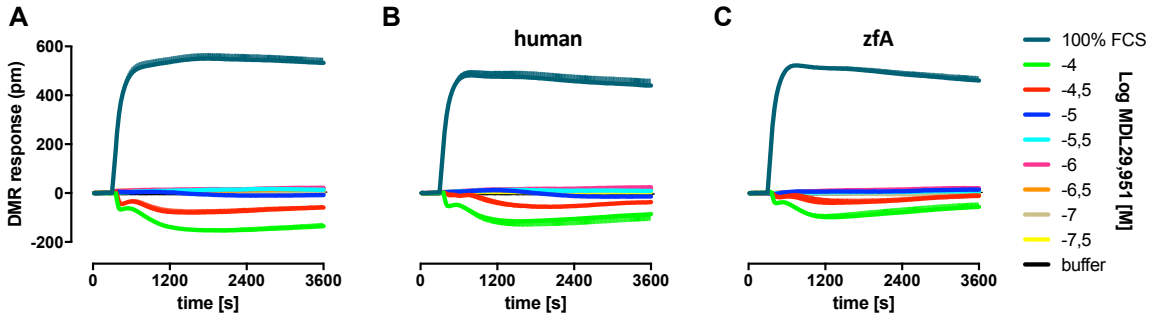

Figure 9: MDL29,951 does not elicit Gpr17 specific DMR responses in zebrafish PAC2 cells. The agonist was applied in increasing concentrations to PAC2 cells that were either untransfected (**A**) or transiently transfected (FuGENE) with human (**B**) and zfA (**C**) Gpr17. FCS control signals were not influenced by the absence or the presence of Gpr17 receptors. DMR responses were recorded for 3600 s. Shown are representative traces (means + SEM) of three independent experiments.

Given this pattern, cell surface expression was determined by ELISA assay. PAC2 cells revealed deficient expression of Gpr17 receptors on the cell membrane similar to empty vector control transfected cells (**Figure 10**). Thus, the lacking DMR response arose from absentee cell surface expression of Gpr17 receptors. Therefore, the need of a fish cellular background for sufficient signalling of zebrafish Gpr17 cannot be concluded from this experiment.

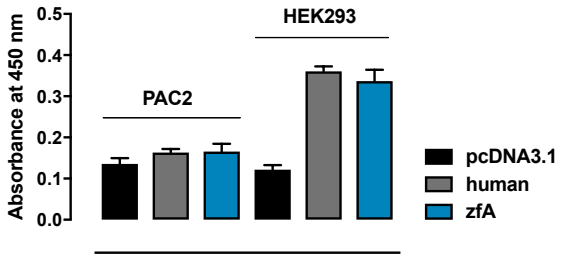

Figure 10: ELISA results display absent cell surface expression of orthologous Gpr17 receptors in PAC2 cells. Cell surface expression was measured with ELISA in fibroblast zebrafish cells and HEK293 cells transiently transfected (FuGENE) with 6 µg of 3HA-tagged Gpr17 receptors. Cells were seeded in a 96-well plate and 3HA-epitope was detected 48 h after transfection. While HEK293 cells revealed sufficient cell surface expression of Gpr17 receptors, expression in PAC2 cells was similar to empty vector control. Shown are the summarized mean values of one representative experiment.

4.2 Analysis of zebrafish embryos after bath treatment with MDL29,951

Since MDL29,951 failed to evoke DMR responses at zebrafish Gpr17 in mammalian HEK293 cells and investigation in a zebrafish cell line proved to be complicated, the zebrafish itself was exposed for several days to the compound. In this case, zebrafish Gpr17 was subjected to the drug in its native environment, which could provide advantages for receptor signalling.

4.2.1 Differentiation of oligodendrocytes is unaffected by MDL29,951 treatment

The use of the zebrafish as an animal to screen for compounds which modulate myelination has become increasingly popular during the last decades (Preston and Macklin, 2015). In search of potential compounds, Buckley et al. developed a screening method by counting migrating oligodendrocyte lineage cells in the dorsal region of the CNS of transgenic zebrafish embryos after bathing exposure. Drugs that significantly changed cell numbers were further investigated by quantitative Polymerase chain reaction (qPCR), revealing direct effects on myelination (Buckley *et al.*, 2010). Hence, tg(*claudink*:EGFP) zebrafish embryos were bath exposed for 96 h with 10 µM MDL29,951 and total number of *claudin K* positive cells were analyzed at 5 dpf. Since Claudin K is a myelin-associated protein, expressed in mature myelinating oligodendrocytes (Münzel *et al.*, 2012), alterations in oligodendrocyte development induced by drug treatment

should be recognized by imaging this transgenic zebrafish line. No difference in numbers of dorsally migrated cells of treated animals compared to DMSO control animals was detected (**Figure 11**). These data suggest that migration and differentiation of the oligodendrocyte lineage is not altered by MDL29,951 treatment.

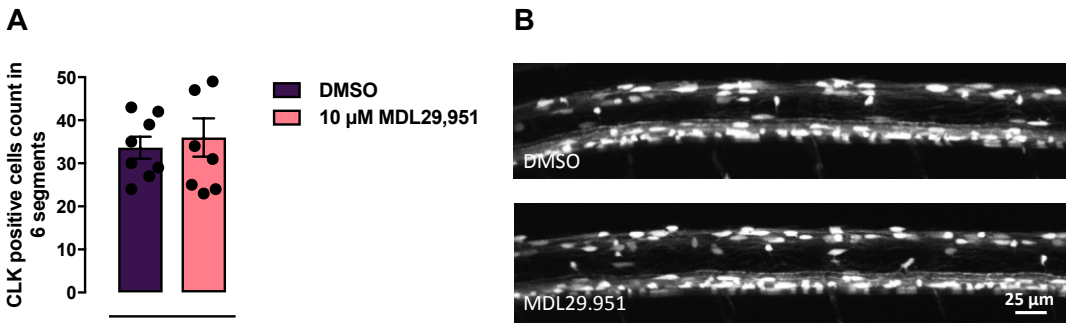

Figure 11: Bath exposure with MDL29,951 does not alter number of *claudin K* positive dorsally migrated cells. After 24 h, tg(*claudink*:EGFP) zebrafish were treated for 96 h with 10 µM MDL29,951 and imaged at 5 dpf. Numbers of dorsally migrated *claudin K* positive cells of MDL29,951 treated and DMSO control animals were almost comparable (**A**). Cells were counted in segments 1 to 6. Presented data are mean values (± SEM) and represent two independent experiments. (**B**) shows representative lateral views, anterior to the left, dorsal up, obtained by Two-photon microscopy (TriM Scope2, LaVision).

4.2.2 MDL29,951 treatment does not alter myelin gene transcripts levels

Even though MDL29,951 did not influence the number of myelinating cells, the question arose if drug treatment directly affects myelination. To this end, *mbp* and *plp* transcript levels of drug exposed and control embryos were examined by qPCR. Since cell number was not altered with 10 µM MDL29,951, embryos were treated with an additional concentration of 30 µM. Drug treatment yielded no difference in myelin gene expression levels of treated larvae compared to the controls at 5 dpf (**Figure 12**). Even the higher compound concentration was inefficient.

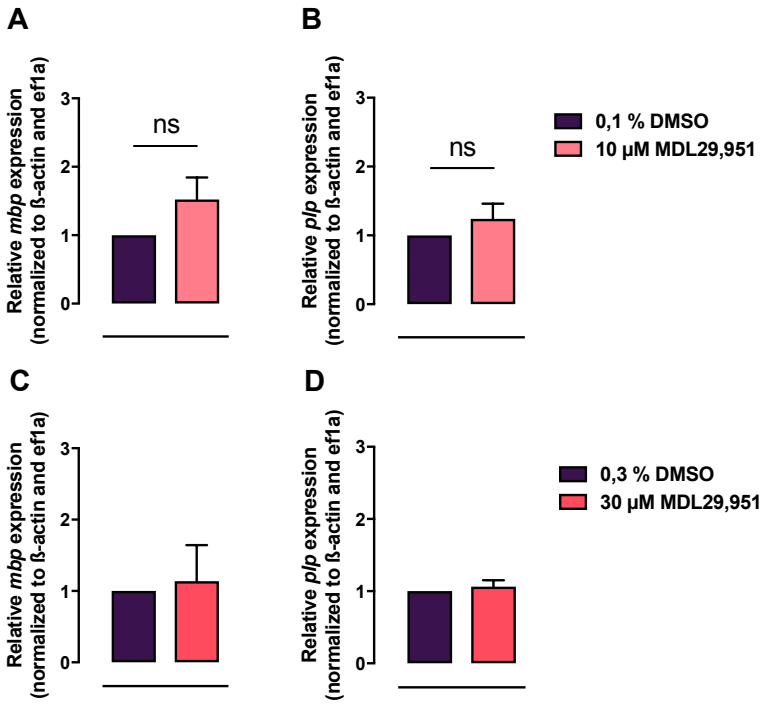

Figure 12: *Mbp* and *plp* expression levels of 5 dpf old zebrafish embryos are not influenced after MDL29,951 treatment. 1 dpf zebrafish larvae were treated for 96 h with MDL29,951 and analysed at 5 dpf by qPCR. Drug treatment with 10 and 30 µM MDL29,951 did not significantly alter *mbp* and *plp* expression levels, respectively. Data shown are mean values (+ SEM) and represent at least four independent experiments, each performed in triplicates with 25 embryos per group. ns = no significant effect to DMSO control group according to the non-parametric Mann Whitney test.

4.2.3 Myelination is not impaired after MDL29,951 treatment

To further verify preceding data, which assumed that drug treatment with MDL29,951 did not affect myelination *in vivo*, Western blot analysis were performed to quantify the expression of 36k, a short-chain dehydrogenase that is expressed in oligodendrocytes as well as in myelin sheaths in the CNS of teleosts (Morris *et al.*, 2004). In congruence with the qPCR results, application of 10 and 30 µM MDL29,951 did not modulate 36k expression levels of treated animals compared to the controls (**Figure 13**).

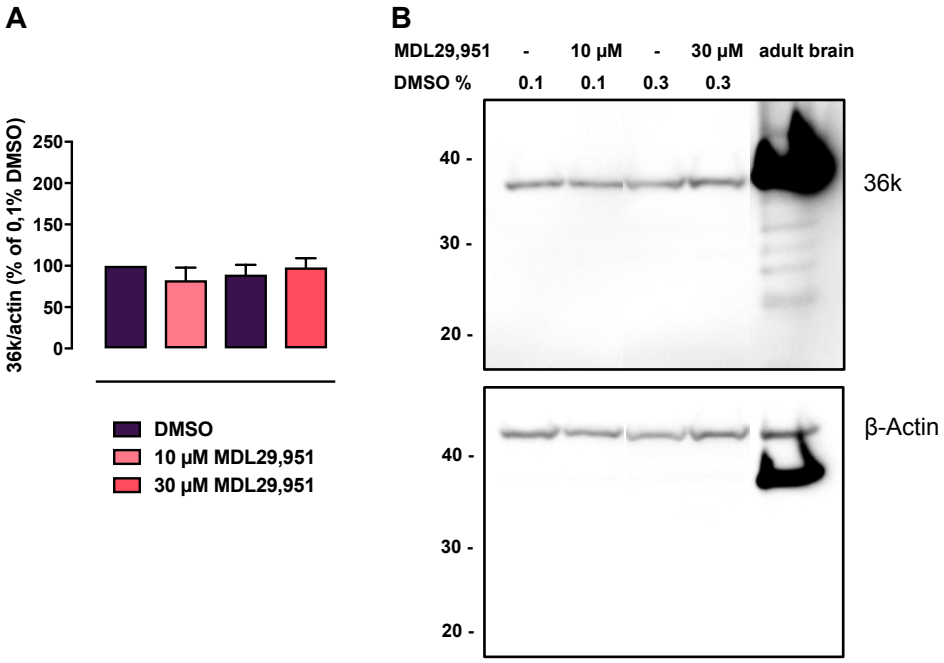

Figure 13: MDL29,951 bath exposure does not affect expression of 36k myelin protein. Western blot analysis of MDL29,951 treated zebrafish larvae revealed no difference in expression of 36k compared to control treated embryos at 5 dpf. Adult zebrafish brain served as a positive control. Shown are densitometric analysis of 36k immunoreactive bands, quantified means (+ SEM) from five independent experiments (**A**). (**B**) depicts a representative Western blot.

Taken together, these results indicate that MDL29,951 treatment does not modulate developmental myelinating processes in zebrafish, neither by altering migration or differentiation of oligodendrocyte lineage cells nor by directly effecting myelin gene expression. Furthermore, this correlates with the *in vitro* results generated in HEK293 cells, where the activation of zebrafish Gpr17 by the agonist could not be portrayed. Therefore, the notion became more evident that the unresponsiveness of zebrafish Gpr17 could arise from impaired ligand binding. Nonetheless, the actual reason could not be firmly concluded.

4.3 Construction and functional analysis of chimeric receptors

Previous experiments suggested that the unresponsiveness of zebrafish Gpr17 versions could be a consequence of impaired ligand binding. To address this, chimeric GPCRs containing the extracellular domains and transmembrane regions of the human Gpr17 and intracellular loops of the zebrafish receptors (h+zfA; h+zfBGpr17) were constructed (**Figure 14**). Additionally, chimeric receptors consisting of zebrafish Gpr17 with intracellular loops of the human Gpr17 (zfA+h; zfB+hGpr17) were generated and analysed upon expression in HEK293 cells by DMR, ELISA and ICC assays.

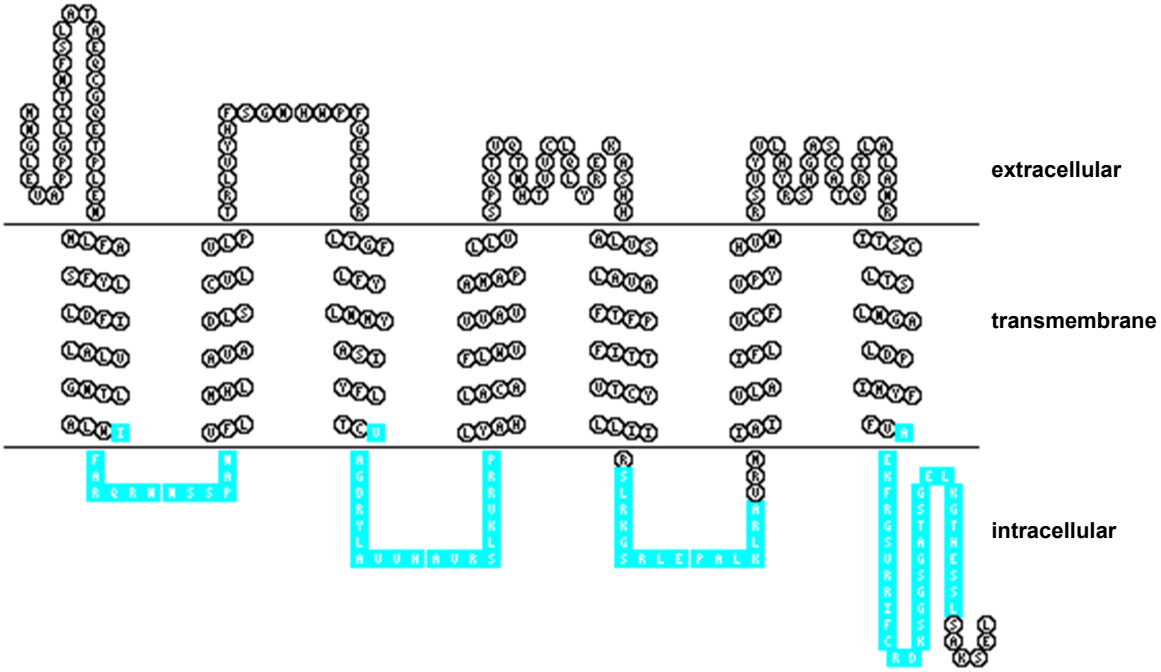

Figure 14: Schematic prediction of chimeric h+zfAGpr17 receptor topology in the cell membrane. Chimeric receptors were constructed by replacing the intracellular loops of the human Gpr17 (black) by the loops of the zebrafish Gpr17 receptors (cyan). Shown is a representative prediction schematic of h+zfAGpr17. Receptors were produced and codon optimized for zebrafish by GeneCust. For prediction HMMTOP software was used.

4.3.1 Chimeric receptors are localized in the cell surface membrane

Thus far, it was examined that the native zebrafish Gpr17 receptors were expressed in the membrane of HEK293 cells, although no functionality was observed after stimulation with the agonist MDL29,951. To validate if the HA-tagged chimeric receptors were equally expressed on the cell surface, ICC analysis with an antibody directed against the 3HA-epitope was performed. The obtained data revealed that all four chimeric receptors, transiently transfected in HEK293 cells, were located in the cell surface membrane (**Figure 15, B, C, E, F**).

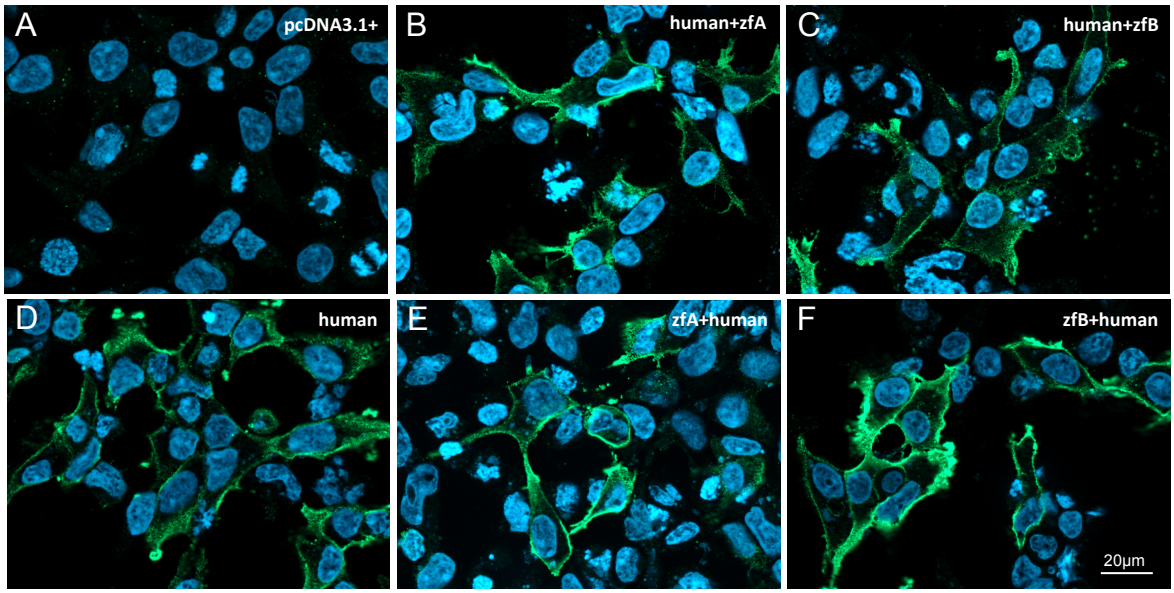

Figure 15: Chimeric Gpr17 receptors are expressed in the cell surface membrane of transiently transfected HEK293 cells. HEK293 cells, transiently transfected with the four chimeric Gpr17 receptors, revealed receptor localisation on the cell membrane (**B, C, E, F**). Receptors were marked by their N-terminal 3HA-Tag, 48 h after transfection. A secondary Cy2-conjugated goat anti-mouse antibody finally led to signals obtained by fluorescent microscopy. Control transfection with human Gpr17 displayed comparable expression (**D**), while cells transfected with empty vector revealed no specific fluorescence (**A**). Shown pictures represent at least three independent experiments.

To further monitor quantitative changes in receptor cell surface expression levels, HEK293 cells transiently transfected with Gpr17 constructs were cultured for 48 h and analysed by ELISA assays. All chimeric receptors displayed declined expression in the cell membrane compared to artless Gpr17 orthologous (**Figure 16**).

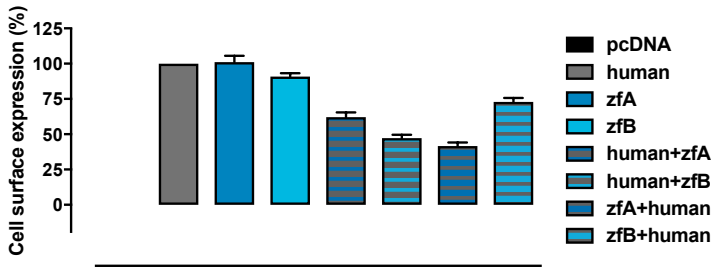

Figure 16: Cell surface expression of chimeric Gpr17 constructs was declined compared to artless Gpr17 orthologous. HEK293 cells transiently expressing 3HA-tagged Gpr17 constructs were investigated 48 h after transfection by ELISA assays. Attenuated cell surface expression levels of chimeric constructs compared to human and zebrafish Gpr17 were observed. Shown are the summarized means (+ SEM), performed in three independent experiments, each in triplicate.

4.3.2 MDL29,951 induces concentration-depended DMR responses at human Gpr17 with intracellular loops of zebrafish receptor

Both ICC and ELISA assays revealed that the chimeric receptors were expressed in the cell surface membrane. To investigate whether these receptors are functional, transiently transfected HEK293 cells were examined by DMR assays. Cell lines expressing human Gpr17 with intracellular loops of zfA (**Figure 17, A**) or zfBGpr17 (**Figure 17, B**) generated label-free responses to MDL29,951 in a concentration-dependent manner, although the responses were diminished compared to human Gpr17 (**Figure 17, C, F**). To the contrary, zfA (**Figure 17, D**) and zfB (**Figure 17, E**) Gpr17 containing intracellular loops of human Gpr17 remained unresponsive to the agonist. Finally, these data argued for an impaired binding of MDL29,951 at the zebrafish receptors.

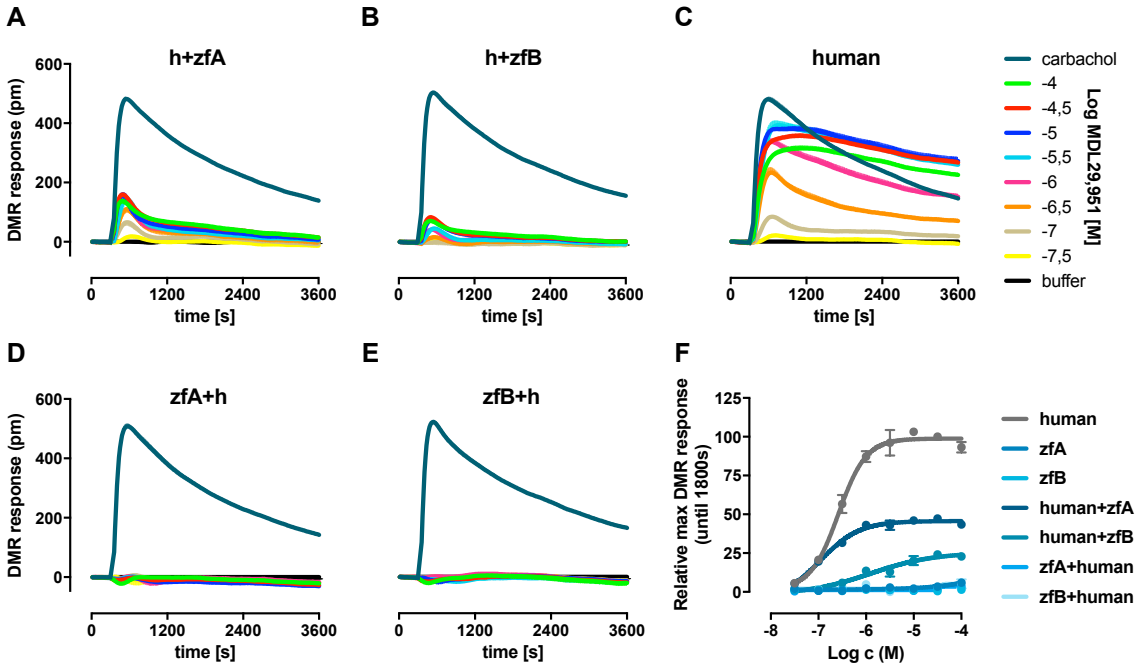

Figure 17: MDL29,951 evokes DMR responses on human Gpr17 containing intracellular loops of zebrafish Gpr17. 48 h after transfection of HEK293 cells, functional analysis of chimeric Gpr17 receptors was performed by DMR. Responses to MDL29,951 and carbachol were recorded over 3600 s. The agonist induced diminished traces at h+zfA (**A**) and h+zfB (**B**) Gpr17s compared to human Gpr17 (**C**), while zfA+h (**D**) and zfB+h (**E**) Gpr17 remained unresponsive. Shown are representative traces (means + SEM) of at least three independent experiments. (**F**) Concentration-effect curves are mean values (± SEM).

Taken together, these observations lead to the assumption that MDL29,951 did not activate zebrafish Gpr17 receptors both *in vitro* and *in vivo* analysis. Given the functionality of chimeric receptors containing the human agonist binding side, it becomes more evident that impaired ligand binding provoked the lack of activity at the fish receptors.

Moreover, the data displayed that the h+zfA and h+zfB chimeric Gpr17 receptors retained wild type characteristic, even though functionality was attenuated. Since MDL29,951 did not induced effects *in vivo*, it might be possible that MDL29,951 treatment on zebrafish transiently expressing the chimeric Gpr17 receptors causes alterations in myelination. If this proves to be true, the chimeric receptors could represent new valuable tools for screening of compounds with activity on human Gpr17 that promote remyelination in humans. But first as a matter of principle, the role of zebrafish Gpr17 *in vivo* has to be examined.

4.4 Gpr17 expression in zebrafish

While preceding investigations have focused on the functional analysis of zebrafish Gpr17, this chapter will explore the temporal and local expression of Gpr17 *in vivo*.

4.4.1 Whole-mount in situ hybridization reveals *gpr17* expression during oligodendrocyte development

Previously published data indicate that Gpr17 is abundant in pre-oligodendrocytes (pre-OLs) during mouse CNS development, but not detectable in mature oligodendrocytes (Chen *et al.*, 2009). Since the zebrafish represent an ideal model system to study oligodendrocyte development and myelination *in vivo* (Preston and Macklin, 2015), *gpr17* RNA expression in zebrafish embryos was determined by Whole-mount in situ hybridization (WISH).

Robust *Gpr17 expression* was found throughout the CNS from 1 to 5 dpf. Initially, a diffuse distribution of RNA was observed in all regions of the spinal cord, in the ventral and the dorsal, as well as in the primary motor neuron domain (pMN) of the neural tube (**Figure 18, A**). At 2 dpf, when oligodendrocyte precursor cells (OPCs) specify (Kirby *et al.*, 2006), mainly the pMN domain displayed high *gpr17* expression levels (**Figure 18, B**), that shifted to the dorsal area of the spinal cord, once OPCs actively start migrating and dividing, and persisted until 5 dpf (**Figure 18, C - E**). Sense control animals did not exhibit any signal, indicating that the staining specifically portrayed *gpr17* expression (**Figure 18, E**). Since expression appeared only in the spinal cord midline (**Figure 18, G-K**), it can be concluded that *gpr17* is abundant in the CNS, while missing in the PNS.

These findings demonstrate *gpr17* expression within the CNS, particularly in dorsal migrating oligodendrocyte-like cells.

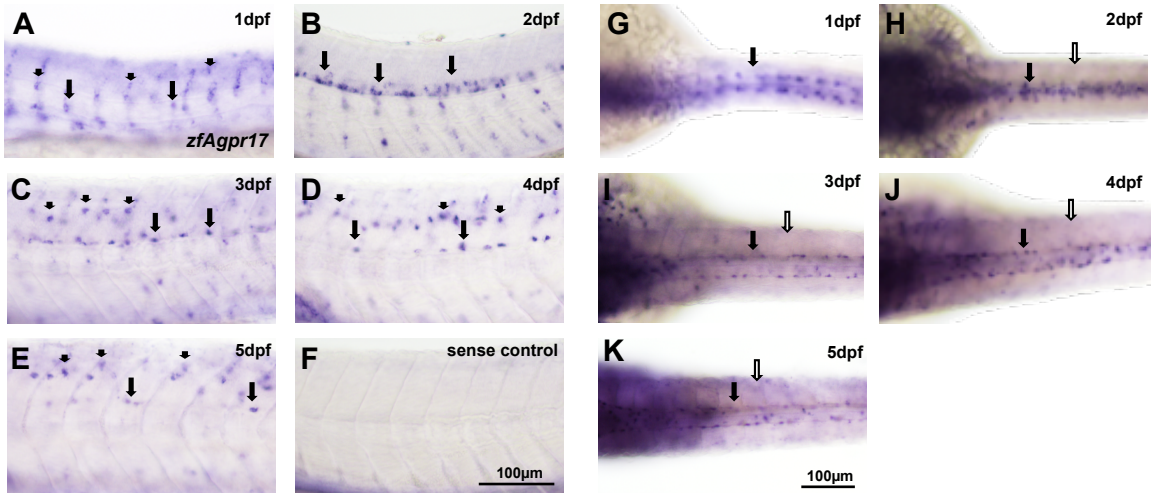

Figure 18: WISH of 1 to 5 dpf old zebrafish larvae reveals *zfAgpr17* expression within the CNS. (**A-E**) Lateral views (dorsal up, anterior to the left) show *gpr17* expression in the pMN region (big arrows) and the dorsal spinal cord (small arrows) of 1 to 5 dpf old zebrafish embryos. (**G-K**). Dorsal views (anterior to the left) depicted *gpr17* expression in the CNS (black arrows), while it was missing in the PNS (white arrows). Images are shown represent at least four independent experiments.

To prove Gpr17 localisation in oligodendrocyte lineage cells, zebrafish were treated with Trichostatin A (TSA), a histone deacetylase inhibitor. Takada et al. (2010) asserted that dorsal migration of OPCs is prevented with TSA. Assuming that Gpr17 is expressed in OPCs, expression of *gpr17* was expected to be vanished in the dorsal spinal cord after treatment with TSA. Indeed, zebrafish treated with TSA revealed significantly decreased *gpr17* expression in the dorsal region of the spinal cord compared to control animals at 4 dpf ($P<0.0001$, student's t-test) (**Figure 19**). In conclusion, our findings strongly suggest that *gpr17* is expressed in dorsally migrating OPCs.

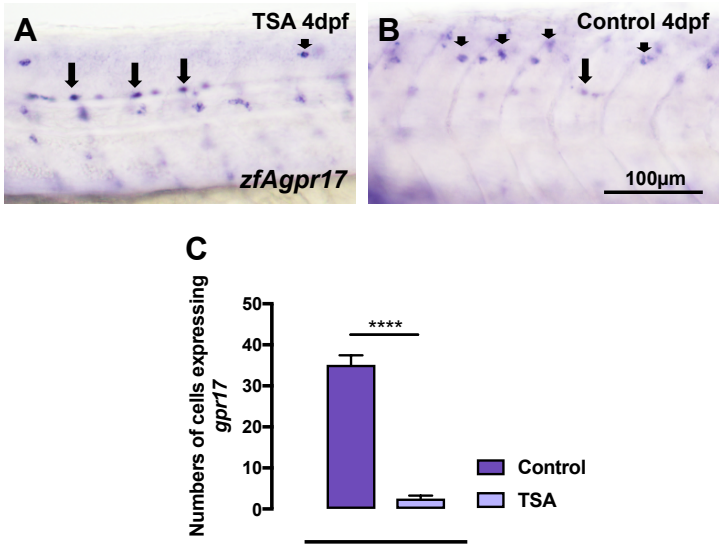

Figure 19: *ZfAgpr17* expression is missing in dorsal spinal cord after Trichostatin A treatment. 4 dpf old zebrafish larvae displayed significantly diminished *gpr17* expression (**C**) in the dorsal region of the spinal cord after treatment with TSA (**A**), while control animals (**B**) depicted normal localization in both dorsal and pMN regions. Data are shown as mean values (+ SEM) from three independent experiments. ****; $p<0.0001$ according to student's t-test.

4.4.2 Gpr17 protein is expressed during zebrafish embryogenesis

In addition to preceding findings displaying the presence of *gpr17* RNA in oligodendrocyte lineage cells, expression of Gpr17 protein was analysed by Western blot analysis. To this end, equal amounts of total protein lysates were isolated from entire embryos at different ages. Throughout the time course, immunoreactive bands at sizes around 40 kDa were detected in samples harvested as early as 3 dpf. After 72 hpf, zfAGpr17 levels increased until 10 dpf, however the band with the highest size disappeared (**Figure 20, A**). Notably, lysates of adult zebrafish brain lacked zfAGpr17 (**Figure 20, B**). These results support the notion that Gpr17 plays a role during CNS development.

On the contrary, zfBGpr17 could not be portrayed by WISH and Western blot analysis. Hence, the following *in vivo* experiments mainly focused on zfAGpr17.

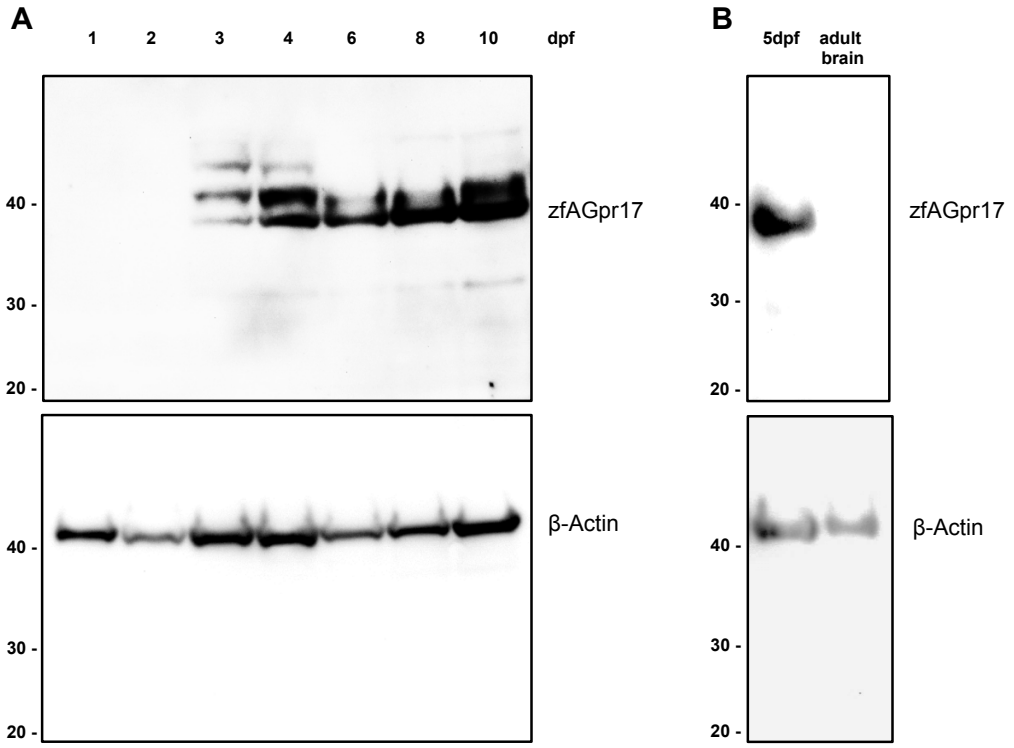

Figure 20: ZfAGpr17 is expressed during oligodendrocyte development. Western blot analysis of Gpr17 expression in zebrafish larvae, harvested at different time points displayed protein expression from 3 to 10 dpf (**A**), while protein was absent in adult brain (**B**). Shown are representative Western blots of three independent experiments.

4.5 Role of Gpr17 in zebrafish

Given the expression pattern of *gpr17* in the developing CNS of zebrafish, the question arose whether Gpr17 may influence oligodendrocyte development. To this end, transient overexpression (OE) and morpholino (MO) knockdown studies served as tools for exploring the role of Gpr17 in zebrafish.

4.5.1 Transient overexpression of Gpr17 in zebrafish embryos does not affect oligodendrocyte development and myelination

Since oligodendrogenesis in zebrafish is accompanied by coordinated expression of distinct transcription factors and proteins (Kirby *et al.*, 2006; Monk and Talbot, 2009; Münzel *et al.*, 2012), effects on oligodendrocyte progression and myelination induced by OE of Gpr17 were determined by several strategies including marker analysis and imaging of fluorescent zebrafish lines at different developmental time points.

4.5.1.1 Evaluation of RNA amount used in OE studies

To identify the suitable RNA concentration for transient OE experiments, mortality rates and phenotypes of tg(*olig2:EGFP*) zebrafish embryos, injected with increasing concentrations of *zfA* and *zfBgpr17* were determined. Since preceding experiments displayed abundances of *gpr17* in dorsally migrating OPCs, numbers of *olig2* positive cells, which correspond to oligodendroglial cells expressing the transcription factor *olig2*, were counted in a representative region of the dorsal CNS (**Figure 21**). Finally, success of microinjection was verified by monitoring the expression of injected *tdTomato* by Two-photon microscopy.

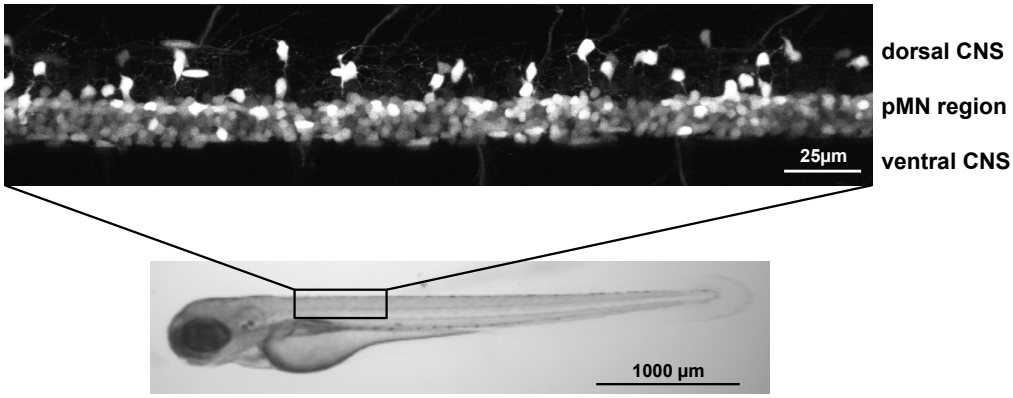

Figure 21: Representative region in the dorsal spinal cord of a 3 dpf tg(*olig2:EGFP*) zebrafish imaged by Two-photon microscopy. For overexpression and knockdown studies, cell numbers were counted in the depicted dorsal CNS region of the spinal cord that encompassed 6 segments.

Microinjections of increasing amounts of *gpr17* RNA in tg(*olig2:EGFP*) zebrafish exhibited enhanced mortality and varied phenotypes (**Figure 22, A-E**). Especially, injections of 1000 pg of *zfBgpr17* caused severe mutations and death rates in about 50 % of zebrafish embryos, while phenotypes of embryos injected with *zfAgpr17* were less pronounced. OE of *zfB* RNA did not alter numbers of dorsally located *olig2* positive cells (**Figure 22, F-I**) compared to *zfA* injections, which produced a significant decrease in cell number ($P<0.05$, one-way ANOVA) (**Figure 22, I**). However, the decrease does not necessarily relate to an effect caused by OE since the difference was only detectable with the highest concentration, which could possibly evoked toxic side effects that influenced CNS development, including cell numbers.

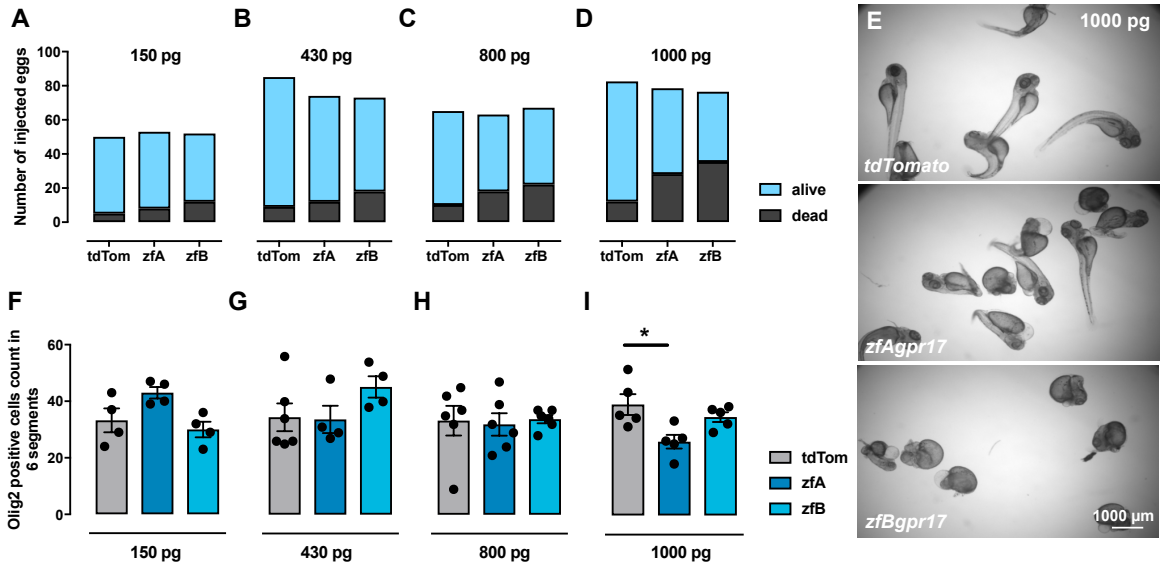

Figure 22: Calibration of RNA amount for OE studies in tg(*olig2:EGFP*) zebrafish embryos suggests 800 pg RNA. 3 dpf old zebrafish embryos, injected in the one-cell stage with increasing RNA concentrations revealed dose-dependent increases in mortality as well as severe phenotypes, while control animals displayed higher survival rates and normal phenotypes (**A-E**). Numbers of dorsally migrating *olig2* positive OPCs were not significantly altered by OE of zfA and zfBGpr17 compared to *tdTomato* injected animals (**F-I**), exclusively 1000 pg of *zfAgpr17* elicited a significant decrease in cell number (**I**). Data are shown as mean values (± SEM); each concentration presents one experiment. One-way ANOVA was used for statistical significance. *, P<0.05.

In order to verify the success of RNA expression, zebrafish embryos were additionally injected with *tdTomato*. The red fluorescent protein was expressed even in the lowest concentration of 150 pg (**Figure 23**). Furthermore, RNA stability studies with tg(*claudinK:EGFP*) zebrafish revealed stable expression of TdTomato protein over 96 h (**Supplementary Figure 1**) concluding that Gpr17 should be expressed in the same manner.

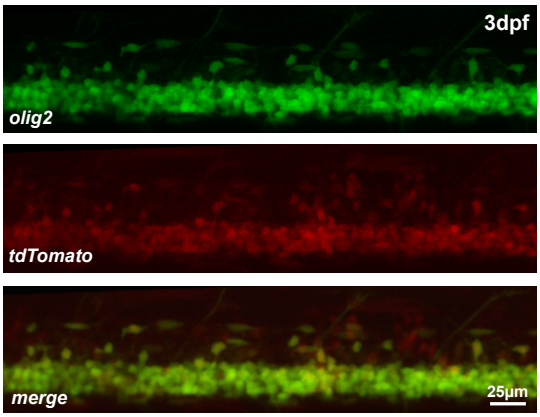

Figure 23: Stable RNA expression after microinjection of 150 pg *tdTomato* in zebrafish embryos. 3 dpf old tg(*olig2:EGFP*) zebrafish embryos, injected with 150 pg *tdTomato* exhibited stable protein expression in the spinal cord. Shown are representative images from one experiment.

The fact that *tdTomato* control injections revealed mellowed death rates compared to *gpr17* injections (**Figure 22, A-E**) infers even more that high amounts of *gpr17* influences zebrafish development in a certain manner. Hence, further OE studies were conducted with 800 pg RNA. Injected animals displayed normal phenotypes (**Figure 24**) and mortality rates about 20 %.

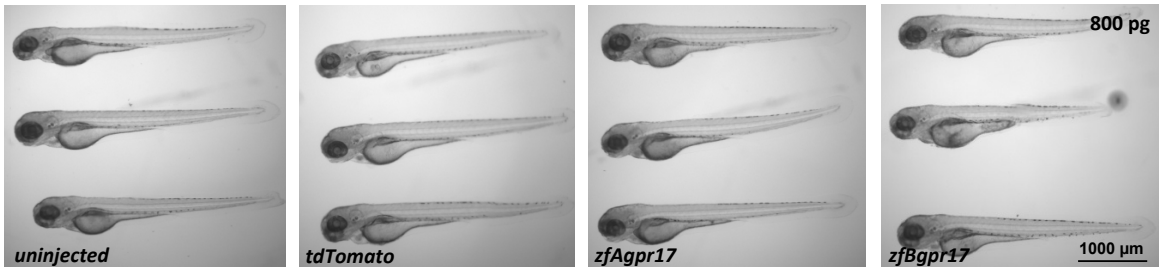

Figure 24: 3 dpf old tg(*olig2:EGFP*) zebrafish embryos display normal phenotypes after injection of 800 pg RNA. Shown are representative images of transgenic zebrafish larvae at 3 dpf, injected with 800 pg *zfA and zfBgpr17* RNA. Success of OE was verified by injection of *tdTomato* RNA.

4.5.1.2 Maturation of oligodendrocytes is not influenced by Gpr17 *OE*

Since OE of GPR17 inhibits oligodendrocyte development and myelination in mice (Chen *et al.*, 2009), it was first examined whether Gpr17 OE in zebrafish interferes with oligodendrocyte maturation. 3 dpf old tg(*claudinK:EGFP*) zebrafish, injected with 800 pg *gpr17* RNA were imaged at 3, 4 and 5 dpf by Two-photon microscopy and cell numbers were ascertained by counting *claudin K* positive cells in the dorsal region of the spinal cord. Tg(*claudinK:EGFP*) zebrafish exhibit expression of exaggerated green fluorescent protein (EGFP) that is driven by the *claudin k* promoter (Münzel *et al.*, 2012), hence EGFP is representative for the generation of Claudin k and differentiation of oligodendrocyte lineage cells. Numbers of *claudin k* positive cells did not significantly differ between *gpr17* and control injected animals, neither at 72 hpf, when OPCs start differentiating, nor at 80 and 96 hpf, when first myelin sheaths are constructed (**Figure 25**). Uninjected animals revealed equal cell numbers, indicating that injection procedure had no effect on oligodendrocyte development.

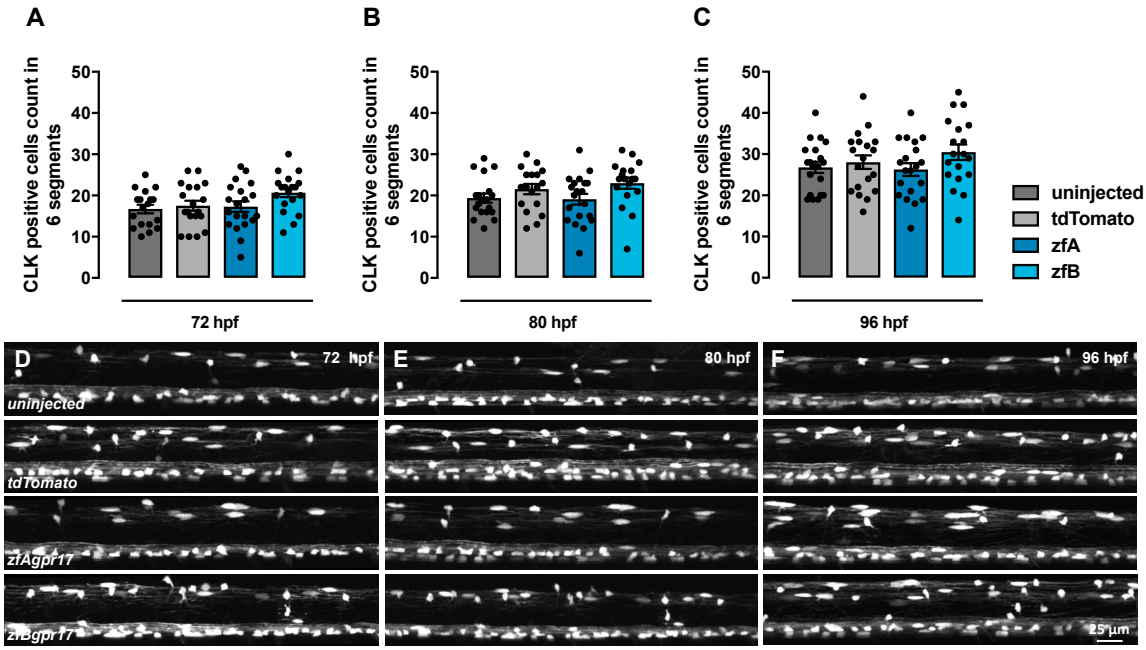

Figure 25: Maturation of oligodendrocyte lineage cells expressing *claudin k* is not altered by Gpr17 OE. Tg(*claudink:EGFP*) zebrafish, injected with 800 pg RNA were imaged by Two-photon microscopy at 72 (**A**), 80 (**B**) and 96 hpf (**C**). Numbers of dorsally migrated *claudin k* positive cells did not differ between *gpr17* injected, control injected and uninjected animals at any time point. Data are presented as mean values (± SEM) of at least four independent experiments. (**D,E,F**) show representative lateral views (anterior to the left, dorsal up).

4.5.1.3 Gpr17 OE does not impair expression of myelin proteins

To question whether unaltered numbers of myelinating oligodendrocytes in overexpressed zebrafish mirror myelin formation, expression of myelin proteins was analysed by Immunohistochemistry (IHC) and Western blot analysis. At first, expression of Myelin basic protein (Mbp) was determined in the spinal cord of 4 dpf old RNA injected zebrafish larvae by Whole-mount IHC analysis. By using an antibody to Mbp, generated data revealed that OE did not alter expression of Myelin protein in the anterior (**Figure 26, A**) and middle region of the spinal cord (**Figure 26, B**) compared to control injected and uninjected embryos.

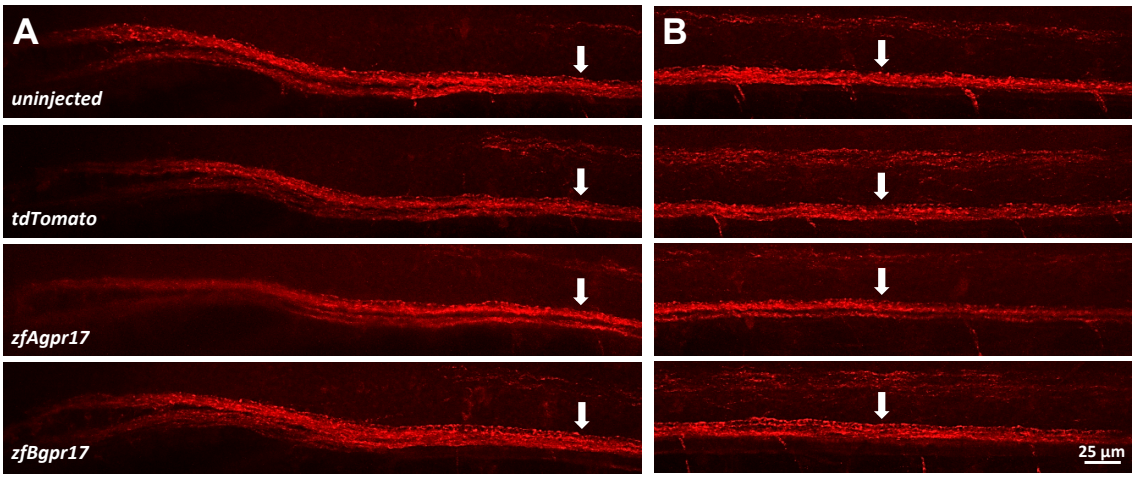

Figure 26: OE of Gpr17 does not alter myelination in 4 dpf old zebrafish larvae. Shown are representative images of Mbp expression in the spinal cord of 4 dpf old zebrafish, injected with 800 pg *zfA and zfBgpr17.* Injected zebrafish exhibited no difference in Myelin basic protein expression in the anterior (**A**) and the middle (**B**) region of the spinal cord compared to *tdTomato* injected and uninjected animals, evaluated by immunolabelling for Mbp. Data are shown are lateral views (dorsal up, anterior to the left) from two independent experiments.

Furthermore, Western blot analysis, evaluating the expression of myelin-associated protein Claudin K (Münzel *et al.*, 2012) (**Supplementary Figure 2**), displayed no difference in expression levels between *gpr17* injected and control injected animals at 4 dpf (**Figure 27**). These results suggest that OE of Gpr17 does not influence the expression of myelin proteins in 4 dpf zebrafish embryos.

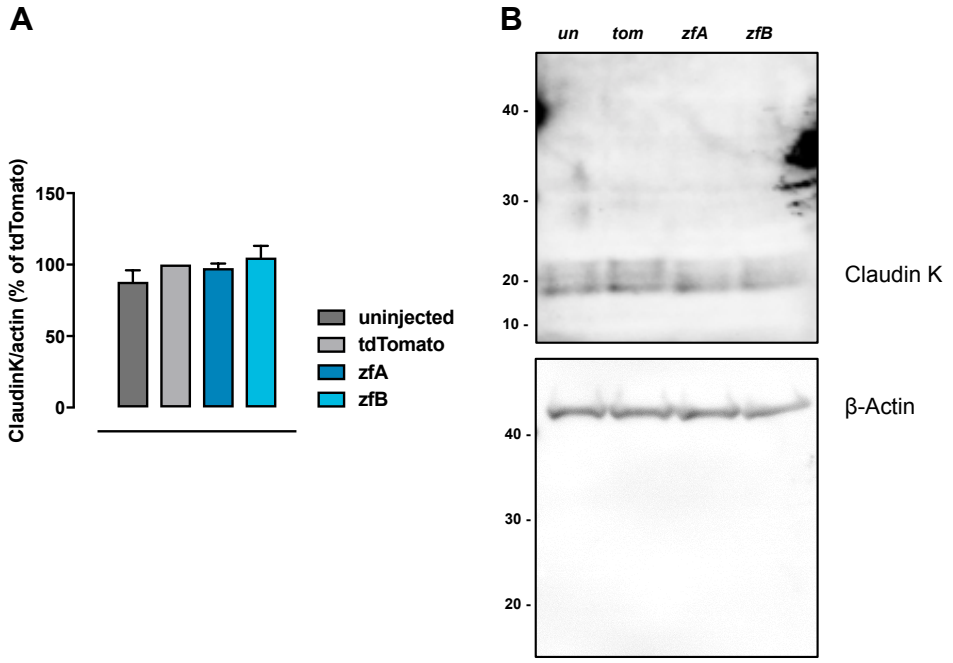

Figure 27: 4 dpf old zebrafish larvae exhibit no difference in Claudin K expression levels after Gpr17 OE. Quantitative evaluation of 4 dpf old zebrafish larvae, injected with 800 pg *gpr17* RNA displayed no difference in expression of myelin protein Claudin K compared to control animals (**A**). (**B**) shows illustrative Western blot from four separate experiments. Data are shown as mean values (+ SEM). *un*= uninjected animals, *tom*= tdTomato injected animals.

4.5.1.4 OE of Gpr17 does not alter number of olig2 positive dorsally migrated OPCs

To ascertain whether OE directly effects development of OPCs, tg(*olig2:EGFP*) zebrafish were injected with 800 pg RNA and imaged by Two-photon microscopy not only at 3 dpf but also 2 dpf, when OPCs proliferate and begin to migrate dorsally. Although a wide dispersion was obtained, no significant difference in numbers of dorsally migrated *olig2* positive cells between *gpr17* and control injected animals was found (**Figure 28**).

To sum up, data obtained with transgenic zebrafish lines demonstrate that OE of Gpr17 does not disturb migration and differentiation of oligodendrocyte lineage cells.

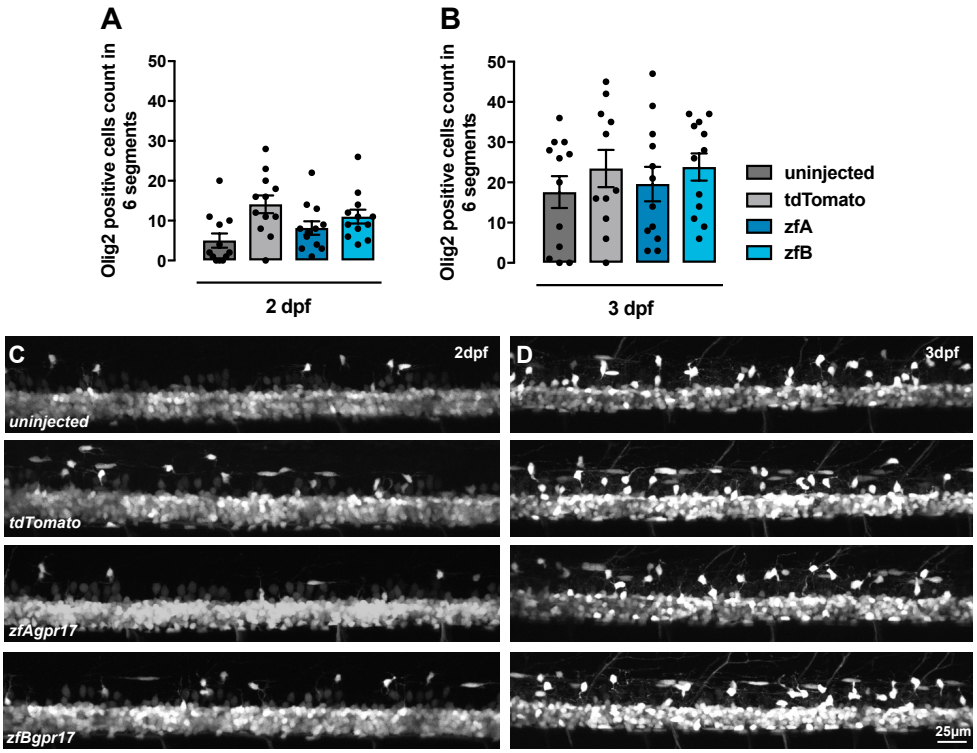

Figure 28: Oligodendrocyte lineage cells expressing transcription factor *olig2* display normal migration after Gpr17 OE. Numbers of *olig2* positive dorsally migrated cells revealed no significant difference between *gpr17* and *tdTomato* (800 pg) injected zebrafish embryos at 2 and 3 dpf (**A,B**). Shown are quantified data (means ± SEM) and representative lateral views (dorsal up, anterior to the left) (**C,D**) of at least three independent experiments.

4.5.1.5 Myelin gene expression levels are unaffected by Gpr17 OE

To evaluate the effect of Gpr17 OE on *mbp* and *plp* expression levels, WISH and qPCR experiments were implemented. To this end, injected zebrafish embryos were analysed at 3 and 4 dpf, at the time when myelination initiates. At both days, myelin gene expression levels were not significantly altered between *gpr17* and control group, as measured by qPCR (**Figure 29**). Even the slight increase in *plp* expression in 4 dpf old animals displayed no significant upregulation (**Figure 29, D**). Again, myelin protein expression in control injected animals resembled expression in uninjected animals, indicating that injection procedure did not influence RNA expression.

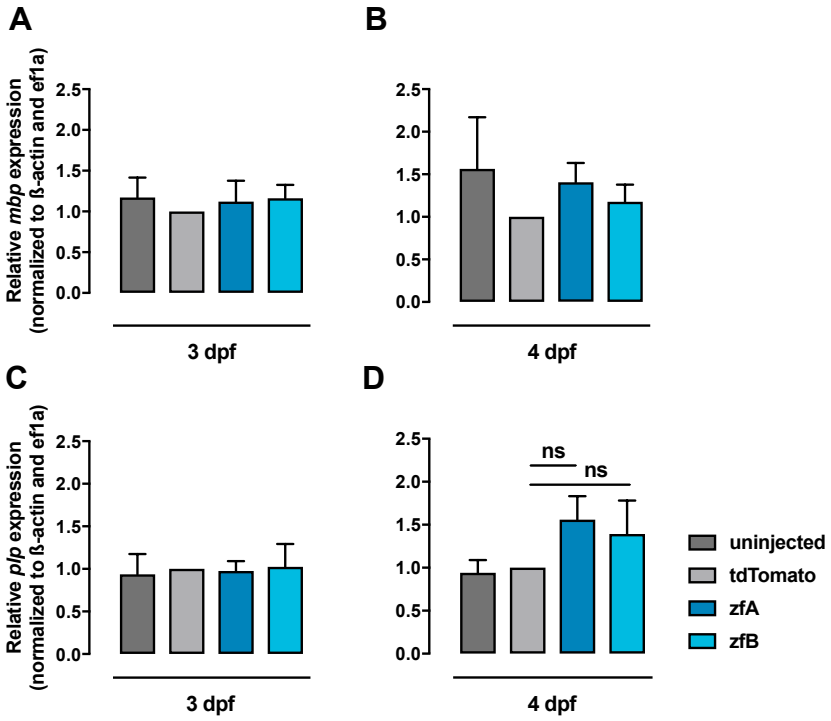

Figure 29: Quantitative polymerase chain reaction revealed no difference in expression levels of myelin proteins *mbp* and *plp* after Gpr17 OE. Zebrafish embryos, injected with 800 pg RNA were analysed at 3 and 4 dpf by qPCR. Expression levels of *mbp* (**A, B**) and *plp* (**C, D**) were not significantly altered between all groups. Mean values (+ SEM) of four independent were summarized, each performed in triplicates with 25 zebrafish per group. ns = no significant effect to *tdTomato* injected zebrafish according to the non-parametric Kruskal-Wallis test.

Consistent with the qPCR data presented above, *mbp* expression ascertained by WISH showed no difference, whether in the CNS including spinal cord and brain regions, nor in the PNS of 3 and 4 dpf zebrafish embryos (**Figure 30**).

Taken together these findings indicate that OE of Gpr17 does not affect transcription of myelin proteins *mbp* and *plp*.

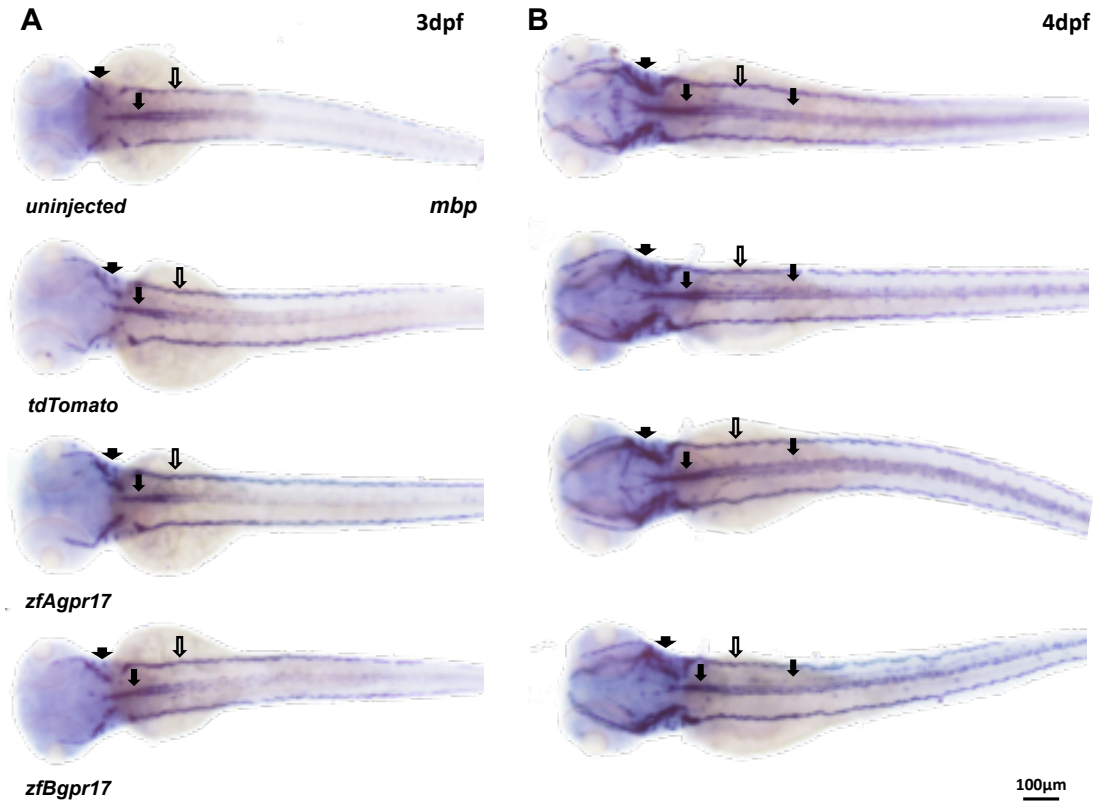

Figure 30: *Mbp* expression pattern determined by WISH is not influenced by Gpr17 OE. WISH of 3 and 4 dpf old zebrafish embryos revealed similar expression of *mbp* in the CNS at the level of the spinal cord (small black arrows) and brain (big black arrows) as well as in the PNS (white arrows). Panels show representative images (dorsal up) of two independent experiments.

4.5.1.6 Initiation of oligodendrocyte differentiation is not impaired by Gpr17 OE

During oligodendrocyte progression, maturation of oligodendrocyte lineage cells is controlled in addition to others by the expression of the transcription factor Nkx2.2. OPCs expressing Nkx2.2 turn into pre-OLs and finally into mature myelinating oligodendrocytes, while OPCs lacking Nkx2.2 remain as non-myelinating progenitor cells (Kucenas, Snell and Appel, 2010). Since preceding results of this thesis demonstrated that both, generation of OPCs and differentiation into myelinating oligodendrocytes are not impaired by Gpr17 OE, it was to investigate whether OE influences the initial stage of differentiation at the level of *nkx2.2* expressing pre-OLs. Therefore, WISH of 2.5 dpf old zebrafish embryos was conducted. Expression of *nkx2.2* gene in the CNS of zebrafish overexpressing Gpr17 did not differ from control injected animals (**Figure 31**). These findings indicate that the generation of pre-OLs is not altered by Gpr17 OE.

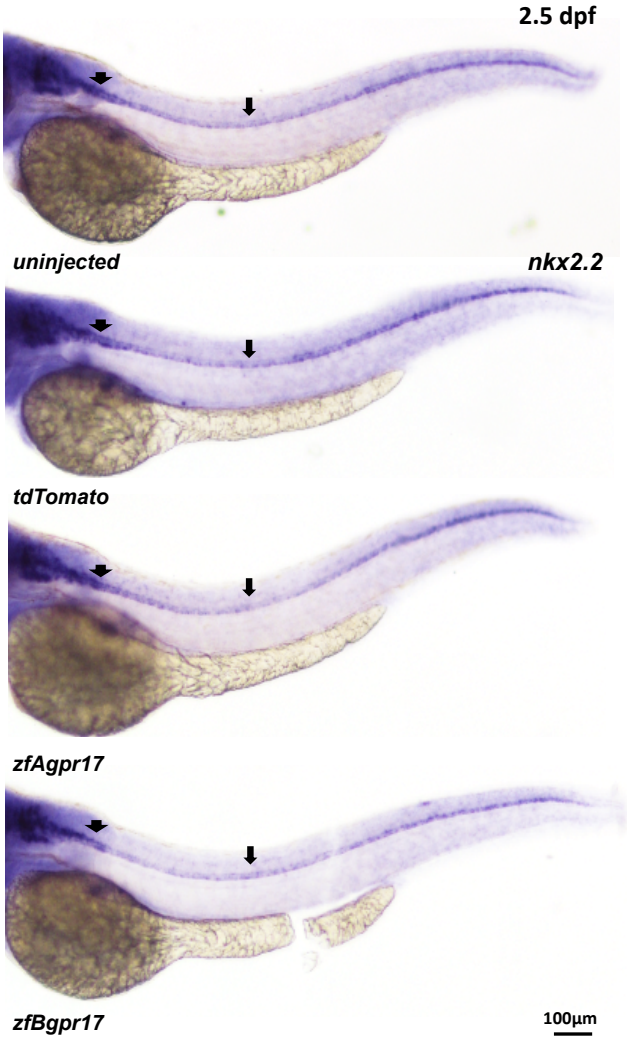

Figure 31: WISH of 2.5 dpf old zebrafish embryos displays equal *nkx2.2* expression in the CNS. WISH images of zebrafish embryos showed no difference in *nkx2.2* expression between *gpr17* and control injected animals (800pg) in the CNS at 2.5 dpf. Depicted are representative images of at least two independent experiments.

To sum up, these data indicate that OE does not affect oligodendrocyte development, neither by changing maturation of oligodendrocyte lineage cells nor by altering their function to myelinate axons. Hence, previous published data sets obtained in mice, indicating that Gpr17 OE inhibits onset of myelination cannot not be confirmed by using zebrafish as model species.

4.5.2 *ZfAgpr17* morpholino injections in zebrafish embryos causes reduced oligodendrocyte numbers and an impaired myelination

The fact that Gpr17 OE did not alter oligodendrocyte formation, differentiation and myelination in zebrafish argues against zebrafish as a suitable model to study Gpr17 *in vivo*. Nevertheless, to definitively decipher the role of this receptor in zebrafish, a morpholino-modified antisense oligonucleotide mediated gene knockdown (Corey and Abrams, 2001) was generated (**Figure 32**). Since zebrafish A version (zfA) of Gpr17 is highly conserved from zebrafish to human showing 56 % homology with the human Gpr17, all knockdown studies were conducted with a morpholino that inhibited the translation of *zfAgpr17*. Thereby, zebrafish embryos were injected at the one-cell stage and effects on oligodendrocyte progression were evaluated by distinct methods throughout the first days of development.

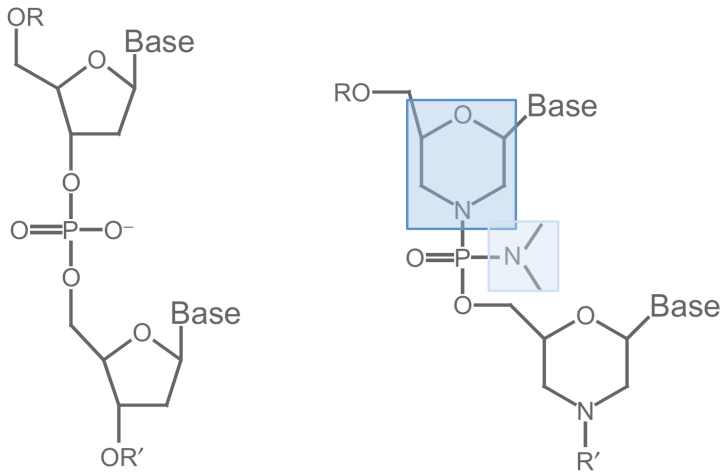

Figure 32: Structure of morpholino antisense oligonucleotide and native DNA. 25 base pairs long morpholino antisense oligonucleotides containing an altered backbone bind to complementary DNA and inhibit the translation process. Figure adapted from (Corey and Abrams, 2001).

4.5.2.1 Morpholino injected animals display smaller sizes and heart oedema

Injections of 2.75 ng *zfAgpr17* morpholino (MO) at the one-cell stage of zebrafish embryos caused weak phenotypes, exhibiting smaller sizes and heart oedema, while control MO injected compared to uninjected animals did not display any abnormalities (**Figure 33**). However, because the survival rate of *zfAgpr17* morphants compared to control and uninjected animals was not significantly altered, all knockdown experiments were conducted with 2.75 ng *zfAgpr17* MO (Reinoß, 2014; Kleinert, 2018).

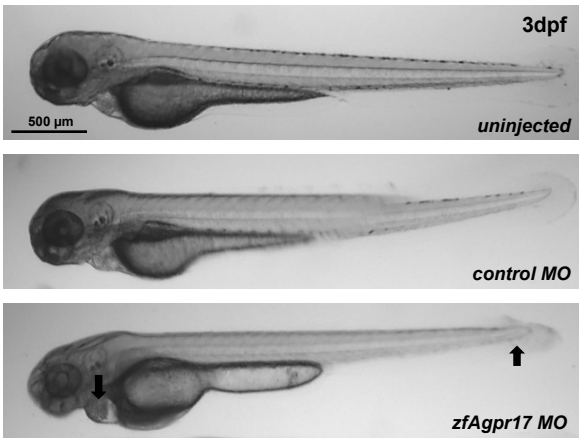

Figure 33: *ZfAgpr17* morpholino injections cause weak phenotypes. Wild type zebrafish injected with 2.75 ng *zfAgpr17* MO displayed weak phenotypes including smaller size and heart oedema compared to control MO injected and uninjected zebrafish. Shown are representative images of at least three independent experiments.

4.5.2.2 Western blot analysis confirm zfAGpr17 knockdown

To verify the specificity of *zfAgpr17* MO, zfAGpr17 expression in 3, 4 and 5 dpf old zebrafish embryos was determined by Western blot analysis after injection of 2.75 ng MO. Protein analysis revealed a decrease in Gpr17 expression levels in zfAGpr17 morphants compared to control animals (**Figure 34**). However, the reduction displayed only significance in 4 dpf old embryos ($P<0.05$, two-way ANOVA) (Kleinert, 2018).

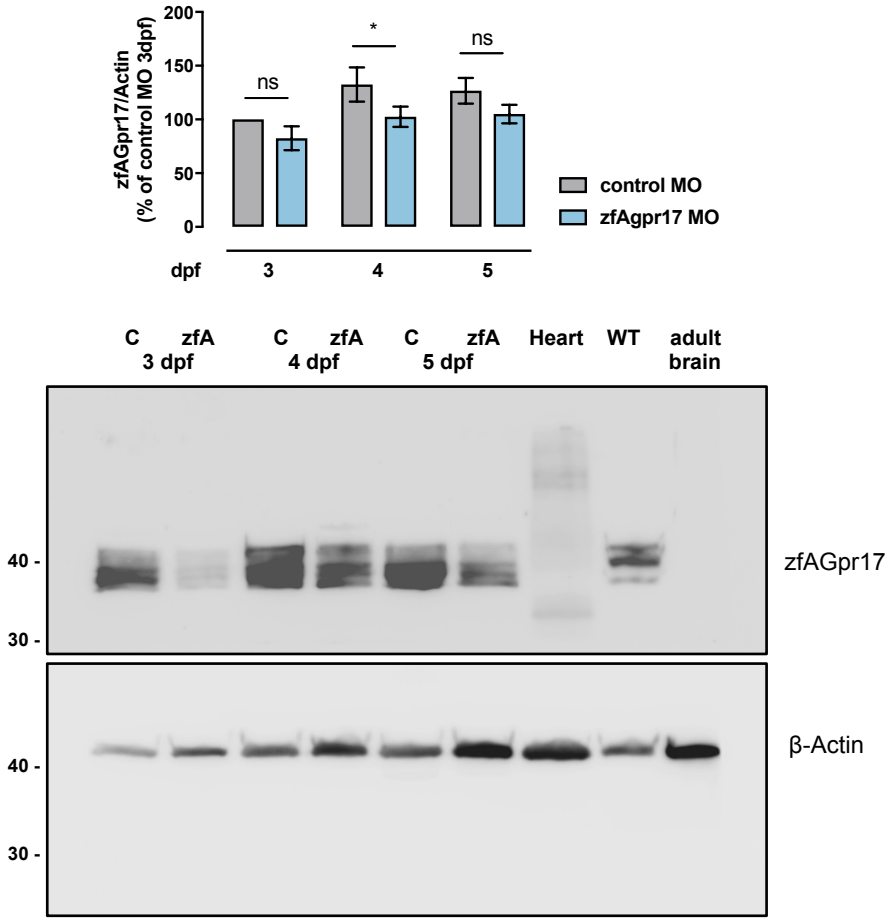

Figure 34: Western blot analysis reveal Gpr17 knockdown after injection of *zfAgpr17* morpholino. Zebrafish embryos injected with 2.75 ng *zfAgpr17* MO displayed decreased Gpr17 expression levels compared to control and uninjected animals, while reduction was only significant in 4 dpf old embryos (Kleinert, 2018). Shown are mean values (+ SEM) from four independent experiments. Two-way ANOVA test was used for statistical significance. *, P<0.05. Data were generated by Philip Reinoß in the Institute of Anatomy, University of Bonn.

ZfAGpr17 knockdown causes impaired expression of myelin proteins in the CNS

Regarding previously published data that demonstrated an early onset of myelination in Gpr17 knockout mice (Chen *et al.*, 2009), expression of myelin proteins in zfAGpr17 morphants was analysed by Whole-mount IHC and Western blot assays.

Using an anti-Mbp antibody, Myelin basic protein expression was imaged in the spinal cord of 4 dpf old zebrafish embryos. By comparison to control MO and uninjected animals a significant decrease in Mbp signal ($P<0.05$, one-way ANOVA) was found in the anterior and middle region of the spinal cord of embryos injected with *zfAgpr17* MO (**Figure 35**).

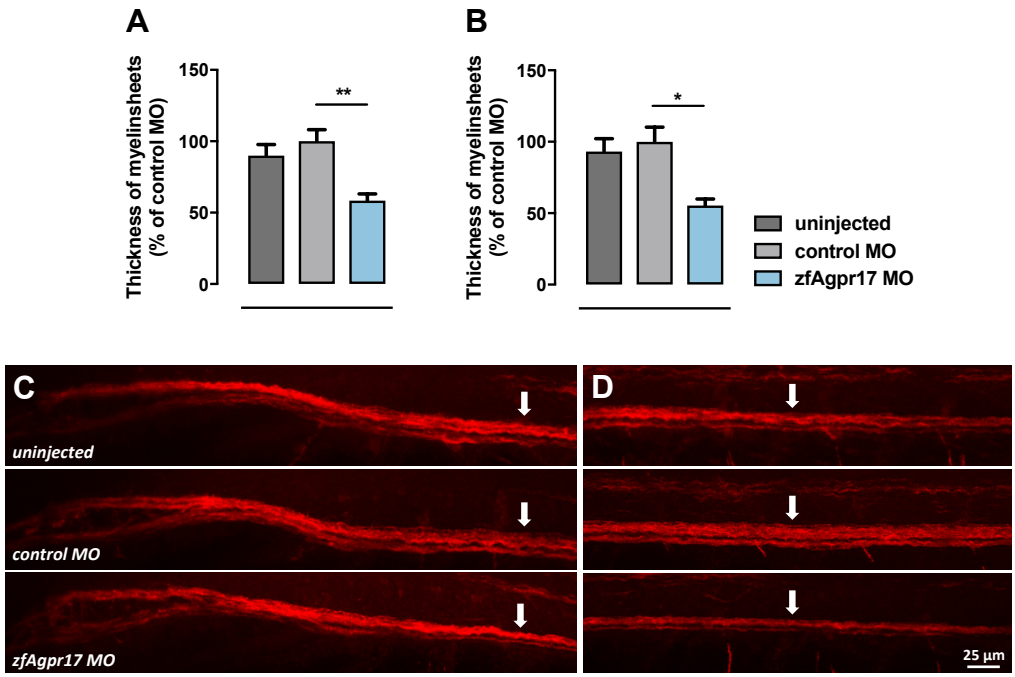

Figure 35: Mbp expression in the spinal cord of 4 dpf old zebrafish embryos is impaired following zfAGpr17 knockdown. Lateral views (dorsal up, anterior to the left) of zebrafish embryos (**C,D**) injected with *zfAgpr17* and control MO were obtained at 4 dpf. Whole-mount IHC was conducted with an antibody directed against Mbp coupling to an AlexaFluor546-conjugated goat anti-guinea pig antibody. One-way ANOVA test comparing MO with control MO injected zebrafish embryos, revealed a significant reduction in Mbp signal in the anterior (**A,C**) and middle (**B,D**) spinal cord, while control MO injected resembled uninjected animals. Data are shown as mean values (+ SEM) from two independent experiments. One-way ANOVA using Bonferroni's multiple comparison test; *,$p<0.016$; **, $p<0.0006$.

Additionally expression of myelin-associated protein Claudin K and myelin Protein zero (P0) (Schweitzer, Becker and Becker, 2003) in 4 dpf old zebrafish was examined by Western blot analysis. While *zfAgpr17* MO injections caused weak decreases in Claudin K expression levels compared to control and uninjected embryos, a significant reduction in protein expression was observed for P0 (P<0.0009, one-way ANOVA) (**Figure 36**).

To sum up, the obtained data reveal impaired myelination following zfAGpr17 knockdown, thus demonstrating the opposing effect observed in knockout mice.

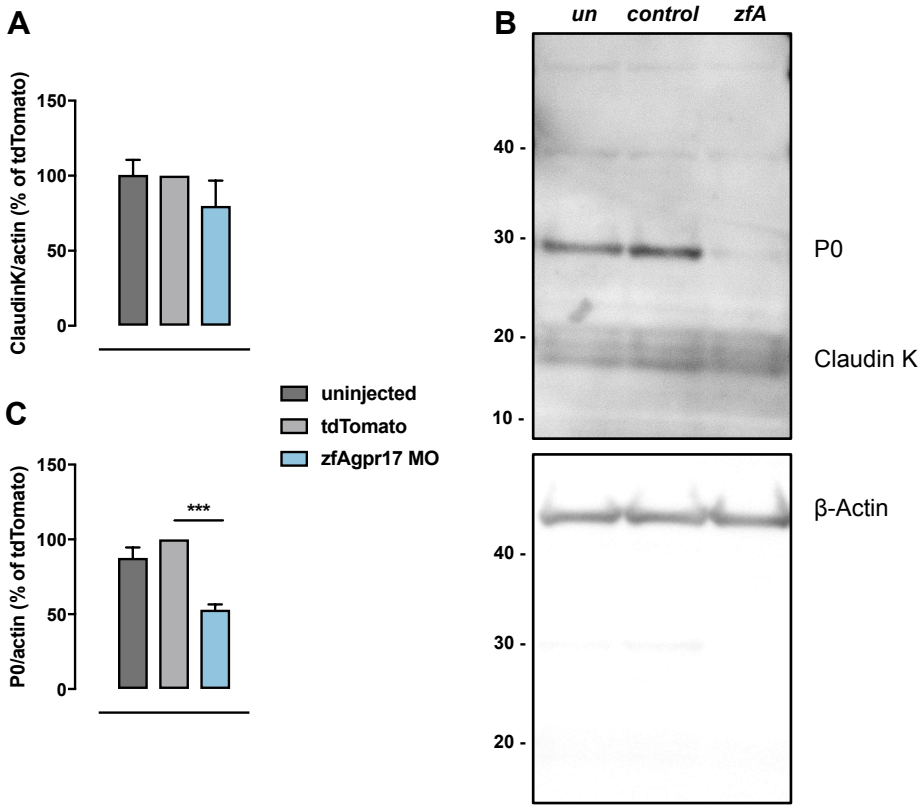

Figure 36: Western blot analysis of zfAGpr17 morphants reveals declined expression of myelin proteins. Expression of myelin proteins Claudin K and P0 was determined in 4 dpf old zebrafish embryos, injected with *zfAgpr17* and control morpholino by Western blot analysis. Data presented as mean values (+ SEM), displayed a decrease in expression of both proteins (**A, C**), while reduction was only significant for P0 (**C**). Shown is the representative Western blot (**B**) of at least three independent experiments. ***; P<0.0009 according to one-way ANOVA using Bonferroni's multiple comparison test. *un* = uninjected animals; *control* = control injected morphants; *zfA* = *zfAgpr17* MO injected animals.

4.5.2.3 WISH demonstrates reduced expression of myelin basic protein in zfAGpr17 morphants

In order to strengthen the IHC assay revealing narrowed Mbp expression in the spinal cord of *zfAgpr17* morpholino injected zebrafish (**Figure 35**), expression of *mbp* at the level of transcription was ascertained by WISH.

Thereby, *mbp* signal in MO injected zebrafish was compared to control MO injected and WT animals at 3 and 4 dpf. While expression of *myelin basic protein* was remarkably reduced in the CNS and in the PNS of 3 dpf old morphants (**Figure 37, A**), the difference was less noticeable at 4 dpf (**Figure 37, B**). Moreover, similarly assayed tg(*olig2:EGFP*) zebrafish, sorted by fluorescent imaging prior the WISH, revealed the same expression pattern, thus supporting previously achieved WISH data (**Supplementary Figure 3**).

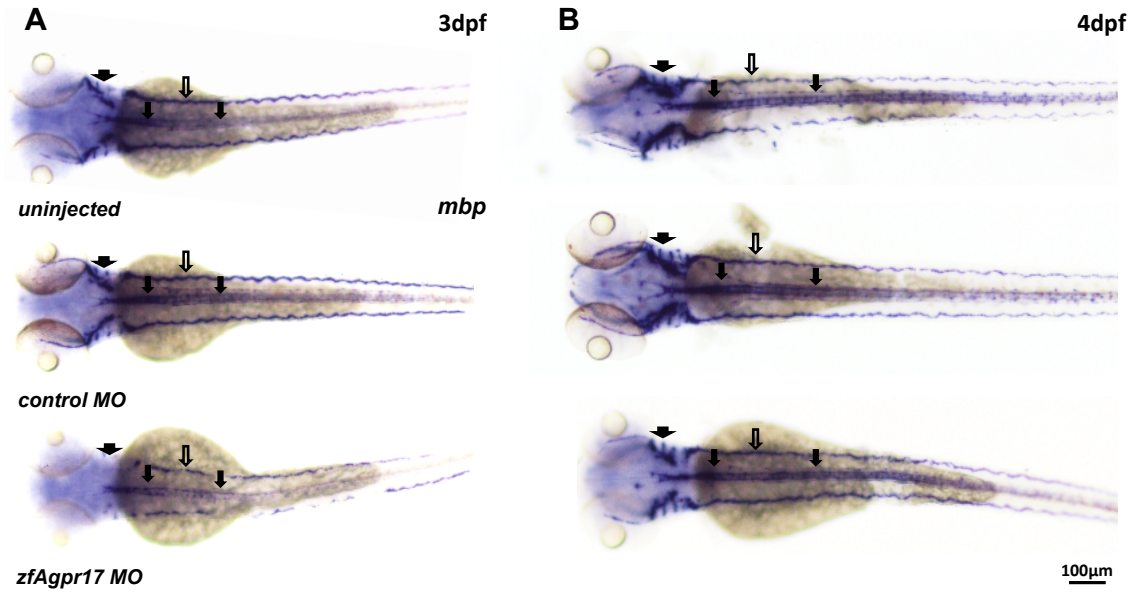

Figure 37: ZfAGpr17 morphants reveal decreased *mbp* expression in the CNS and PNS. *zfAgpr17* MO injected embryos displayed a decrease in *mbp* expression in the CNS at the level of the spinal cord (small black arrows) and brain (big black arrows) as well as in the PNS (white arrows) at 3 dpf (**A**). At 4 dpf the difference was still noticeable, albeit it was diminished (**B**). Shown are representative images (dorsal up) of two independent experiments.

4.5.2.4 Numbers of mature oligodendrocytes are narrowed in zfAGpr17 morphants

One explanation for the narrowed myelination in zfAGpr17 morphants could be fewer mature oligodendrocytes.

To test this, Two-photon microscopy images of representative spinal cord regions of tg(*claudink:EGFP*) zebrafish were acquired to quantify cell numbers in *zfAgpr17* MO injected embryos. At 3 dpf, zfAGpr17 morphants revealed a significantly reduced number of dorsally migrated *claudin k* positive oligodendrocytes ($P<0.0025$, one-way ANOVA) compared with the controls (**Figure 38**), indicating diminished oligodendrocyte maturation.

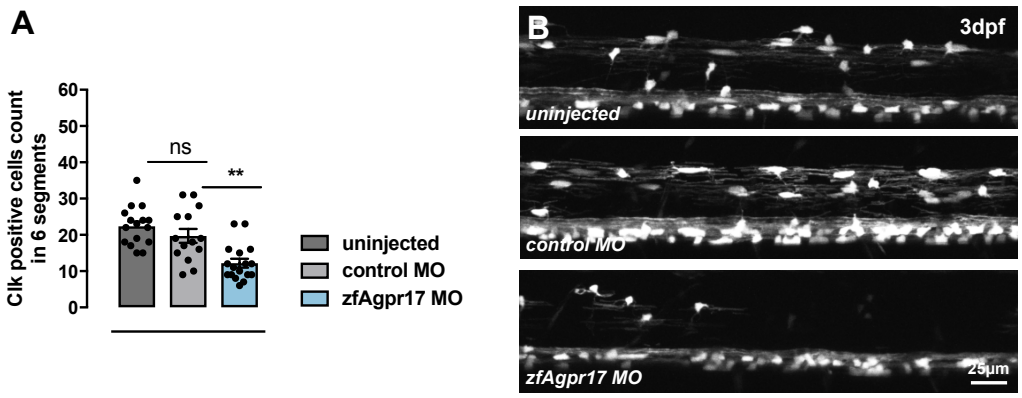

Figure 38: ZfAGpr17 morphants reveal reduced numbers of *claudin k* expressing dorsally migrated cells. Tg(*claudink:EGFP*) zebrafish, injected with 2.75 ng *zfAgpr17* MO RNA were imaged by Two-photon microscopy at 3 dpf. Numbers of dorsally migrated *claudin k* positive cells significantly differed between *zfAgpr17* and control MO injected animals (**A**). Figure (**B**) shows representative lateral views (anterior to the left, dorsal up) of spinal cord regions. Data are presented as mean values (± SEM) from at least three independent experiments. One-way ANOVA was performed using Bonferroni's multiple comparison test. **, P<0.0025.

4.5.2.5 ZfAGpr17 morphants display reduced numbers of dorsally migrated olig2 positive cells

Since oligodendrocytes differentiate from Olig2 positive OPCs, it was to delineate whether the reduction in number of dorsally located *claudin k* positive oligodendrocyte in zfAGpr17 morphants resulted from fewer OPCs.

Hence, fluorescent images of spinal cord regions of tg(*olig2:EGFP*) zebrafish injected with 2.75 ng *zfAgpr17* MO were taken by Two-photon microscopy. A significant reduction (P<0.0001, one-way ANOVA) in the percentage of *olig2* positive cell numbers in mutant embryos compared with control and WT was found at 3 dpf (**Figure 39, A, C**). These results were also reproducible by imaging higher numbers of injected zebrafish with the EnSight plate reader® representing a high-throughput zebrafish imaging technology (**Figure 39, B**).

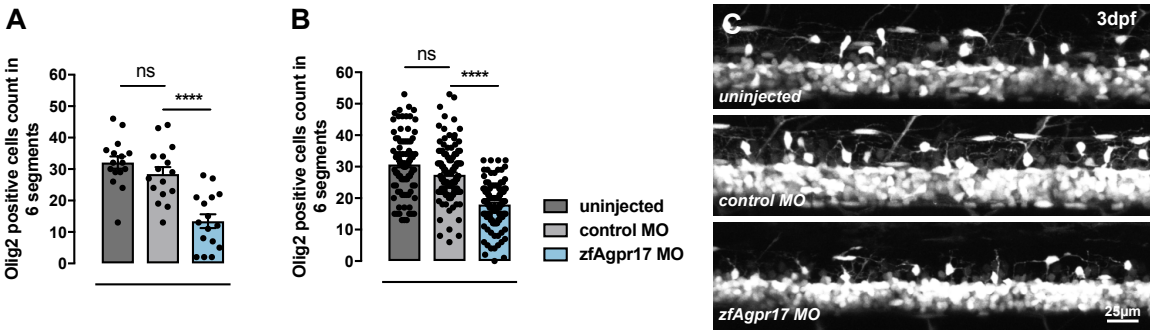

Figure 39: Migration of *olig2* positive OPCs is inhibited after zfAGpr17 knockdown. At 3 dpf, injections of 2.75 ng *zfAgpr17* MO in tg(*olig2:EGFP*) zebrafish caused a significant reduction in *olig2* positive dorsally migrated cells in morphants compared to control injected and WT animals (**A**). Results achieved with EnSight® plate reader confirmed data obtained by Two-photon microscopy (**B**). Figure (**C**) presents lateral views (dorsal up, anterior to the left) of representative spinal cord regions. Shown are mean values (± SEM) from three independent experiments. ****; P<0.0001 according to one-way ANOVA using Bonferroni's multiple comparison test. Results obtained with EnSight® were generated by Enrico Mingardo in the lab of Prof. Dr. Evi Kostenis, University of Bonn.

Collectively, the imaging data demonstrate, that zfAGpr17 knockdown reduces numbers of dorsally located oligodendrocyte lineage cells in two stages of development, at the level of OPC proliferation/migration and at the level of oligodendrocyte differentiation. Hence, the reduced cell numbers could result either from decreased OPC proliferation and differentiation, and/or increased death. To distinguish between these possibilities, IHC and WISH analysis were conducted.

4.5.2.6 ZfAGpr17 knockdown does not induce apoptosis

To determine whether the reduced numbers of oligodendrocyte lineage cells in zfAGpr17 morphants resulted from increased cell death, whole-mount zebrafish embryos, injected with *zfAgpr17* and control MO were labelled for the active form of Caspase-3 (Cleaved Caspase-3) at 3 dpf. Numbers of cells that stained positive for Caspase-3 did not markedly differ between MO and control MO injected animals (**Figure 40**), indicating that *zfAgpr17* MO does not induce cell death in the spinal cord of zebrafish embryos.

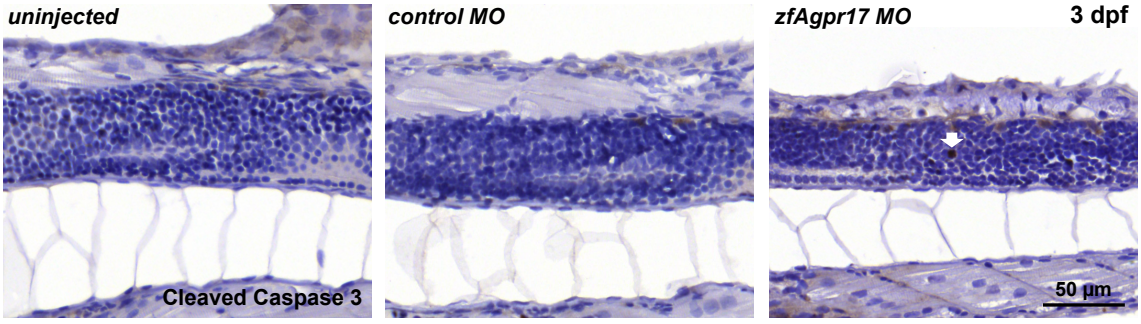

Figure 40: Cleaved Caspase-3 is not upregulated in 3 dpf zebrafish embryos after *zfAgpr17* MO injection. Expression of Cleaved Caspase-3 was determined in 3 dpf old zebrafish, injected with *zfAgpr17* and control MO by IHC assay. Cells stained positive for Cleaved Capsase-3 (white arrow) were not markedly present after *zfAgpr17* MO injections compared to control MO injected and uninjected animals. Data are representative images of two independent experiments. Stainings and images were generated by Dr. Anna Japp in the lab of Prof. Dr. Torsten Pietsch, Medical Centre, University of Bonn.

4.5.2.7 Enhanced nkx2.2 expression in zfAGpr17 morphants indicates precocious initiation of oligodendrocyte differentiation

As expression of the transcription factor Nkx2.2 initiates the terminal differentiation pathway, allowing OPCs turn into pre-OLs (Kucenas, Snell and Appel, 2010), it was to ascertain whether Gpr17 knockdown intervene in this developmental stage.

To test this, *nkx2.2* expression in zfAGpr17 morphants and control embryos was determined by WISH. *ZfAgpr17* MO injected zebrafish revealed a markedly increase in *nkx2.2* gene expression in the spinal cord compared to control animals at 2.5 dpf (**Figure 41**), suggesting that differentiation of OPCs into pre-OLs is not inhibited but rather preceded compared WT animals.

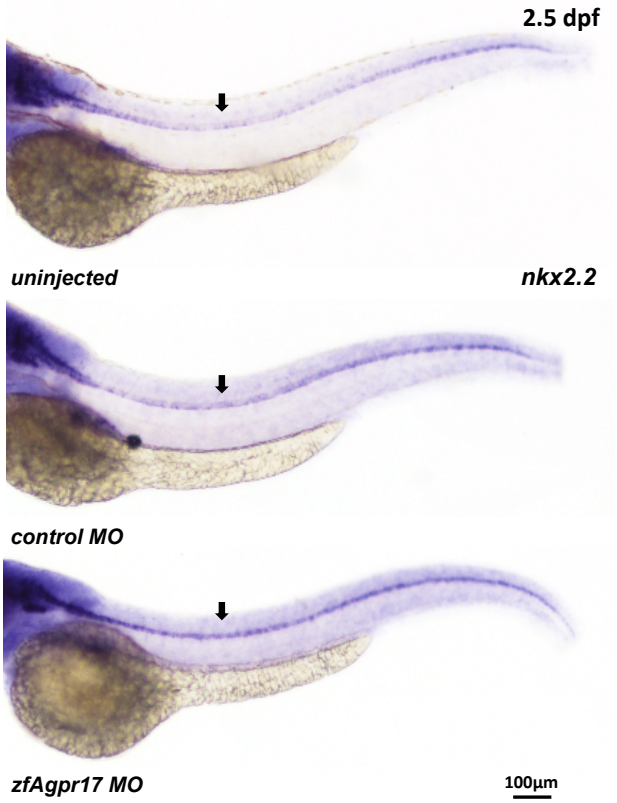

Figure 41: *Nkx2.2* expression in the spinal cord of zfAGpr17 morphants was markedly increased at 2.5 dpf. WT zebrafish injected with 2.75 ng *zfAgpr17* MO exhibited enhanced *nkx2.2* gene expression in the spinal cord at 2.5 dpf compared to control MO injected and uninjected animals. Shown are representative lateral views (dorsal up) of two independent experiments.

Together, these data suggest that Gpr17 knockdown induced precocious differentiation of OPCs into *nkx2.2* expressing pre-OLs. However, as being restrained in the pMN region, oligodendrocyte lineage cells fail to migrate into the dorsal spinal cord region, which finally leads to insufficient myelination. Whether Gpr17 knockdown affects OPC proliferation cannot be concluded by these experiments.

4.5.2.8 zfAgpr17 RNA rescues morpholino-induced reduction of dorsally migrated oligodendrocyte lineage cells

Since preceding studies revealed that OE of Gpr17 by RNA injections did not affect oligodendrocyte development, one could argue that protein is not translated. Hence, the ability of *zfAgpr17* RNA to rescue MO-induced reduction of dorsally migrated cells was determined by co-injection of *zfAgpr17* MO and RNA. As expected, injections of *zfAgpr17* MO caused a significant decrease in numbers of *olig2* positive cells at 3 dpf (P<0.0001, one-way ANOVA). Notably, co-injection of 800 pg *zfAgpr17* RNA rescued the amounts of *olig2* positive cells (**Figure 42**). No significant differences were observed between control injected and co-injected animals. Together, these data indicate both successful translation of *gpr17* RNA within zebrafish embryos as well as specificity of *zfAgpr17* MO.

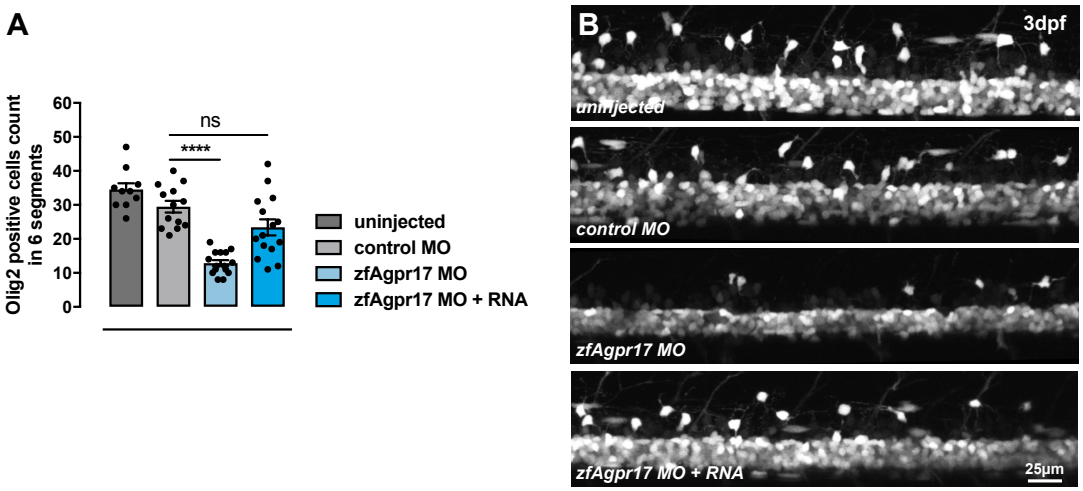

Figure 42: Reduction in numbers of *olig2* positive cells in zfAGpr17 morphants can be rescued by *zfAgpr17* RNA. Gpr17 rescue was evaluated by imaging representative spinal cord regions of 3 dpf old tg(*olig2:EGFP*) zebrafish embryos, injected with *zfAgpr17* MO alone as well as together with *zfAgpr17* RNA. While MO injected animals displayed a significant difference in number of dorsally migrated *olig2* positive cells compared to control injected animals, the reduction was completely rescued after co-injection of *zfAgpr17* MO with RNA (**A**). (**B**) shows representative lateral views (dorsal up, anterior to the left). Data presented as mean values (± SEM) of at least three independent experiments. One-way ANOVA was performed using Bonferroni's multiple comparison test. ****; P<0.0001.

5 Discussion

Myelination, the deposition of multi-layered membrane sheaths on axons by specialized glia cells, constitutes the basis for several neurophysiological processes in the vertebrate nervous system (Pfeiffer, Warrington and Bansal, 1993). However, to date, the underlying mechanism of myelination is not completely clarified; consequently, ongoing research in this field is crucial. An improved understanding of myelination would further support the investigation of diseases such as multiple sclerosis (MS) (Compston and Coles, 2008), Alzheimer's disease (George Bartzokis, 2011), cerebral palsy (Azzarelli *et al.*, 1996) or schizophrenia (Azzarelli *et al.*, 1996), all displaying demyelination as pathological feature.

Recently, G-protein coupled receptors have been identified as key regulators during oligodendrocyte development and myelination (Mogha, Rozario and Monk, 2016), and may therefore promise new targets in the treatment of demyelinating diseases. One of them, the orphan rhodopsin family G-protein coupled receptor 17, which is enriched in oligodendrocyte lineage cells, has been implicated in the maturation of oligodendrocytes (Chen *et al.*, 2009; Fumagalli *et al.*, 2011). In addition to its role during oligodendrocyte development, GPR17 was found to be upregulated in human white matter plaques of MS patients (Chen *et al.*, 2009). However its function in the disease remains speculative at the time. Despite the intensive knowledge about this GPCR, published literature reveals inconsistences concerning expression pattern, role and activation by distinct ligands; thus, there is an urgent need of further research clarifying outstanding issues (Marucci *et al.*, 2016).

Herein, the zebrafish (Danio rerio), a freshwater teleost (Kari, Rodeck and Dicker, 2007), might represent a potential model organism to gain new insights in the role of Gpr17 in oligodendrocyte myelination, not only during development but also in disease. This chapter will discuss receptor functionality of zebrafish Gpr17 examined in *in vitro* and *in vivo* assays as well as the potential of artificial chimeric Gpr17 receptors as promising screening tools. Furthermore, specific *in vivo* results concerning receptor expression and function will be discussed and compared with existing literature to finally debate whether the zebrafish is a suitable animal model as *in vivo* screening platform for new ligands of human Gpr17.

5.1.1 Zebrafish Gpr17 lacks functionality *in vitro*

After identification and characterization of the orphan G-protein coupled receptor 17 (Raport *et al.*, 1996; Bläsius *et al.*, 1998; Heise *et al.*, 2000), researchers aimed to ascertain the ligand that endogenously activates this GPCR. In 2006, Ciana *et al.* postulated a dual pharmacological profile, whereupon Gpr17 responds to both uracil nucleotides and cysteinyl leukotrienes. Based on that deorphaning report, follow-up studies by the same group examined function of this receptor during oligodendrocyte development by using the two family ligands, with the conclusion that Gpr17 activation promotes oligodendrocyte maturation (Lecca *et al.*, 2008; Ceruti *et al.*, 2009; Fumagalli *et al.*, 2011). However, Gpr17 activation through the proposed agonists could not be verified by several independent laboratories (Heise *et al.*, 2000; Maekawa *et al.*, 2009; Benned-Jensen and Rosenkilde, 2010; Simon *et al.*, 2017). Additionally, Hennen and collaborators identified a small-molecule agonist, MDL29,951, which activated Gpr17 mainly, but not exclusively, via the $G_{\alpha i/o}$ pathway in a concentration-dependent manner. Noteworthy, experimental results from this group emphasised an inhibitory role of Gpr17 on maturation of oligodendrocytes (Hennen *et al.*, 2013a; Simon *et al.*, 2016), in agreement with reports from several independent laboratories (Chen *et al.*, 2009; Daniele *et al.*, 2014).

In an attempt to clarify these conflicting data, ongoing research should focus on finding new model systems in which the activation and role of Gpr17 can be analysed. While prior studies utilized rodent models to study Gpr17 in myelination (Lecca *et al.*, 2008; Chen *et al.*, 2009; Fumagalli *et al.*, 2011; Hennen *et al.*, 2013a; Simon *et al.*, 2016), future efforts might consider the smaller vertebrate model zebrafish, which displays a powerful alternative to study myelination *in vivo* (Driever *et al.*, 1994; Buckley, Goldsmith and Franklin, 2008; Ackerman and Monk, 2015; Preston and Macklin, 2015). Hence, primary experiments of this work aimed to answer two questions: firstly, whether zebrafish Gpr17 can be activated by postulated uracil nucleotides and cysteinyl leukotrienes; and secondly, whether MDL29,951 could induce robust responses comparable to those on human, mouse and rat Gpr17 (Hennen *et al.*, 2013).

The data obtained in label-free Dynamic mass redistribution assays revealed missing responses of zebrafish Gpr17 transfected mammalian HEK293 cells towards both the proposed endogenous agonists and MDL29,951. The lack of activity of uracil nucleotides and cysteinyl leukotrienes on zebrafish Gpr17 was rather expected and entirely consistent with previous observations showing unresponsiveness of human, mouse and rat Gpr17 in various recombinant, immortalized and primary cells (Simon *et al.*, 2017). Thus, the notion of Simon and collaborators considering Gpr17 as orphan is further supported by the results of this work. Conversely, the lacking response of

MDL29,951 on zebrafish Gpr17 examined within this work was rather surprising, since Simon and collaborators proved that MDL29,951 activates Gpr17 orthologous from human, mouse and rat in a similar manner. The missing response may be grounded on three reasons: Firstly, zebrafish Gpr17 is insufficiently expressed in the cell membrane of the mammalian HEK293 cell line. Secondly, the intracellular interaction between the zebrafish receptor and the mammalian G-proteins is circumvented. Thirdly, the small molecule agonist does not bind appropriately to the zebrafish receptor.

Beginning with the membrane availability of the receptor, ELISA and ICC assays verified its expression on the cell surface, thus a lack of response based on missing membrane expression can be actually excluded. Nevertheless, it might be possible that zebrafish receptors need increased expression levels in mammalian cell lines for an appropriate detectable signaling. A future generation of a stable cell line expressing the zebrafish Gpr17 at a higher level than transient transfected cells might offer better signalling conditions in the extrinsic mammalian background.

Intricacies in the analysis of zebrafish receptors in mammalian cell lines have already been described by existing literature. Studies of Ringvall and collaborators demonstrated lower binding affinities and less potency of zebrafish neuropeptide Y (NPY) receptors in CHO cells compared to mammalian NPY receptors (Ringvall, Berglund and Larhammar, 1997). Thereby, inappropriate interaction of mammalian G-proteins with zebrafish receptors was assumed to be the cause. Within this work, this assumption was supposed to be resolved by use of a zebrafish fibroblast cell line, which exhibits zebrafish G-proteins. However, sufficient zebrafish Gpr17 expression levels could not be achieved upon transfection into this cell line. Since zebrafish cell lines do not appear in current literature to date, their use as an *in vitro* platform might be inappropriate.

In a multiple alignment, human Gpr17 (Gpr17-S) shared 56 % identical residues with zfA and 44 % with zfBGpr17. Moreover, according to mutagenesis studies (unpublished data), the residue motif involved in receptor activation by MDL29,951 is identical from zebrafish to mammals. Therefore, considering the level of conservation, there are no actual reasons for a lack of agonist binding at the zebrafish receptors. However, the missing receptor functionality queried the binding capacity of MDL29,951. One way to overcome this open question was the construction of chimeric receptors, exchanging the extracellular loops together with the transmembrane regions, which contain the ligand binding domain, between human and zebrafish Gpr17s. In DMR assays, chimeras containing the human binding domain region and either zfA or zfBGpr17 intracellular loops showed functionality after stimulation with MDL29,951, although the responses were diminished compared to human Gpr17. Conversely, chimeric receptors exhibiting the zebrafish

binding domain remained unresponsive, despite containing the human intracellular loops responsible for the interaction with G-proteins in HEK293 cells. Altogether, these results suggest an impaired binding of MDL29,951 on zebrafish Gpr17. Clearly, future GTPγS-binding analysis should be carried out to prove this hypothesis.

Even though our results suggest an impeded receptor-ligand interaction, it may have happened that the fish receptor lacked its normal microenvironment. In the animal, zebrafish Gpr17 signals at 28°C, while experiments conducted within this work in the HEK293 cell line were performed at 37°C. The temperature may influence the folding of the receptor and the following signalling behaviour. Thus, it could have occurred that although membrane expression was present, the receptor remained non-functional in this cell line. Therefore, functionality of zebrafish Gpr17 should be also analysed in its native signalling environment.

5.1.2 MDL29,951 treatment of zebrafish embryos does not influence myelination *in vivo*

The highly important research area of developmental and disease biology has been complemented during the last two decades by the small fresh-water vertebrate zebrafish since it provides an ideal *in vivo* model organism for gene and target validation, as well as for disease investigations. The high genome conservation between zebrafish and humans makes them a popular and currently used model organism in many important medical areas (Langheinrich, 2003; Taylor *et al.*, 2010; Howe *et al.*, 2013). Especially in the field of myelination, several genes and cell lineage properties are highly conserved between zebrafish and mammals, wherefore questions concerning CNS development, myelin function and repair can be investigated with zebrafish (Brösamle and Halpern, 2002; Raphael and Talbot, 2011; Czopka, 2015).

Furthermore, due to its small size and rich fertility, the animal provides also optimal conditions for drug discovery studies by high-throughput screenings of large compound libraries. Particularly suited for this purpose is the zebrafish embryo since it is permeable to drugs and can be easily genetically modified. For instance, Buckley *et al.* used a transgenic reporter line for high-throughput screening of drugs with pro-myelinating features. Compounds that altered numbers of oligodendrocyte lineage cells were further examined by qPCR and finally evaluated in tertiary screens for suitability for research progression (Buckley *et al.*, 2010). Likewise, Fang *et al.* demonstrated that treatment of zebrafish embryos with metronidazole caused demyelination that regenerated after metronidazole withdrawal within seven days (Fang *et al.*, 2014). In both studies, drugs were easily applied in the aquaria water where the zebrafish were housed in.

Accordingly, an effect of MDL29,951 acting on zebrafish Gpr17 and thereby influencing the myelination process could be examined in an analogous way. On this occasion, functionality of zebrafish Gpr17 would be analysed in its native signalling environment. Obviously, this method cannot exclude target unspecific effects and merely yields an indirect way to analyse responsiveness of MDL29,951 at zebrafish Gpr17. However, it substantiates evidence whether distinct signalling backgrounds influence receptor signal transduction in a certain manner and whether knockout approaches are essential for further studies.

Similar to Buckley and collaborators (Buckley *et al.*, 2010), who used imaging methods as a first and quick experiment in the entire drug-screening cascade, numbers of migrated mature *claudin K* positive oligodendrocytes of treated and control animals were evaluated at 5 dpf. While Buckley *et al.* screened for immature oligodendrocyte precursor cells at earlier time points, hence achieving further premonitions about cell proliferation and migration, experiments within this work rather focused on myelin producing cells, aiming to mirror myelination. The results show that MDL29,951 treatment of zebrafish embryos for five days did not change *claudin K* positive oligodendrocyte numbers, thus indicating no altered oligodendrocyte development nor myelination. This was further confirmed by Western blot analysis of 5 dpf old embryos revealing stable expression of myelin protein 36k after MDL29,951 treatment compared to untreated controls. Noteworthy, 36k, a newly discovered myelin protein that was found to be highly expressed in oligodendrocytes of zebrafish (Morris *et al.*, 2004), may not represent myelination in the approved manner as prominent myelin proteins such as Mbp or Plp (Schweitzer *et al.*, 2006; Nawaz *et al.*, 2013). However, antibodies detecting zebrafish Mbp and Plp did not work in Western blot analysis. Nevertheless, qPCR analysis reflected unaltered expression of myelin genes *mbp* and *plp* after MDL29,951 treatment, further supporting the 36k analysis. It is important to note that a disadvantage of Western blot and qPCR studies constitutes the sample acquisition, since entire embryos were collected for analysis of myelin protein expression and, consequently, potential differences in particular regions of the zebrafish nervous system may be undetectable. Future studies using electron microscopy of transverse spinal cord sections would be desirable in order to screen for specific potential alterations in myelinated axons (Ackerman and Monk, 2015).

Overall, these results additionally underscore the unresponsiveness of zebrafish Gpr17 obtained in preceding *in vitro* experiments and plead once more for impaired ligand binding. Therefore, MDL29,951, a selective activator for Gpr17 of human, rat and mouse Gpr17, turned out to be unsuitable for a Gpr17-dependent manipulation of oligodendrocyte myelination in zebrafish.

5.1.3 Chimeric Gpr17 receptors may represent suitable tools for target validation and drug discovery

While the Greek mythology delineates chimeras as monstrous fire-breathing composites of parts from lion, goat and serpent, in the scientific literature the designation stands for molecules composed of domains from various receptors. Especially, the 7-transmembrane G-protein coupled receptors comprising three basic domains (extracellular, intracellular and transmembrane region) can be perfectly converted into chimeras. During the last two decades several independent research groups established more than 100 chimeric receptors to study inter alia ligand binding and downstream signalling (Yin *et al.*, 2004).

While existing literature occasionally reports about chimeric receptors consisting of homologous receptors, first time within this work, orthologous Gpr17 receptors from zebrafish and human were merged into chimeras with the view to unravel the unresponsiveness of zebrafish Gpr17 towards a small molecule agonist. As described in preceding chapters, DMR assays proved functionality of chimeras containing the human binding site upon activation with MDL29,951, while receptors exhibiting the zebrafish binding domain remained unresponsive. The functional chimeric receptors provoked varied DMR traces and 2-fold lower responses than those of the human Gpr17. One of the reasons for the constrained responses was the 2-fold decreased membrane expression compared to the human receptor. The phenomenon of declined expression of chimeric receptors is also found in different studies (e.g., Gearing *et al.* studying ligand binding of chimeric leukotriene receptors (Gearing *et al.*, 2003)). A second reason was elucidated in further experiments that analyzed chimeric Gpr17 receptors in the presence of the G-protein inhibitors pertussis toxin (PTX) and UBO-QIC. The obtained data revealed exclusive coupling of the chimeric receptors through $G_{\alpha i}$, exemplified by the depressed, sharpened trace shape, while human Gpr17 activates both, $G_{\alpha i/o}$ and $G_{\alpha q}$ pathways (**Supplementary Figure 4**).

In particular, the established chimeric receptors are not only applicable for clarifying the binding incompatibilities of zebrafish Gpr17, but may also represent smart tools for *in vivo* screening of compounds with activating or inhibiting properties on human Gpr17. Stably expressed in different zebrafish reporter lines, endogenous zebrafish signalling pathways would be triggered while ligand binding and receptor activation would proceed as in humans. On this occasion, compounds that alter myelination in zebrafish would allow drawing conclusion concerning effects in humans. Nevertheless, the reduced membrane expression and impaired signalling behaviour of chimeric receptors observed in the mammalian cell line should not be disregarded when considering potency of compounds *in vivo*. It may be that both restrictions are vanished in the

animal; however, it remains speculative to what extent that impacts on the effects. In the same sense, to prevent biased results, the expression of chimeras in zebrafish Gpr17 null mutants should be also considered. Although MDL29,951 failed in activating zebrafish Gpr17, this does not mean that other compounds act in the same way.

To conclude, Gpr17 chimeras would indeed facilitate the *in vivo* screening of human Gpr17 targeting compounds, although their usability *in vivo* has to be shown in future experiments. Before this, however, additional investigations have to prove a crucial role of Gpr17 in myelination of the aquatic vertebrate zebrafish.

5.1.4 Gpr17 is expressed in developmental stages of zebrafish CNS

In 2006, Kirby *et al.* illustrated oligodendrocyte development and myelination in zebrafish by *in vivo* time-lapse imaging of transgenic reporter lines. Confocal images of zebrafish embryos revealed that at 2 dpf, OPCs derived from NP cells start migrating dorsally from the pMN region in the neural tube. Once they stop proliferating and migrating, OPCs differentiate into pre-OLs that finally transition into myelinating oligodendrocytes, so that at 5 dpf first myelin sheaths can be observed. Consistent with this reported zebrafish oligodendrocyte development, WISH experiments of this work displayed an expression pattern of *gpr17* RNA within the first five days of zebrafish development. Deletion of OPCs with TSA (Takada et al., 2010) induced a significant demise of *gpr17* expression in the dorsal spinal cord region, thus suggesting Gpr17 presence in dorsally migrated oligodendrocyte lineage cells in zebrafish. Remarkably, diffuse expression of *gpr17* is detected already at 1 dpf within the dorsal and the ventral spinal cord, suggesting an existence of *gpr17* before initiation of oligodendrocyte development. This presumption was previously described by Maisel *et al.* proposing *gpr17* gene as marker of adult NG2 positive progenitor cells of human hippocampus (Maisel, Herr, *et al.*, 2007). Whether Gpr17 is expressed in developmental NG2 progenitor cells of the zebrafish has to be confirmed by future experiments. Last but not least, WISH experiments revealed missing *gpr17* expression in the PNS, thereby supporting previously published data obtained with mice (Chen *et al.*, 2009). Altogether, these data suggest that *gpr17* is expressed in oligodendroglial cells. Future experiments to finally corroborate this finding are necessary, such as co-localization in oligodendrocyte lineage cells by simultaneous signal amplification of *gpr17* RNA with *olig2* or *claudin K* by RNAscope technology®, or by IHC assays detecting the corresponding proteins.

In addition to WISH analysis that visualized expression of *gpr17* RNA, implemented Western blot analysis displayed Gpr17 protein abundance during embryogenesis, commencing at 3 dpf and

remaining stable until 10 dpf, the period when myelination progresses. Moreover, Gpr17 could not be detected in brains of healthy adult zebrafish. These results correlate with the pattern of expression found in mice, where Gpr17 is present during the period of myelinogenesis from P3 to P21, whereupon its expression declines markedly until adulthood (Chen *et al.*, 2009).

To sum up, experiments of this work demonstrate Gpr17 expression during zebrafish CNS development, which is consistent with the reported expression in mice and suggests an involvement of this receptor in the regulation of oligodendrocyte development.

5.1.5 The impact of zebrafish Gpr17 on myelination needs to be further explored

The potential of zebrafish serving as tool in drug discovery is further extended by its utilization in target identification and validation studies. Thus, zebrafish provide prominent platforms for genetic screens, either for forward screenings to identify mutated genes after inducing phenotypes by chemical mutagenesis or for investigations of specific phenotypes following mutations of disease-related targets. The latter, also known as reverse screening, usually takes advantage of overexpression (OE) and knockout (KO) methodologies implemented inter alia by use of the CRISPR/cas9 system (Yoganantharjah and Gibert, 2017). While transient OE can be quickly achieved by injection of mRNA or plasmid DNA into the one-cell stage of zebrafish embryos, the generation of KO animals takes far longer. A timesaving alternative represents the morpholino (MO)-induced gene knockdown. By complementary binding of backbone-altered oligomers to specific nucleic acid sequences, the translation machinery is impaired (Corey and Abrams, 2001). Noteworthy, during the last 15 years an growing number of scientists claimed about MO-induced off-target effects causing misleading results and thus degrading their scientific relevance (Blum *et al.*, 2015). However, Stainier and co-workers recently published a guideline recommending utility of MO oligomers while taking account of some rules, for instance by verifying MO-induced effects in rescue experiments (Stainier *et al.*, 2017). Hence, for validating the role of Gpr17 during oligodendrocyte development and myelination, Gpr17 expression was manipulated by injections of *3HA-tagged zfgpr17* mRNA or MO oligonucleotides into one-cell stage zebrafish embryos.

Transient OE of Gpr17 within the first days of zebrafish life had no influence on oligodendrocyte development or myelination. Imaging results of transgenic reporter lines revealed unaltered numbers of oligodendrocyte lineage cell in both, pre-mature and mature developmental stages. In addition, comparable expression pattern of the transcription factor *nkx2.2* labelling pre-OLs indicated neither premature nor delayed initiation of oligodendrocyte development. Finally, unchanged expression of myelin genes such as *mbp* and *plp*, evaluated by qPCR and WISH, coincided with Mbp expression obtained in IHC assays as well as myelin protein expression in Western blot analysis. These results may question the successful OE of Gpr17; however, control injections of tdTomato resulted in sufficient protein expression, as verified by fluorescence microscopy. Obviously, that control is not evidence that Gpr17 is translated in the same manner; nevertheless, it proved an effective RNA generation as well as a flawless injection procedure.

The lack of effect of Gpr17 OE could be due to the injection procedure, since injection of mRNA into the one-cell stage causes a mosaic expression within the entire animal. This means that the protein could be expressed in each cell type, while the abundance in cells endogenously expressing the protein may be insufficient for inducing clear phenotypes. This limitation could be prevented by injecting the constructs together with their promoter, although that is unknown for Gpr17. Alternatively, it might be used the Olig2 promoter to drive expression in OPCs that presumably express Gpr17 and mainly contribute to oligodendrocyte development. Whether this would cause distinct phenotypes might be investigated in future studies. Additionally, coupling of Gpr17 with EGFP and subsequent injection could be a complementary alternative to visualize expression of Gpr17, although it should be considered the possibility that the large fluorescent protein may reduce functionality *in vivo*.

Intriguingly, OE of Gpr17 in mice that resulted in hypomyelination was provoked in late-stage oligodendrocytes already expressing CNPase, thus at a time point when Gpr17 is almost down regulated (Chen *et al.*, 2009). On the contrary, in zebrafish embryos, where *gpr17* mRNA was injected in one-cell stage embryos, OE probably appears even before Gpr17 is endogenously abundant. Hence, additional amounts of Gpr17 in that stage of development might not further contribute to the following effect of endogenous Gpr17, wherefore obtained results showed no effect on oligodendrocyte development and myelination. In comparison, OE of Gpr56, another GPCR that is essential for oligodendrocyte proliferation and already present before OPC specification, evoked preceded *mbp* expression in 2.5 dpf old zebrafish embryos (Ackerman *et al.*, 2015). Contrarily to Gpr17, in this study OE was implemented in the stage of endogenous receptor expression.

However, further experiments demonstrating that injected zebrafish *gpr17* mRNA could rescue the MO-induced effect finally proved the successful expression of Gpr17 OE and, moreover, the specificity of the *gpr17* MO. Additional to the rescue experiments, Western blot analysis verified MO-induced knockdown of Gpr17, albeit reduction of protein amount was only significant at 4 dpf (Kleinert, 2018). Nevertheless, as previously mentioned, slight differences between protein levels seem to be difficult to detect by this method. Collectively, knockdown of Gpr17 adversely affected oligodendrocyte development as well as myelination. In the almost absence of Gpr17, OPCs deficiently migrated into the dorsal spinal cord, the region where terminal differentiation is achieved. Subsequently, reduced numbers of OPCs resulted in fewer mature oligodendrocytes, which failed to sufficiently myelinate axons. Impaired myelination was demonstrated by reduced Mbp expression within the spinal cord and further by Western blot analysis revealing mellowed levels of myelin proteins Claudin K and P0. Conversely, the apparent increase of *nkx2.2*

expression within the pMN region of morphants at 2.5 dpf is likely the result of greater numbers of pre-OLs at that developmental stage, suggesting preceded pre-maturation of oligodendrocyte lineage cells. This observation could be further confirmed by future experiments quantifying *nkx2.2* expression by qPCR and *mbp* expression within the pMN region by RNAscope technology® or immunostaining. Since a MO-induced cell death figured as Cleaved Caspase-3 in IHC assays can be excluded as reason for the reduced cell numbers, summarized data argue for a Gpr17 knockdown-induced premature differentiation of OPCs into *nkx2.2* expressing pre-OLs. As being restrained in the pMN region, pre-OLs fail to migrate into the dorsal spinal cord, which finally leads to insufficient myelination in this region.

This hypothesis approximately correlates with findings of Chen *et al.* demonstrating a preceded onset of myelination in Gpr17 null mutant mice. Noteworthy, Chen and collaborators did not examine numbers or migration of oligodendrocyte lineage cells. Hence, it could be possible that pre-mature myelin-forming oligodendrocytes of mice are still able to migrate and myelinate axons, while migration in zebrafish might be additionally inhibited after Gpr17 knockdown. If this proves true, migration ability of oligodendrocyte lineage cells could be examined by time-laps imaging of distinct zebrafish reporter lines such as tg(*olig2*:EGFP) (Shin *et al.*, 2003) or tg(*nkx2.2a*:GFP) (Pauls *et al.*, 2007). A positive influence of Gpr17 on OPC migration was already published by Coppi and collaborators (2013), however results were obtained by use of the dubious UDP ligands.

Previous knockdown studies using specific small interfering RNAs (siRNAs) in primary OPCs observed similar effects as this work, particularly reduced numbers of Gpr17 positive cells as well as mature myelin-forming oligodendrocytes (Fumagalli *et al.*, 2011), though effects on myelination were not described. Nevertheless, one should be cautious when comparing knockdown with knockout results. The observation that knockdown strategies could cause distinct phenotypes than knockout approaches was recently described in literature (El-Brolosy and Stainier, 2017). For instance, Kok *et al.* demonstrated that different generated zebrafish knockout mutants could not recapitulate those phenotypes obtained in previous MO knockdown studies. Additionally, another working group examining an endothelial extracellular matrix gene (egfl7) in zebrafish uncovered severe vascular defects in MO injected animals, while knockout mutants revealed normal phenotypes (Rossi *et al.*, 2015).

Hence, it becomes evident that Gpr17 knockout animals are mandatorily required to further clarify the impact of Gpr17 on oligodendrocyte development and myelination.

5.1.6 Conclusion & outlook

In conclusion, this work demonstrates in several approaches the suitability of zebrafish to study G-protein coupled receptor 17 *in vivo*. Receptor expression in the CNS during the first days coincided with expression pattern found in mice and indicates a crucial role in oligodendrocyte development, which is further strengthened by reduced cell numbers, impaired myelination and assumed pre-maturation of oligodendrocytes after MO-induced knockdown of Gpr17.

Further studies are clearly necessary to finally conclude the developmental function of Gpr17 in zebrafish. This includes the confirmation of Gpr17 localisation in OPCs, the investigation whether Gpr17 additionally impacts on OPCs migration and the evidence of OPC pre-maturation after gene knockdown. Moreover, obtained knockdown experiments should be confronted to following knockout studies, examining whether both methodologies evoke the same or distinct phenotypes. Last but not least, Gpr17 mRNA could be injected once more into the yolk of 1 dpf old zebrafish embryos for achieving OE during endogenous Gpr17 expression.

Since the overall project aims to use zebrafish as screening platform for substances interacting with Gpr17 to support remyelination in demyelinating diseases, it should be considered that this work investigated Gpr17 during embryogenesis. It may be that the role of Gpr17 during oligodendrocyte development differs from that under pathological conditions and that inhibition or activation of Gpr17 may have distinct implications on disease progression. This is underlined by two studies investigating the role of Gpr37, another GPCR involved in the myelination process. While KO of Gpr37 induced hypermyelination during development (Yang *et al.*, 2016), a recent study demonstrated that absence of Gpr37 in the cuprizone disease model resulted in increased susceptibility of demyelination (Smith *et al.*, 2017). Therefore, function of Gpr17 in neurodegenerative pathologies remains also speculative. Although Gpr17 is found upregulated in several demyelinating conditions, such as in MS plaques of human white matter or EAE mouse models (Chen *et al.*, 2009), in a rat neonatal model of ischemic periventricular leukomalacia (PVL) (Mao *et al.*, 2012), in post-traumatic brain injury (Franke *et al.*, 2013) or in a transgenic model of Alzheimer's disease (Boda *et al.*, 2011), these reports implicate that depending on the pathology either inhibition or activation of Gpr17 positively contribute to the disease progression. Consequently, further investigations clarifying Gpr17 function under pathological conditions have to be driven, for instance, by use of an adult MOG-induced EAE zebrafish model (Kulkarni *et al.*, 2017) or, otherwise, by induction of spinal lesions in adult but also in juvenile zebrafish might represent an alternative method. Nevertheless, high-throughput screening of compounds affecting myelination could be initially conducted in developing Gpr17 zebrafish null mutants

stably expressing chimeric human/zebrafish Gpr17 receptors. Subsequently, substances that induced alterations should be finally tested under pathological conditions.

6 Summary

Myelination of axons represents an obvious evolutionary condition for efficient and rapid nerve conduction (Pfeiffer, Warrington and Bansal, 1993). Although intense studies aimed to attain improved understanding of this essential process during the last decades, several questions pertaining to the differentiation of myelinating glia cells remain unacknowledged. In this context, ongoing research has identified G-protein coupled receptors such as Gpr17 as crucial regulators of oligodendrocyte development and myelination (Chen *et al.*, 2009; Mogha, Rozario and Monk, 2016). Nevertheless, further investigations are required to finally conclude about function of GPCRs in CNS development but also in demyelinating pathologies such as MS.

Within this work, the zebrafish, a powerful model system for studying myelination *in vivo* (Preston and Macklin, 2015), served as animal model to gain further insights in expression and function of Gpr17 during CNS development. Additionally, functionality of zebrafish Gpr17 towards proposed agonists was evaluated in mammalian cellular backgrounds.

In the first part of this work, Dynamic mass redistribution assays revealed missing functionality of zebrafish Gpr17 towards the postulated endogenous ligands (Ciana, Fumagalli, M. L. Trincavelli, *et al.*, 2006) as well as the small molecule MDL29,951 (Hennen *et al.*, 2013b) upon transfection in mammalian HEK293 cells. Since results obtained with uracil nucleotides and cysteinyl leukotrienes coincided with previous reports, further experiments focused on the complete lack of response of MDL29,951. Sufficient cell surface expression indicated an impaired ligand binding that was confirmed by the analysis of chimeric human/zebrafish receptors. Chimeric constructs containing the binding and transmembrane domain of human and the intracellular loops of zebrafish Gpr17 responded to MDL29,951 in a concentration-dependent manner, while receptors exhibiting the zebrafish binding domain remained unresponsive. These preceded *in vitro* data were further validated by *in vivo* experiments, displaying unaltered oligodendrocyte development and myelination in 5 dpf old zebrafish embryos after a 5-day bath treatment with MDL29,951. Hence, summarizing data revealed the unsuitability of this small molecule agonist as a selective manipulator of Gpr17 in zebrafish. Interestingly, chimeric receptors stably expressed in zebrafish might represent a smart alternative for a MDL29,951-dependet activation and further function analyses of Gpr17 *in vivo*.

The second part of this work dealt with the expression and role of zebrafish Gpr17 *in vivo*. WISH and Western blot experiments verified Gpr17 expression in oligodendrocyte lineage cells of the CNS throughout embryogenesis, which was consistent with the expression pattern found in mice

(Chen *et al.*, 2009), suggesting a role of Gpr17 during zebrafish oligodendrocyte development. While transient OE of Gpr17 did not affect developing oligodendrocytes or myelination, MO-induced receptor knockdown led to significant reduction of dorsally migrated pre-mature and mature oligodendrocyte numbers as well as impaired myelination. Additional experiments indicated a preceded pre-maturation of pre-OLs, which were restrained in the region of OPC specification and thus impaired to migrate and myelinate dorsal axons. These findings approximately correlate with data obtained in Gpr17 knockout mice, demonstrating an early onset of oligodendrocyte maturation (Chen *et al.*, 2009). Due to the dissimilarity between knockdown and knockout methodologies, further knockout studies in zebrafish are required to finally clarify the role of Gpr17 in this animal model.

In summary, the present study reveals that Gpr17 notably contributes to oligodendrocyte development and myelination in zebrafish. Clearly, upcoming studies with Gpr17 knockout zebrafish have to be assessed for the future use of this aquaria animal model as screening platform of compounds affecting myelination.

7 Supplementary

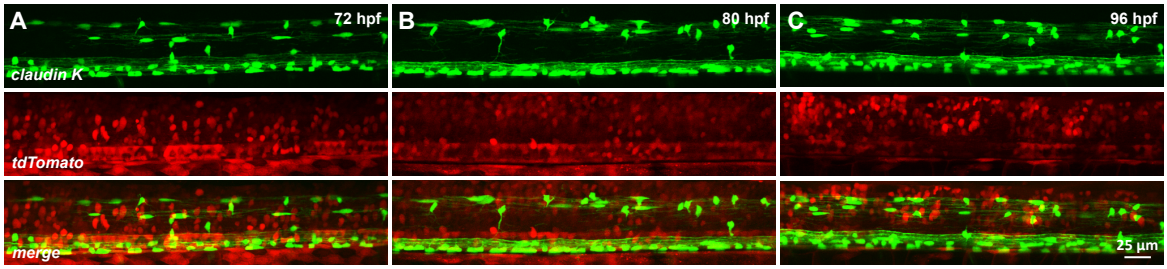

Supplementary Figure 1: Tg(*claudinK*:EGFP) zebrafish embryos injected with 800 pg tdTomato displayed stable RNA expression over 96 h. Transient microinjection of 800 pg *tdTomato* in tg(*claudinK*:EGFP) zebrafish embryos caused stable protein expression for 96 h. Shown are representative images of three independent experiments.

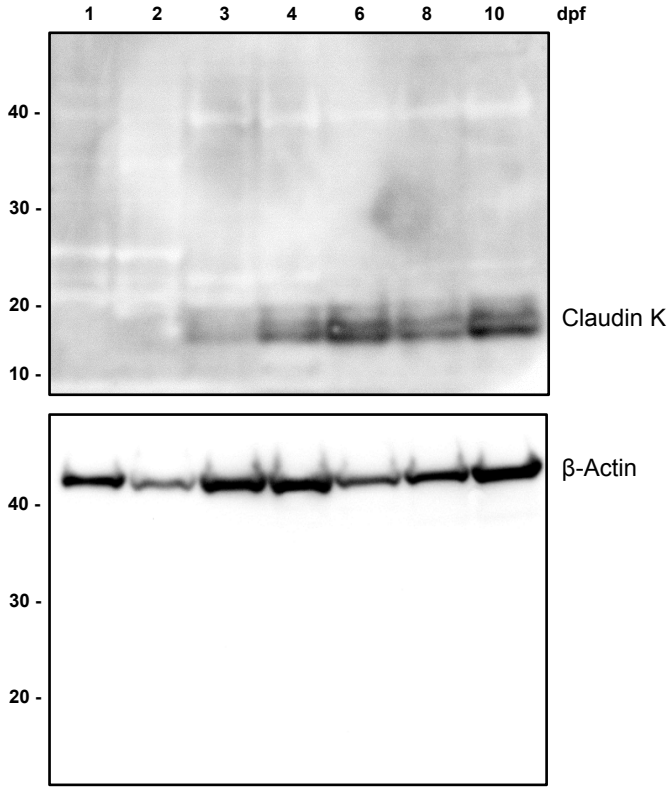

Supplementary Figure 2: Expression of myelin protein Claudin K in 1 to 10 dpf old zebrafish embryos. Representative Western blot displayed expression of Claudin K starting at 3 dpf, when myelination initiates and increasing until 10 dpf. Claudin K was also expressed in adult zebrafish brain (data are not shown).

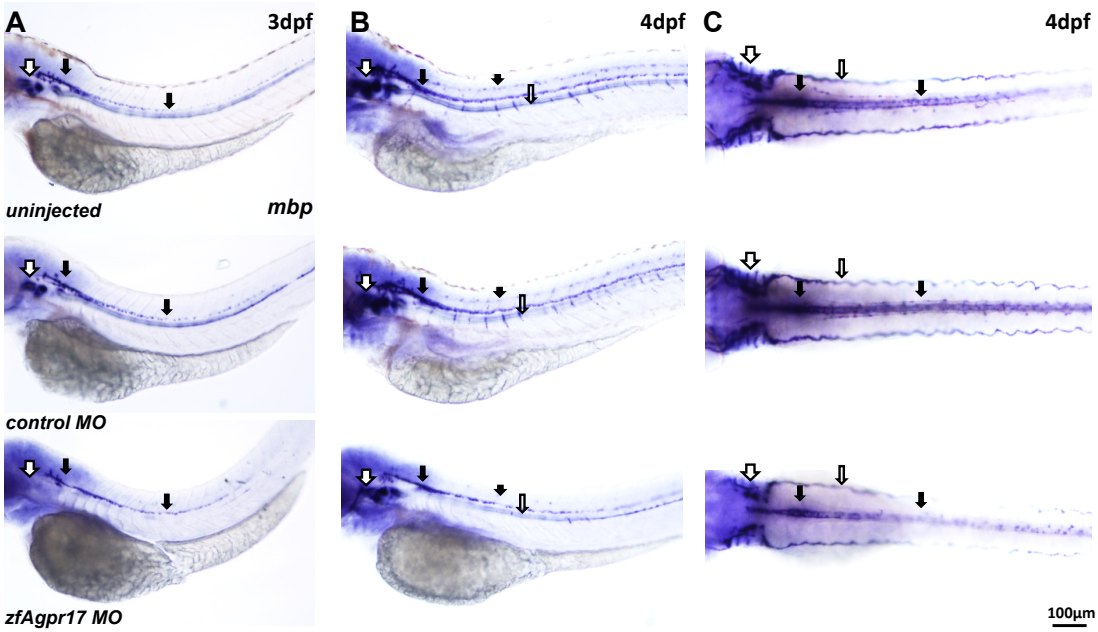

Supplementary Figure 3: Tg(*olig2*:EGFP) zebrafish revealed impaired *mbp* expression in CNS and PNS after *zfAgpr17* MO injections. *Tg*(*olig2:EGFP*) zebrafish, exhibiting a decrease in numbers of dorsally migrated *olig2* positive OPCs after injections of *zfAgpr17* MO, were sorted for WISH experiments. Lateral (**A, B**) and dorsal (**C**) views showed markedly decrease in *mbp* expression in the CNS at the level of the ventral (big black arrows) and dorsal (small black arrows) spinal cord , in the brain (big white arrows) and PNS (small white arrows) at 3 and 4 dpf. Presented data are from two independent experiments.

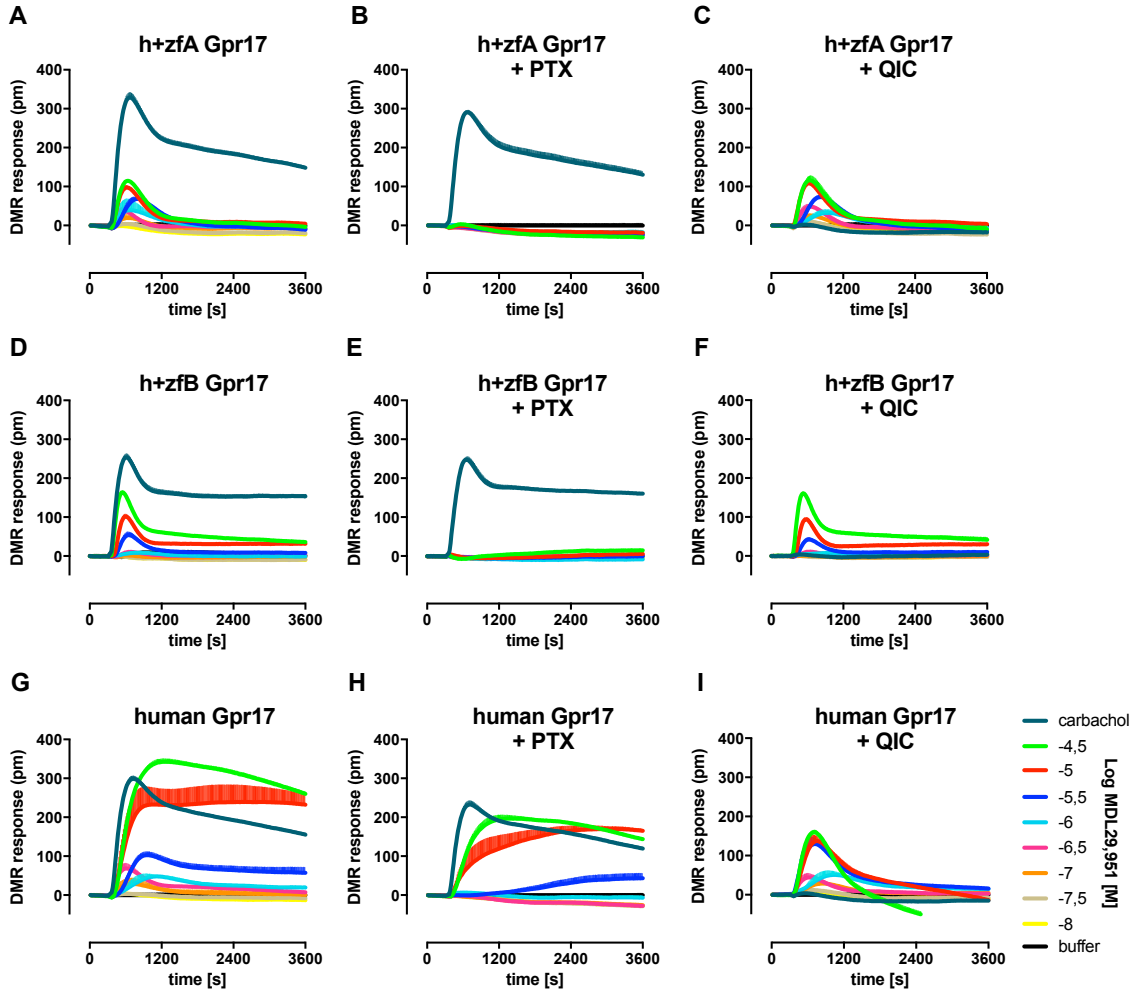

Supplementary Figure 4: Chimeric Gpr17 receptors exclusively couple via $G_{\alpha i}$ pathway. MDL29,951 elicited DMR responses on 3-HA tagged chimeric Gpr17 transiently (**A-C**) and stably (**D-F**) expressed in HEK293 cells. In the presence of PTX, responses of h+zfA (**B**) and h+zfBGpr17 (**E**) were abolished, while stimulation with UBO-QIC merely eliminated carbachol signal (**C,F**). On the contrary, DMR responses of human Gpr17 transiently expressed in HEK293 cells (**G-I**) were diminished in the presence of both inhibitors, PTX (**H**) and UBO-QIC (**I**). Label-free recordings are shown as representative traces, each performed in triplicates (means + SEM). Data were generated by Dr. Nicole Merten in the Institute of Pharmaceutical Biology, University of Bonn.

8 List of abbreviations

ad	latin word for up to
Claudin k	Zebrafish myelin-associated protein
CNS	central nervous system
CXCR4	chemokine 4 receptor
CysLTR	cysteinyl leukotriene receptor
dH_2O	demineralized water
DMR	dynamic mass redistribution
dpf	days post fertilization
EAE	experimental autoimmune encephalomyeli- tis (animal model of multiple sclerosis)
EGFP	exaggerated green fluorescent protein
ELISA	enzyme-linked immunosorborent assay
et al.	Et alii, Latin word for and others
FRET	fluorescence resonance energy transfer
g	acceleration by gravity
GPCR	G-protein coupled receptor
G protein	guanine nucleotide-binding protein
Gpr17	G-protein coupled receptor 17
Gpr30	G-protein coupled receptor 37
Gpr37	G-protein coupled receptor 37
Gpr56	G-protein coupled receptor 56

Gpr98	G-protein coupled receptor 98
h	human
h	hour(s)
HA-tag	human influenza hemagglutinin Tag
hpf	hours post fertilization
hGpr17	Human Gpr17
h+zfAGpr17	chimeric human (in) and zebrafish version A (out) Gpr17
h+zfBGpr17	chimeric human (in) and zebrafish version B (out) Gpr17
IgM	immunoglobuline M
ICC	immunocytochemistry
IHC	immunohistochemistry
KOR	κ-Rezeptor
Lingo-1	leucine rich repeat and Ig-like domain-containing Nogo receptor interacting protein 1
LTC4	leukotriene C4
LTD4	leukotriene D4
M	molar concentration (mol/liter)
MAG	myelin associated glycoprotein
MBP	myelin basic protein
mGlu4	glutamate receptor 4
min	minutes
MO	morpholino anti-sense oligonucleotide

MOG	myelin oligodendrocyte glycoprotein
ms	milliseconds
MS	multiple sclerosis
µL	microliter
µM	micromolar
nm	nanometer
NG2	neural/glial antigen 2 proteoglycan
Nkx2.2	transcription factor
NP	Neuronal precursor
OE	overexpression
OL	oligodendrocytes
Olig2	transcription factor
OPC	oligodendrocyte precursor cells
P	latin abbreviation for after birth
PCR	polymerase chain reaction
qPCR	quantitative polymerase chain reaction
Plp	proteolipid protein
PNS	peripheral nervous system
Pre-OL	pre-mature oligodendrocyte
PTX	Pertussis toxin
PY2 receptors	purinergic receptors
s	seconds

S1P1	sphingosin-1-phosphat receptor
siRNA	small-interfering RNA
UDP	uridine diphosphate
UDP-glc	uridine diphosphate-glucose
UDP-gal	uridine diphosphate-galactose
WISH	whole-mount in situ hybridization
zf	zebrafish
zfAGpr17	zebrafish version A Gpr17
zfA+hGpr17	chimeric zebrafish version A (in) and human (out) Gpr17
zfBGpr17	zebrafish version B Gpr17
zfB+hGpr17	chimeric zebrafish version B (in) and human (out) Gpr17
36k	zebrafish myelin protein 36k

9 List of figures

Figure 1: Oligodendrocyte development (Oligodendrogenesis) in zebrafish. 3

Figure 2: Expression of GPCRs during oligodendrocyte development. 5

Figure 3: Development of zebrafish during the first 5 days post fertilization (dpf). 9

Figure 4: Calculation for injected amount of morpholino. 53

Figure 5: Zebrafish Gpr17 version A is unresponsive towards uracil nucleotides and cysteinyl leukotrienes. 66

Figure 6: Stimulation of zebrafish Gpr17 with MDL29,951 does not display any sign of activity in holistic DMR assays. 68

Figure 7: Immunocytochemical localisation of 3HA-tagged Gpr17 constructs reveals no difference. 69

Figure 8: Quantification of cell surface expression of Gpr17 constructs displays almost equivalent expression levels in HEK293 cells. 70

Figure 9: MDL29,951 does not elicit Gpr17 specific DMR responses in zebrafish PAC2 cells. 71

Figure 10: ELISA results display absent cell surface expression of orthologous Gpr17 receptors in PAC2 cells. 72

Figure 11: Bath exposure with MDL29,951 does not alter number of *claudin K* positive dorsally migrated cells. 73

Figure 12: *Mbp* and *plp* expression levels of 5 dpf old zebrafish embryos are not influenced after MDL29,951 treatment. 74

Figure 13: MDL29,951 bath exposure does not affect expression of 36k myelin protein. 75

Figure 14: Schematic prediction of chimeric h+zfA Gpr17 receptor topology in the cell membrane.. 76

Figure 15: Chimeric Gpr17 receptors are expressed in the cell surface membrane of transiently transfected HEK293 cells. 77

Figure 16: Cell surface expression of chimeric Gpr17 constructs was declined compared to artless Gpr17 orthologous. 78

Figure 17: MDL29,951 evokes DMR responses on human Gpr17 containing intracellular loops of zebrafish Gpr17. 79

Figure 18: WISH of 1 to 5 dpf old zebrafish larvae reveals *zfAgpr17* expression within the CNS.... 81

Figure 19: *ZfAgpr17* expression is missing in dorsal spinal cord after Trichostatin A treatment. ... 82

Figure 20: ZfAGpr17 is expressed during oligodendrocyte development. 83

Figure 21: Representative region in the dorsal spinal cord of a 3 dpf tg(*olig2:EGFP*) zebrafish imaged by Two-photon microscopy. 85

Figure 22: Calibration of RNA amount for OE studies in tg(*olig2:EGFP*) zebrafish embryos suggests 800 pg RNA. 86

Figure 23: Stable RNA expression after microinjection of 150 pg *tdTomato* in zebrafish embryos. 87

Figure 24: 3 dpf old tg(*olig2:EGFP*) zebrafish embryos display normal phenotypes after injection of 800 pg RNA. 87

Figure 25: Maturation of oligodendrocyte lineage cells expressing *claudin k* is not altered by Gpr17 OE..... 89

Figure 26: OE of Gpr17 does not alter myelination in 4 dpf old zebrafish larvae..... 90

Figure 27: 4 dpf old zebrafish larvae exhibit no difference in Claudin K expression levels after Gpr17 OE..... 91

Figure 28: Oligodendrocyte lineage cells expressing transcription factor *olig2* display normal migration after Gpr17 OE. 92

Figure 29: Quantitative polymerase chain reaction revealed no difference in expression levels of myelin proteins *mbp* and *plp* after Gpr17 OE. 93

Figure 30: *Mbp* expression pattern determined by WISH is not influenced by Gpr17 OE. 94

Figure 31: WISH of 2.5 dpf old zebrafish embryos displays equal *nkx2.2* expression in the CNS.... 95

Figure 32: Structure of morpholino antisense oligonucleotide and native DNA. 96

Figure 33: *ZfAgpr17* morpholino injections cause weak phenotypes..... 97

Figure 34: Western blot analysis reveal Gpr17 knockdown after injection of *zfagpr17* morpholino.

..... 98

Figure 35: Mbp expression in the spinal cord of 4 dpf old zebrafish embryos is impaired following zfAGpr17 knockdown. 99

Figure 36: Western blot analysis of zfAGpr17 morphants reveals declined expression of myelin proteins. 100

Figure 37: ZfAGpr17 morphants reveal decreased *mbp* expression in the CNS and PNS.....102

Figure 38: ZfAGpr17 morphants reveal reduced numbers of *claudin k* expressing dorsally migrated cells. 103

Figure 39: Migration of *olig2* positive OPCs is inhibited after zfAGpr17 knockdown.....104

Figure 40: Cleaved Caspase-3 is not upregulated in 3 dpf zebrafish embryos after *zfAgpr17* morpholino injection. 105

Figure 41: *Nkx2.2* expression in the spinal cord of zfAGpr17 morphants was markedly increased at 2.5 dpf.....106

Figure 42: Reduction in numbers of *olig2* positive cells in zfAGpr17 morphants can be rescued by *zfAgpr17* RNA. 107

Supplementary Figure 1: Tg(*claudinK*:EGFP) zebrafish embryos injected with 800 pg tdTomato displayed stable RNA expression over 96 h…….125

Supplementary Figure 2: Expression of myelin protein Claudin K in 1 to 10 dpf zebrafish embryos……126

Supplementary Figure 3: Tg(*olig2*:EGFP) zebrafish revealed impaired *mbp* expression in CNS and PNS after *zfAgpr17* MO injections…..127

Supplementary Figure 4: Chimeric Gpr17 receptors exclusively couple via Gαi pathway……128

10 Bibliography

Ackerman, S. D. *et al.* (2015) 'The adhesion GPCR Gpr56 regulates oligodendrocyte development via interactions with Gα12/13 and RhoA', *Nature Communications*. Nature Publishing Group, 6(May 2014), pp. 1–14. doi: 10.1038/ncomms7122.

Ackerman, S. D. and Monk, K. R. (2015) 'The scales and tales of myelination: using zebrafish and mouse to study myelinating glia', *Brain Research*. doi: 10.1016/j.brainres.2015.10.011.

Acorda Therapeutics; PRA Health Sciences (2015) 'An intravenous infusion study of rHIgM22 in patients with multiple sclerosis.', *ClinicalTrials.gov*. Available at: https://clinicaltrials.gov/ct2/show/NCT01803867.

Aharoni, R. and Aharoni, R. (2016) 'Expert Review of Neurotherapeutics long-standing challenge Remyelination in multiple sclerosis : realizing a long-standing challenge', *Expert Review of Neurotherapeutics*. Informa Healthcare, 15(12), pp. 1369–1372. doi: 10.1586/14737175.2015.1112740.

Azzarelli, B. *et al.* (1996) 'Hypoxic-ischemic encephalopathy in areas of primary myelination: A neuroimaging and PET study', *Pediatric Neurology*, 14(2), pp. 108–116. doi: 10.1016/0887-8994(96)00010-0.

Bai, Q. *et al.* (2011) 'Major isoform of zebrafish P0 is a 23,5 kDa myelin glycoprotein expressed in selected white matter tracts of the central nervous system', *J Comp Neurol*, 519(8), pp. 1580–1596. doi: 10.1002/cne.22587.Major.

Becker, C. G. and Becker, T. (2008) 'Adult zebrafish as a model for successful central nervous system regeneration', *Restorative neurology and neuroscience*, 26(2–3), pp. 71–80.

Benned-Jensen, T. and Rosenkilde, M. M. (2010) 'Distinct expression and ligand-binding profiles of two constitutively active GPR17 splice variants', *British Journal of Pharmacology*, 159(5), pp. 1092–1105. doi: 10.1111/j.1476-5381.2009.00633.x.

Bjarnadóttir, T. (2006) 'Comprehensive repertoire and phylogenetic analysis of the G protein-coupled receptors in human and mouse', *Genomics*, 88, pp. 263–273.

Blackburn, P. *et al.* (2013) 'The CRISPR system- Keeping zebrafish gene targeting fresh', *Zebrafish*, 10, pp. 116–118.

Bläsius, R. *et al.* (1998) 'A Novel Orphan G Protein-Coupled Receptor Primarily Expressed in the Brain Is Localized on Human Chromosomal Band 2q21', *Journal of Neurochemistry*, 70(4), pp.

1357–1365. doi: 10.1046/j.1471-4159.1998.70041357.x.

Blum, M. *et al.* (2015) 'Morpholinos: Antisense and Sensibility', *Developmental Cell*. Elsevier Inc., 35(2), pp. 145–149. doi: 10.1016/j.devcel.2015.09.017.

Boda, E. *et al.* (2011) 'The GPR17 receptor in NG2 expressing cells: Focus on in vivocell maturation and participation in acute trauma and chronic damage', *Glia*, 59(12), pp. 1958–1973. doi: 10.1002/glia.21237.

Brösamle, C. and Halpern, M. E. (2002) 'Characterization of myelination in the developing zebrafish', *Glia*, 39(1), pp. 47–57. doi: 10.1002/glia.10088.

Buckley, C. E. *et al.* (2010) 'Drug reprofiling using zebrafish identifies novel compounds with potential pro-myelination effects', *Neuropharmacology*, 59, pp. 149–159. doi: 10.1016/j.neuropharm.2010.04.014.

Buckley, C. E., Goldsmith, P. and Franklin, R. J. M. (2008) 'Zebrafish myelination: a transparent model for remyelination?', *Disease models & mechanisms*, 1, pp. 221–228. doi: 10.1242/dmm.001248.

Campbell, J. *et al.* (2012) 'New and TALENted genome engineering toolbox', *Circ Res*, 113, pp. 571–587.

Ceruti, S. *et al.* (2009) 'The P2Y-like receptor GPR17 as a sensor of cord injury', pp. 2206–2218. doi: 10.1093/brain/awp147.

Chen, Y. *et al.* (2009a) 'The oligodendrocyte-specific G protein-coupled receptor GPR17 is a cell-intrinsic timer of myelination.', *Nature neuroscience*. Nature Publishing Group, 12(11), pp. 1398–406. doi: 10.1038/nn.2410.

Chen, Y. *et al.* (2009b) 'The oligodendrocyte-specific G protein – coupled receptor GPR17 is a cell-intrinsic timer of myelination', *Nature Neuroscience*, 12(11). doi: 10.1038/nn.2410.

Ciana, P., Fumagalli, M., Trincavelli, M. L., *et al.* (2006) 'The orphan receptor GPR17 identified as a new dual uracil nucleotides/cysteinyl-leukotrienes receptor.', *The EMBO journal*. EMBO Press, 25(19), pp. 4615–27. doi: 10.1038/sj.emboj.7601341.

Ciana, P., Fumagalli, M., Trincavelli, L., *et al.* (2006) 'The orphan receptor GPR17 identified as a new receptor', (April), pp. 4615–4627. doi: 10.1038/sj.emboj.7601341.

Cole, K. L. H. *et al.* (2017) 'Drug discovery for remyelination and treatment of MS', (April), pp. 1–25. doi: 10.1002/glia.23166.

Compston, A. and Coles, A. (2008) 'Multiple sclerosis', *The Lancet*. Elsevier Ltd, 372(9648), pp. 1502–1517. doi: 10.1016/S0140-6736(08)61620-7.

Coppi, E. *et al.* (2013) 'UDP-glucose enhances outward K+ currents necessary for cell differentiation and stimulates cell migration by activating the GPR17 receptor in oligodendrocyte precursors', *Glia*, 61(7), pp. 1155–1171. doi: 10.1002/glia.22506.

Corey, D. R. and Abrams, J. M. (2001) 'Morpholino antisense oligonucleotides: tools for investigating vertebrate development.', *Genome biology*, 2(5), p. REVIEWS1015. doi: 1015.1.

Czopka, T. (2015) 'Insights into mechanisms of central nervous system myelination using zebrafish', *Glia*, p. n/a-n/a. doi: 10.1002/glia.22897.

Daniele, S. *et al.* (2014) 'Does GRK–β arrestin machinery work as a "switch on" for GPR17-mediated activation of intracellular signaling pathways?', *Cellular Signalling*, 26(6), pp. 1310–1325. doi: https://doi.org/10.1016/j.cellsig.2014.02.016.

Driever, W. *et al.* (1994) 'Zebrafish: genetic tools for studying vertebrate development.', *Trends in genetics : TIG*, 10(5), pp. 152–159. doi: 10.1016/0168-9525(94)90091-4.

El-Brolosy, M. A. and Stainier, D. Y. R. (2017) 'Genetic compensation: A phenomenon in search of mechanisms', *PLoS Genetics*, 13(7), pp. 1–17. doi: 10.1371/journal.pgen.1006780.

Emery, B. (2010) 'Regulation of oligodendrocyte differentiation. [Review]', *Trends Neurosci.*, 330(November), pp. 359–362. Available at: http://science.sciencemag.org.ezproxy.library.tufts.edu/content/sci/330/6005/779.full.pdf.

Fang, Y. *et al.* (2007) 'Dynamic mass redistribution: a novel physiological signal of cells for cell systems biology and pharmacology', *Catalog2.Corning.Com*, (1), pp. 1–4. Available at: http://catalog2.corning.com/Lifesciences/media/pdf/2007_REDLines_DMR.pdf.

Fang, Y. *et al.* (2014) 'A novel model of demyelination and remyelination in a GFP-transgenic zebrafish.', *Biology open*, pp. 1–7. doi: 10.1242/bio.201410736.

Foran, D. R. and Peterson, A. C. (1992) 'Myelin acquisition in the central nervous system of the mouse revealed by an MBP-Lac Z transgene', *Journal of Neuroscience*, 12(12), pp. 4890–4997.

Franke, H. *et al.* (2013) 'Changes of the GPR17 receptor, a new target for neurorepair, in neurons and glial cells in patients with traumatic brain injury', *Purinergic Signalling*, 9(3), pp. 451–462. doi: 10.1007/s11302-013-9366-3.

Fumagalli, M. *et al.* (2011) 'Phenotypic changes, signaling pathway, and functional correlates of

GPR17-expressing neural precursor cells during oligodendrocyte differentiation', *Journal of Biological Chemistry*, 286(12), pp. 10593–10604. doi: 10.1074/jbc.M110.162867.

Fumagalli, M. *et al.* (2015) 'The ubiquitin ligase Mdm2 controls oligodendrocyte maturation by intertwining mTOR with G protein-coupled receptor kinase 2 in the regulation of GPR17 receptor desensitization', *Glia*, 63(12), pp. 2327–2339. doi: 10.1002/glia.22896.

Gearing, K. L. *et al.* (2003) 'Complex chimeras to map ligand binding sites of GPCRs', *Protein Engineering Design and Selection*, 16(5), pp. 365–372. doi: 10.1093/protein/gzg045.

George Bartzokis (2011) 'Alzheimer's disease as homeostatic responses to age-related myelin breakdown', *Neurobiol Aging*, 32(8), pp. 1341–1371. doi: 10.1109/TMI.2012.2196707.Separate.

Giera, S. *et al.* (2015) 'The adhesion G protein-coupled receptor GPR56 is a cell-autonomous regulator of oligodendrocyte development', *Nature Communications*. Nature Publishing Group, 6(May 2014), pp. 1–12. doi: 10.1038/ncomms7121.

Goldsmith, P. (2004) 'Zebrafish as a pharmacological tool : the how , why and when', *Current Opinion in Neurobiology*, 4, pp. 504–512. doi: 10.1016/j.coph.2004.04.005.

Goldsmith, P. and Solari, R. (2003) 'The role of zebrafish in drug discovery', *Drug Discovery World, Spring*, pp. 74–78.

Goldsmith, Y. *et al.* (2012) 'Fgf-dependent glial cell bridges facilitate spinal cord regeneration in zebrafish', *Journal of Neuroscience*, 32, pp. 7477–7492.

Guo, P. *et al.* (2015) 'Zebrafish as a model for studying the developmental neurotoxicity of propofol', *Journal of Applied Toxicology*, (April), p. n/a-n/a. doi: 10.1002/jat.3183.

Haffter, P. *et al.* (1996) 'The identification of genes with unique and essential functions in the development of the zebrafish, Danio rerio', *Development (Cambridge, England)*, 123, pp. 1–36. Available at: papers2://publication/uuid/7B13B1E7-8407-494D-BDAF-B88A09B73AB2.

Hagemeier, K. J. (2012) 'Multiple sclerosis - remyelination failure as a cause of disease progression.', *Histology and histopathology*, 27(3), pp. 277–287. doi: 10.14670/HH-27.277.

Harlow, D. E., Honce, J. M. and Miravalle, A. A. (2015) 'Remyelination therapy in multiple sclerosis', *Frontiers in Neurology*, 6(DEC), pp. 1–13. doi: 10.3389/fneur.2015.00257.

Hartline, D. K. and Colman, D. R. (2007) 'Rapid Conduction and the Evolution of Giant Axons and Myelinated Fibers', *Current Biology*, 17(1), pp. 29–35. doi: 10.1016/j.cub.2006.11.042.

Heise, C. E. *et al.* (2000) 'Characterization of the human cysteinyl leukotriene 2 receptor', *Journal*

of Biological Chemistry, 275(39), pp. 30531–30536. doi: 10.1074/jbc.M003490200.

Hennen, S. *et al.* (2013a) 'Decoding signaling and function of the orphan G protein-coupled receptor GPR17 with a small-molecule agonist.', *Science signaling*, 6(298), p. ra93. doi: 10.1126/scisignal.2004350.

Hennen, S. *et al.* (2013b) 'Decoding Signaling and Function of the Orphan G Protein – Coupled Receptor GPR17 with a Small-Molecule Agonist', 6(298), pp. 1–17.

Howard, A. *et al.* (2011) 'Orphan G-protein-coupled receptors and natural ligand discovery', *Trends in Pharmacological Sciences*, 22, pp. 132–140.

Howe, K. *et al.* (2013) 'The zebrafish reference genome sequence and its relationship to the human genome', *Nature*, 496(7446), pp. 498–503. doi: 10.1038/nature12111.The.

Joeng, J. *et al.* (2008) 'Functional and developmental analysis of the blood-brain barrier in zebrafish', *Brain Res Bull*, 75, pp. 619–628.

Jung, S. *et al.* (2009) 'Visualization of myelination in GFP-transgenic zebrafish', *Developmental Dynamics*. Wiley-Blackwell, 239(2), pp. 592–597. doi: 10.1002/dvdy.22166.

Kari, G., Rodeck, U. and Dicker, A. P. (2007) 'Zebrafish: An emerging model system for human disease and drug discovery', *Clinical Pharmacology and Therapeutics*, 82(1), pp. 70–80. doi: 10.1038/sj.clpt.6100223.

Kirby, B. B. *et al.* (2006) 'In vivo time-lapse imaging shows dynamic oligodendrocyte progenitor behavior during zebrafish development', 9(12), pp. 1506–1511. doi: 10.1038/nn1803.

Kleinert, H. (2018) *Charakterisierung von gpr17 und dessen Einfluss auf die Myelinisierung im Zebrafish (Danio rerio)*, *University of Bonn*.

Kok, F. O. *et al.* (2015) 'Reverse genetic screening reveals poor correlation between morpholino-induced and mutant phenotypes in zebrafish', *Developmental Cell*. Elsevier Inc., 32(1), pp. 97–108. doi: 10.1016/j.devcel.2014.11.018.

Kucenas, S., Snell, H. and Appel, B. (2010) 'nkx2.2a promotes specification and differentiation of a myelinating subset of oligodendrocyte lineage cells in zebrafish', 4(2). doi: 10.1017/S1740925X09990123.nkx2.2a.

Kulkarni, P. *et al.* (2017) 'Novel Zebrafish EAE model: A quick in vivo screen for multiple sclerosis', *Multiple Sclerosis and Related Disorders*, 11(August 2016), pp. 32–39. doi: 10.1016/j.msard.2016.11.010.

Langheinrich, U. (2003) 'Zebrafish: A new model on the pharmaceutical catwalk', *BioEssays*, pp. 904–912. doi: 10.1002/bies.10326.

Lecca, D. *et al.* (2008) 'The Recently Identified P2Y-Like Receptor GPR17 Is a Sensor of Brain Damage and a New Target for Brain Repair', *PLOS ONE*. Public Library of Science, 3(10), p. e3579. Available at: https://doi.org/10.1371/journal.pone.0003579.

Livak, K. J. and Schmittgen, T. D. (2001) 'Analysis of relative gene expression data using real-time quantitative PCR and the 2-ΔΔCT method', *Methods*, 25(4), pp. 402–408. doi: 10.1006/meth.2001.1262.

Lu, P. H. *et al.* (2013) 'Myelin breakdown mediates age-related slowing in cognitive processing speed in healthy elderly men', *Brain and Cognition*, 81(1), pp. 131–138.

Maekawa, A. *et al.* (2009) 'GPR17 is a negative regulator of the cysteinyl leukotriene 1 receptor response to leukotriene D4.', *Proceedings of the National Academy of Sciences of the United States of America*, 106(28), pp. 11685–11690. doi: 10.1073/pnas.0905364106.

Maisel, M., Alexander, H., *et al.* (2007) 'Transcription Profiling of Adult and Fetal Human Neuroprogenitors Identifies Divergent Paths to Maintain the Neuroprogenitor Cell State', *STEM CELLS*. Wiley-Blackwell, 25(5), pp. 1231–1240. doi: 10.1634/stemcells.2006-0617.

Maisel, M., Herr, A., *et al.* (2007) 'Transcription Profiling of Adult and Fetal Human Neuroprogenitors Identifies Divergent Paths to Maintain the Neuroprogenitor Cell State', *Stem Cells*, 25(5), pp. 1231–1240. doi: 10.1634/stemcells.2006-0617.

Mao, F. *et al.* (2012) 'Periventricular leukomalacia long-term prognosis may be improved by treatment with UDP-glucose, GDNF, and memantine in neonatal rats', *Brain Research*, 1486, pp. 112–120. doi: https://doi.org/10.1016/j.brainres.2012.09.033.

Marinelli, C. *et al.* (2016) 'Systematic Review of Pharmacological Properties of the Oligodendrocyte Lineage', 10(February), pp. 1–19. doi: 10.3389/fncel.2016.00027.

Marucci, G. *et al.* (2016) 'The G Protein-Coupled Receptor GPR17 : Overview and Update', pp. 1–9. doi: 10.1002/cmdc.201600453.

Mellion, M. *et al.* (2017) 'Efficacy Results from the Phase 2b SYNERGY Study: Treatment of Disabling Multiple Sclerosis with the Anti-LINGO-1 Monoclonal Antibody Opicinumab (S33.004)', *Neurology*, 88(16 Supplement). Available at: http://n.neurology.org/content/88/16_Supplement/S33.004.abstract.

Mi, S. *et al.* (2005) 'LINGO-1 negatively regulates myelination by oligodendrocytes', *Nature*

Neuroscience, 8(6), pp. 745–751. doi: 10.1038/nn1460.

Mi, S. *et al.* (2007) 'LINGO-1 antagonist promotes spinal cord remyelination and axonal integrity in MOG-induced experimental autoimmune encephalomyelitis', *Nature medicine*, 13(10), pp. 1228– 1233. doi: 10.1038/nm1664.

Milligan, G. (2011) 'Orthologue selectivity and ligand bias: Translating the pharmacology of GPR35', *Trends in Pharmacological Sciences*. Elsevier Ltd, 32(5), pp. 317–325. doi: 10.1016/j.tips.2011.02.002.

Mingardo, E. (2017) *Establishing a multi-well plate reader system for high- throughput imaging and analysis of fluorescent zebrafish larvae to investigate the central nervous system*. University of Bonn.

Mogha, A., Rozario, M. D. and Monk, K. R. (2016) 'Review G Protein-Coupled Receptors in Myelinating Glia', *Trends in Pharmacological Sciences*. Elsevier Ltd, 37(11), pp. 977–987. doi: 10.1016/j.tips.2016.09.002.

Monk, K. *et al.* (2011) 'Gpr126 is essential for peripheral nerve development and myelination in mammals.', *Development*, 138, p. 2673–2680.

Monk, K. R. *et al.* (2009) 'A G Protein-Coupled Receptor Is Essential for Schwann Cells to Initiate Myelination', *Science*, 325(5946), pp. 1402–1405. doi: 10.1126/science.1173474.

Monk, K. R. and Talbot, W. S. (2009) 'Genetic dissection of myelinated axons in zebrafish', *Current Opinion in Neurobiology*, 19(5), pp. 486–490. doi: 10.1016/j.conb.2009.08.006.

Morris, J. K. *et al.* (2004) 'The 36K Protein of Zebrafish CNS Myelin Is a Short-Chain Dehydrogenase', *GLIA*, 45(4), pp. 378–391. doi: 10.1002/glia.10338.

Münzel, E. J. *et al.* (2012) 'Claudin k is specifically expressed in cells that form myelin during development of the nervous system and regeneration of the optic nerve in adult zebrafish', *Glia*, 60(July 2011), pp. 253–270. doi: 10.1002/glia.21260.

Nave, K. A. (2010) 'Myelination and support of axonal integrity by glia', *Nature*, 468(7321), pp. 244–252. doi: 10.1038/nature09614.

Nawaz, S. *et al.* (2013) 'Molecular evolution of myelin basic protein, an abundant structural myelin component', *Glia*, 61(8), pp. 1364–1377. doi: 10.1002/glia.22520.

Neves, S., Ram, P. and Iyengar, R. (2002) 'G protein pathways. Part A, Receptors', 296(May), p. 680.

Ohnmacht, J. *et al.* (2016) 'Spinal motor neurons are regenerated after mechanical lesion and genetic ablation in larval zebrafish', *Development*, 143(9), pp. 1464–1474. doi: 10.1242/dev.129155.

Ou, Z. *et al.* (2016) 'Regulates Oligodendrocyte Survival in Response to Lysolecithin-Induced Demyelination', 36(41), pp. 10560–10573. doi: 10.1523/JNEUROSCI.0898-16.2016.

Paavola, K. J. *et al.* (2014) 'Type IV collagen is an activating ligand for the adhesion G protein-coupled receptor GPR126', *Science Signaling*, 7(338), pp. 1–10. doi: 10.1126/scisignal.2005347.

Pauls, S. *et al.* (2007) 'Function and regulation of zebrafish nkx2.2a during development of pancreatic islet and ducts', *Developmental Biology*, 304(2), pp. 875–890. doi: 10.1016/j.ydbio.2007.01.024.

Pepinsky, R. B. *et al.* (2011) 'Exposure Levels of Anti-LINGO-1 Li81 Antibody in the Central Nervous System and Dose- Efficacy Relationships in Rat Spinal Cord Remyelination Models after Systemic Administration', *Journal of Pharmacology and Experimental Therapeutics*, 339(2), pp. 519–529. doi: 10.1124/jpet.111.183483.

Perier, O. and Gregoire, A. (1965) 'Electron microscopic features of multiple sclerosis lesions', *Brain*, 88(6), pp. 937–952.

Petersen, S. C. *et al.* (2015) 'The adhesion GPCR GPR126 has distinct, domain-dependent functions in Schwann cell development mediated by interaction with laminin-211.', *Neuron*, 85, pp. 755–69. doi: 10.1016/j.neuron.2014.12.057.

Pfeiffer, S. E., Warrington, A. E. and Bansal, R. (1993) 'The oligodendrocyte and its many cellular processes', *Trends in Cell Biology*, 3(6), pp. 191–197. doi: 10.1016/0962-8924(93)90213-K.

Preston, M. a and Macklin, W. B. (2015) 'Zebrafish as a model to investigate CNS myelination.', *Glia*, 63(2), pp. 177–93. doi: 10.1002/glia.22755.

Pruvot, B. *et al.* (2014) 'Developmental defects in zebrafish for classification of EGF pathway inhibitors.', *Toxicology and applied pharmacology*, 274(2), pp. 339–49. doi: 10.1016/j.taap.2013.11.006.

Qi, A.-D. *et al.* (2013) 'Is GPR17 a P2Y/leukotriene receptor? examination of uracil nucleotides, nucleotide sugars, and cysteinyl leukotrienes as agonists of GPR17', *J. Pharmacol. Exp. Ther.*, 347(1), pp. 38–45. doi: 10.1124/jpet.113.207647.

Raphael, A. R. and Talbot, W. S. (2011) 'Chapter one - New Insights into Signaling During Myelination in Zebrafish', in Birchmeier, C. B. T.-C. T. in D. B. (ed.) *Growth Factors in*

Development. Academic Press, pp. 1–19. doi: https://doi.org/10.1016/B978-0-12-385975-4.00007-3.

Raport, C. J. *et al.* (1996) 'New members of the chemokine receptor gene family', *Journal of Leukocyte Biology*. Wiley Online Library, 59(1), pp. 18–23. doi: 10.1002/jlb.59.1.18.

Reinoß, P. (2014) *Functional analysis of the transmembrane receptor Gpr17 for CNS myelination in zebrafish*. University of Bonn.

Ringvall, M., Berglund, M. M. and Larhammar, D. (1997) 'Multiplicity of neuropeptide Y receptors: cloning of a third distinct subtype in the zebrafish.', *Biochemical and biophysical research communications*, 241(3), pp. 749–755.

Rossi, A. *et al.* (2015) 'Genetic compensation induced by deleterious mutations but not gene knockdowns', *Nature*. Nature Publishing Group, a division of Macmillan Publishers Limited. All Rights Reserved., 524, p. 230. Available at: http://dx.doi.org/10.1038/nature14580.

Schaefer, K. and Brosamle, C. (2009) 'Zwilling-A and -B, two related myelin proteins of teleost, which originate from a single bicistronic transcript', *Mol Biol Evol*, 26, pp. 495–499.

Schneider, S. *et al.* (2016) 'GPR17 Expressing NG2-Glia : Oligodendrocyte Progenitors Serving as a Reserve Pool After Injury'. doi: 10.1002/glia.22929.

Schröder, R. *et al.* (2011) 'Applying label-free dynamic mass redistribution technology to frame signaling of G protein-coupled receptors noninvasively in living cells.', *Nature protocols*. Nature Publishing Group, a division of Macmillan Publishers Limited. All Rights Reserved., 6(11), pp. 1748–60. doi: 10.1038/nprot.2011.386.

Schweitzer, J. *et al.* (2006) 'Evolution of myelin proteolipid proteins; Gene duplication in teleosts and expression pattern divergence', *Mol Cell Neurosci*, 31, pp. 161–177.

Schweitzer, R. N., Becker, T. and Becker, C. G. (2003) 'Expression of Protein Zero Is Increased in Lesioned Axon Pathways in the Central Nervous System of Adult Zebrafish', 317(August 2002), pp. 301–317. doi: 10.1002/glia.10192.

Seyedsadr, X. M. S. and Ineichen, X. B. V. (2017) 'Gpr17 , a Player in Lysolecithin-Induced Demyelination , Oligodendrocyte Survival , and Differentiation', 37(9), pp. 2273–2275. doi: 10.1523/JNEUROSCI.3778-16.2017.

Shin, J. *et al.* (2003) 'Neural cell fate analysis in zebrafish using olig2 BAC transgenics', *Methods Cell Sci*, 136, pp. 62–67.

Simon, K. *et al.* (2016) 'The Orphan G Protein-coupled Receptor GPR17 Negatively Regulates Oligodendrocyte Differentiation via G __ i / o and Its Downstream Effector Molecules *', 291(2), pp. 705–718. doi: 10.1074/jbc.M115.683953.

Simon, K. *et al.* (2017) 'The Orphan Receptor GPR17 Is Unresponsive to Uracil Nucleotides and Cysteinyl Leukotrienes s', pp. 518–532.

Smith, B. M. *et al.* (2017) 'Mice lacking Gpr37 exhibit decreased expression of the myelin-associated glycoprotein MAG and increased susceptibility to demyelination', *Neuroscience*. IBRO, 358, pp. 49–57. doi: 10.1016/j.neuroscience.2017.06.006.

Stainier, D. Y. R. *et al.* (2017) 'Guidelines for morpholino use in zebrafish', *PLoS Genetics*, 13(10), pp. 6–10. doi: 10.1371/journal.pgen.1007000.

Starback, P. *et al.* (1999) 'Neuropeptide Y receptor subtype with unique properties cloned in the zebrafish : the zYa receptor 1', pp. 242–252.

Stoffels, J. *et al.* (2013) 'Fibronectin aggregation in multiple sclerosis lesions impairs remyelination', *Brain*, 136, pp. 116–31. doi: 10.1093/brain/aws313.

Sun, T. *et al.* (2006) 'Evidence for motoneuron lineage-specific regulation of Olig2 in the vertebrate neural tube', *Developmental Biology*, 292(1), pp. 152–164. doi: 10.1016/j.ydbio.2005.12.047.

Takada, N. and Appel, B. (2010) 'Identification of Genes Expressed by Zebrafish Oligodendrocytes Using a Differential Microarray Screen', (May), pp. 2041–2047. doi: 10.1002/dvdy.22338.

Taylor, K. L. *et al.* (2010) 'Small molecule screening in zebrafish : an in vivo approach to identifying new chemical tools and drug leads', pp. 1–14.

Thisse, C. and Thisse, B. (2008) 'High-resolution in situ hybridization to whole-mount zebrafish embryos', 3(1), pp. 59–69. doi: 10.1038/nprot.2007.514.

Urnov, F. *et al.* (2010) 'Genome edeting with engineered zinc finger nucleases', *Nat Rev Genet*, 11, pp. 636–646.

Waterston, R. H. *et al.* (2002) 'Initial sequencing and comparative analysis of the mouse genome', *Nature*, 420(6915), pp. 520–562. doi: 10.1038/nature01262.

Watzlawik, J. *et al.* (2013) 'Cellular targets and mechanistic strategies of remyelination-promoting IgMs as part of the naturally occurring autoantibody repertoire', *Expert Rev Neurother*, 13, pp. 1017–29. doi: 10.1586/14737175.2013.835601 133.

van Wijngaarden, P. and Franklin, R. J. M. (2013) 'Ageing stem and progenitor cells: implications for rejuvenation of the central nervous system', *Development*, 140(12), pp. 2562–2575. doi: 10.1242/dev.092262.

Yang, H.-J. *et al.* (2016) 'G protein-coupled receptor 37 is a negative regulator of oligodendrocyte differentiation and myelination', *Nature Communications*. Nature Publishing Group, 7, p. 10884. doi: 10.1038/ncomms10884.

Yin, D. *et al.* (2004) 'Probing Receptor Structure / Function with Chimeric G-Protein-Coupled Receptors', *Molecular pharmacology*, 65(6), pp. 1323–1332. doi: 10.1124/mol.65.6.1323.

Yoganantharjah, P. and Gibert, Y. (2017) 'The Use of the Zebrafish Model to Aid in Drug Discovery and Target Validation', *Current Topics in Medicinal Chemistry*, 17(18), pp. 2041–2055. doi: 10.2174/1568026617666170130112109.

Yoshida, M. and Macklin, W. B. (2005) 'Oligodendrocyte development and myelination in GFP-transgenic zebrafish', *Journal of Neuroscience Research*. Wiley-Blackwell, 81(1), pp. 1–8. doi: 10.1002/jnr.20516.

Zada, D. *et al.* (2016) 'Pharmacological treatment and BBB-targeted genetic therapy for MCT8-dependent hypomyelination in zebrafish', *Disease Models & Mechanisms*, 9(11), pp. 1339–1348. doi: 10.1242/dmm.027227.

Zhao, B. *et al.* (2012) 'The new P2Y-like receptor G protein-coupled receptor 17 mediates acute neuronal injury and late microgliosis after focal cerebral ischemia in rats', *Neuroscience*, 202, pp. 42–57. doi: https://doi.org/10.1016/j.neuroscience.2011.11.066.

Zon, L. I. and Peterson, R. T. (2005) 'IN VIVO DRUG DISCOVERY IN THE ZEBRAFISH', 4(January). doi: 10.1038/nrd1606.

Publications

Publications

Grundmann M, Merten N, Malfacini D, Inoue A, Preis P, Simon K, Rüttiger N, Ziegler N, Benkel T, **Schmitt NK**, Ishida S, Müller I, Reher R, Kawakami K, Inoue A, Rick U, Kühl T, Imhof D, Aoki J, König GM, Hoffmann C, Gomeza J, Wess J, Kostenis E. Lack of beta-arrestin signaling in the absence of active G proteins. Nat Commun. 2018 Jan 23;9(1):341. doi: 10.1038/s41467-017-02661-3.

Simon K, Merten N, Schröder R, Hennen S, Preis P, **Schmitt NK**, Peters L, Schrage R, Vermeiren C, Gillard M, Mohr K, Gomeza J, Kostenis E. The Orphan Receptor GPR17 Is Unresponsive to Uracil Nucleotides and Cysteinyl Leukotrienes. Mol Pharmacol. 2017;91(5):518-532

Sosic A, Zuravka I, **Schmitt NK**, Miola A, Göttlich R, Fabris D, Gatto B. Direct and Topoisomerase II Mediated DNA Damage by Bis-3-chloropiperidines: The Importance of Being an Earnest G. ChemMedChem. 2017;12(17):1471-1479

Poster Presentations

Schmitt NK, Simon K, Merten N, Preis P, Kleinert H, Schröder R, Hennen S, Peters L, Odermatt B, Gomeza J, Kostenis E. On the value of uracil nucleotides and cysteinyl- leukotrienes as molecular probes to explore GPR17 biology in nonhuman species. DPhG Annual Meeting 2015 (Düsseldorf, DE, September 23.-25.)

Acknowledgments

Zunächst bedanke ich mich bei meiner Doktormutter Frau Prof. Dr. Evi Kostenis für die wissenschaftliche Betreuung meines Projektes, für ihre Unterstützung und ihr Vertrauen während der letzten 4 Jahre. Ein besonderer Dank gilt auch Herrn Dr. Jesús Gomeza, für die uneingeschränkte Hilfsbereitschaft, insbesondere für die zahlreichen Gespräche, die ich stets als Motivation und Ermutigung empfunden habe.

Des Weiteren, danke ich meinem Zweitgutachter Prof. Dr. Benjamin Odermatt für die Bereitstellung seines Labors sowie für seine hilfsbereite Betreuung.

Auch bedanke ich mich bei Frau Prof. Dr. Dorothea Bartels für das Mitwirken als fachfremdes und Herrn Prof. Dr. Ulrich Jaehde fachnahes Mitglied meiner Prüfungskommission.

Ein großer Dank gilt auch meinen Kollegen aus der AG Kostenis, der AG Odermatt sowie der AG König, die in vielerlei Hinsicht mein Vorankommen während der Promotion unterstützt haben. Vielen Dank an Dr. Nicole Merten und Dr. Katharina Simon, für die gute Einarbeitung in der Anfangsphase und die fortlaufende Unterstützung während der gesamten Promotionszeit. Weiterhin bedanke ich mich bei Öznur Yilmaz für die große Hilfe im Labor. Besonders bedanke ich mich auch bei Felix Häberlein und Bhuvaneswari Nagarajan, für ihr Vertrauen, ihre Hilfsbereitschaft, ihre Teamfähigkeit und ihr offenes Ohr, sowohl in beruflichen als auch privaten Angelegenheiten. Ansonsten bedanke ich mich bei den Sportlern (Suvi Eymann, Julian Patt und Paul Barac), den „Mamis“ (Nina Heycke und Ulrike Rick), den Island-Urlaubern (Caroline Maria Kolvenbach, Bhuvaneswari Nagarajan, Felix Häberlein, Stephan Terporten), den Mensa-Gängern (AG Kostenis und AG Odermatt), den Fischleuten (AG Odermatt), der Weihnachtsfeier/Karneval Community (AG Kostenis und AG König) und den BIOIII Leuten (Dr. Christel Drewke, Benjamin Libor, Tobias Benkel, Ekaterina Egereva, Emilia Goralski) für die wunderbare gemeinsame Zeit.

Nicht zuletzt danke ich meinen Freunden und meiner Familie, insbesondere meinen Eltern und meinem Freund Gerrit für ihre uneingeschränkte, liebevolle und vielseitige Unterstützung während meiner Promotionszeit.